Hydrogeologic Investigation of the Northern Taos Plateau, Taos County, New Mexico

Final Technical Report
February 2012
Open File Report 544
updated November 2012

New Mexico Bureau of Geology and Mineral Resources

Peggy S. Johnson
Paul W. Bauer

AQUIFER MAPPING PROGRAM

New Mexico Bureau of Geology and Mineral Resources

A division of New Mexico Institute of Mining and Technology

Socorro, NM 87801
(575) 835-5490
Fax (575) 835-6333
www.geoinfo.nmt.edu

Hydrogeologic Investigation of the Northern Taos Plateau, Taos County, New Mexico

Final Technical Report
February 2012
Open File Report 544

Peggy S. Johnson
Paul W. Bauer

November 2012
This report was edited to correct missing "-" characters, which had been inadvertently dropped from portions of the isotopic data results. None of the interpretations within the report have changed.

AQUIFER MAPPING PROGRAM

New Mexico Bureau of Geology and Mineral Resources

PROJECT FUNDING

New Mexico Interstate Stream Commission
The Healy Foundation, with Taos County as the fiscal agent
The New Mexico Bureau of Geology & Mineral Resources,
Aquifer Mapping Program

TABLE OF CONTENTS

FIGURES

TABLES

APPENDICES

EXECUTIVE SUMMARY

The Taos Plateau in northern Taos County is a high-elevation, basalt-capped plain that lies between the Rio Grande and the Tusas Mountains. The plateau overlaps the New Mexico-Colorado border and forms the west rim of the Rio Grande gorge. The hydrogeologic field investigation of the northern Taos Plateau, conducted between October 2007 and October 2009, is the first comprehensive assessment of groundwater conditions on the Taos Plateau and interactions between local aquifers and the Rio Grande. The investigative approach integrates new and existing geologic, geophysical, hydrologic, and geochemical data. This study has been undertaken in parallel with a major investigation of the springs in the Rio Grande gorge (Bauer et al., 2007). These studies advance understanding of the groundwater system in the northern Taos Plateau, and the interconnection of groundwater and surface water along the Rio Grande in northern Taos County.

This report contains seven detailed geologic cross sections and a regional geologic map, maps of surface drainages and closed basins, locations of inventoried wells, and data tables of well characteristics, water-level measurements, and results of geochemical sampling. It also contains interpretive maps of a regional water-table surface, the physical, chemical and isotopic characteristics of groundwater including temperature, distribution of dissolved ions and elements, and apparent ^{14}C, tritium (^{3}H), and chlorofluorocarbon groundwater ages. Interpretive plots of groundwater geochemistry provide insight into controlling hydrogeochemical processes, sources of groundwater, and groundwater flow paths. When integrated, these multiple data sets support a conceptual hydrogeologic model of the groundwater and surface water systems of the Taos Plateau.

The northern Taos Plateau study area extends westward from the Rio Grande gorge to the west edge of the plateau where the Tusas Mountains begin to rise. The Tusas Mountains represent the western flank of the Rio Grande rift, with peaks that exceed 11,000 feet in elevation. The study area then runs northward from the line of large Pliocene volcanoes east of Tres Piedras (No Agua Peaks, Cerro del Aire, Cerro de la Olla, and Cerro Chiflo) to just north of the town of Antonito, Colorado, and includes a short reach of the Rio San Antonio and the southernmost San Luis Hills.

The northern Taos Plateau is geomorphically remarkable due to the complexity of surface drainages and the scarcity of drainage integration. Only two second-order stream systems exist along the edges of the plateau: the Conejos River drainage to the northwest and the Arroyo Aguaje de la Petaca drainage to the southwest. Most of the study area (453 mi^2) consists of closed basins and poorly developed surface drainage systems. Two large closed basins in the center of the plateau originate on San Antonio Mountain and contain numerous, large active playas that contain standing water following storms and local snowmelt. Large basins with narrow outlets to the Rio Grande gorge occupy 278 mi^2 and include Punche, Pinabetoso, Chiflo, Brushy Mountain, and Montoso. The open basins contain small playas that hold water following large storm and melt events.

The perennial Rio San Antonio flows from the northern Tusas Mountains northward into Colorado, then joins the Conejos River in the San Luis Valley. The transition between the Taos Plateau and the San Luis Valley is roughly coincident with a subtle, but highly significant, surface drainage divide that separates the Rio San

Antonio drainage from Punche Arroyo by less than 10 feet of elevation.

The Taos Plateau lies within the southern San Luis Basin, the northernmost large basin of the Rio Grande rift. The basin is roughly divided into two major provinces, the San Luis Valley of southern Colorado and the Taos Plateau of northern New Mexico. The San Luis Basin is asymmetric, with a deep, narrow structural trough east of the gorge, known as the Taos graben in New Mexico, and a shallow bedrock ramp west of the gorge. The northern half of the rift basin is structurally complex, with a number of sub-basins and structural highs, including the Alamosa and Taos-Costilla sub-basins and the San Luis Hills and Brushy-Timber Mountain horsts. The major geologic features in the study area are the Taos Plateau volcanic field (TPVF), the Rio Grande gorge, the San Luis Hills, and the Brushy Mountain and Timber Mountain horsts.

The Pliocene to Pleistocene TPVF is the largest and compositionally most diverse volcanic field of the Rio Grande rift. Volcanic units capping the plateau include the Servilleta flood basalts and at least 35 extinct volcanoes of a variety of compositions, sizes, and shapes. Lava domes (such as San Antonio Mountain, Ute Mountain, Cerro Chiflo, No Agua Peaks, Cerro del Aire, Cerro de la Olla, and Cerro Montoso) are high-relief volcanoes ranging from about 8600 to nearly 11,000 ft in elevation. The Servilleta basalts are highly fractured, and consist of many, thin, laterally extensive, pahoehoe flows. Lava domes are also highly fractured with rubble-covered surfaces. Servilleta Basalt progressively thins to the northwest and pinches out just south of Antonito, Colorado.

The Rio Grande gorge deepens southward from a small canyon in southern Colorado to 850 ft deep near the Red River confluence in the southeastern study area. Over most of its length, the gorge consists of highly fractured, sub-horizontal, thinly layered Servilleta basalt flows. Locally, thin layers of alluvial sediments crop out between basalt flows. These silt-sand-gravels represent the Santa Fe Group, which probably also underlies the oldest Servilleta basalt layer over most of the study area.

The Taos Plateau aquifer is generally unconfined within the Servilleta Basalt and the underlying Santa Fe Group alluvial deposits. Most wells on the Taos Plateau in New Mexico draw groundwater from the Servilleta Basalt. Virtually all Colorado wells tap Santa Fe Group alluvium. Between the state line and the Rio San Antonio, thin Servilleta Basalt is generally unsaturated and lies above saturated Santa Fe group. Wells completed in the Servilleta Basalt have water depths ranging from 241 to 620 ft and yields ranging from 2.5 to 100 gallons per minute (gpm). In Colorado, wells tapping the Santa Fe Group aquifer have water depths from 18 to 294 ft and an average well yield of 375 gpm.

Wells on or near large volcanic domes generally have water levels elevated slightly or significantly above the regional aquifer and produce significant yields (10 to 56 gpm). The elevated water levels indicate either a local perched aquifer, or signify a recharge mound in the regional aquifer. Downward migration of groundwater from these perched zones, through fracture and rubble zones in the lava rock, is believed to recharge the regional aquifer with groundwater sourced from precipitation at higher elevations on the volcanic peaks.

The San Luis Hills form a topographic and structural high between the Taos Plateau and the Alamosa sub-basin. The hills represent the surface expression of a large intrarift horst (the San Luis Hills horst) that is mainly composed of middle Tertiary volcanic rocks and related sedimentary units of the Conejos, Los Pinos, and Hinsdale Formations. These units are also exposed at Brushy Mountain and Timber Mountain, which are believed to represent a southward extension of the San Luis Hills horst. Although the subsurface extent of these middle Tertiary rocks is unknown, it is assumed that they underlie much of the study area. The Hinsdale and other lower Tertiary formations have low relative permeability that alters groundwater flow direction and hydraulic gradients in the Taos Plateau aquifer. The Hinsdale

Formation forms the principal aquifer along the western edge of the study area, west of the inferred Western Plateau fault, where depth to water ranges from 600 to 727 ft and well yields range from 15 to 35 gpm.

Proterozoic granitic rocks crop out in the southwestern study area, near Tres Piedras. The top of the basement is a major unconformity that probably contains extensive topographic relief. Similar rocks certainly underlie all of the study area, but appear to be shallow enough to interact with the top of the regional aquifer only in the southwest corner of the study area. Where Proterozoic granitic rocks comprise the aquifer near Tres Piedras, the wells vary from 780 to 960 ft in depth and yield about 1 gpm.

Several faults and associated horst structures influence regional groundwater flow on the Taos Plateau: 1) the Red River fault zone; 2) the Gorge fault zone; 3) the Cerro de la Olla-Ute Mountain fault zone; 4) the San Luis Hills-Taos Plateau-Brushy/Timber Mountain horsts; and 5) the inferred Western Plateau fault. We infer the existence of a buried, continuous, structural high—informally named the Taos Plateau horst—connecting the San Luis Hills and Brushy-Timber Mountain horsts beneath the eastern Taos Plateau. All of the mapped faults displace rocks as young as the Servilleta Basalt, and all are thought to be normal faults related to the Rio Grande rift. Where exposed, the faults are characterized by complex strands of high-angle faults that can include significant fracture zones. In the volcanic rocks, the faults appear to be effective conduits for groundwater flow.

A water table surface for the Taos Plateau aquifer shows that groundwater generally flows from the Tusas Mountains eastward toward the Rio Grande gorge. At the western margin of the plateau, a decrease in the hydraulic gradient across the Western Plateau fault, from 70 ft/mi to as little as 2.5 ft/mi, reflects a contrast in aquifer permeability between the Hinsdale Formation to the west and the Servilleta Basalt to the east, which are juxtaposed across the fault. A flat water table under the eastern half of the plateau is caused by high permeability in the fractured-basalt aquifer, flat topography, and recharge through the lava-capped plateau. Just west of the Rio Grande gorge, the water table surface shows southerly and southeasterly flow flanking the Taos Plateau horst.

The water table surface shows recharge mounds beneath the Rio Grande in the Ute Mountain reach, and the Rio San Antonio near Antonito, Colorado. The Rio San Antonio mound forms a subtle groundwater divide that is generally coincident with the surface drainage divide separating the Rio San Antonio drainage from Punche Arroyo. From the divide, groundwater flows southeast into New Mexico and north into the San Luis Valley. There is no hydraulic evidence of groundwater flow from the San Luis Valley north of Antonito into the Taos Plateau aquifer. The San Luis Hills appear to form a flow barrier between the two provinces.

Gains in flow to the Rio Grande in New Mexico from adjacent aquifers are focused in two large spring zones that coincide with the Ute Mountain, Gorge, and Red River fault zones. The Ute Mountain spring zone discharges 37 cfs in a 1.5-mile reach of river beginning at river mile 19.5, where the Ute Mountain fault intersects the Rio Grande gorge. The spring zone ends at the Lava Tube spring, a large subaqueous spring discharging approximately 13 cfs (6000 gpm) from a cavern in the river channel that spatially coincides with the Gorge fault. The Bear Crossing-Felsenmeere spring zone consists of two spring clusters in a 1.5-mile reach of the Upper Taos Box. The Bear Crossing springs discharge an estimated 14 cfs (6400 gpm) from multiple vents located 50 to 100 or more feet above the river, starting where the Red River fault zone intersects the west wall of the Rio Grande gorge. The three Felsenmeere springs, visible from the eastern rim as high-velocity, high-discharge columns of water that emerge from the basalt talus about 100 ft above the river, discharge an estimated 21.6 cfs (9700 gpm). The large volume of groundwater discharging via springs in the west canyon wall is a response to the high channel gradient (84 ft/mi) and deep incision of the Rio Grande through this reach. Seepage data and spring observations in the intervening 10-mile reach of the Rio Grande, coincident with the Sunshine Valley and between these two large spring zones, indicate a stream loss of more than 13 cfs.

Thermal anomalies due to convection (the transport of heat by flowing groundwater) are common in deep basin aquifers of the Rio Grande rift, including the San Luis Basin. Groundwater discharge temperatures from wells and springs on the Taos Plateau range from 10.5 to 31 ºC (50.9 to 87.8 ºF) and identify thermal anomalies between San Antonio Mountain and No Agua, and along the eastern edge of the plateau near the Red River fault zone and the inferred Taos Plateau horst. Two hot wells and three warm wells with discharge temperatures of 18 to 31 ºC, and large warm springs at Bear Crossing (TS-8, 16.5 ºC) and Felsenmeere (TS-61, 16.8 ºC) that discharge from the Red River fault zone, are associated with these thermal anomalies. Cool groundwater (<16 ºC) characterizes the center of the Taos Plateau. This study shows that thermal water upwelling along large rift structures influences both the flow, and thermal and chemical characteristics, of shallow groundwater in parts of the Taos Plateau regional aquifer.

Multiple chemical, isotopic, and age-dating methods were applied to identify and distinguish sources of inflow and recharge to the Taos Plateau aquifer. Discharge temperatures, ion and trace element chemistry, stable isotopes of hydrogen (^{2}H) and oxygen (^{18}O), and groundwater age dating using radiocarbon (^{14}C), tritium (^{3}H), and chlorofluorocarbon (CFC) composition, each contribute unique information regarding water source and chemical processes affecting the groundwater. When interpreted in the hydrogeologic framework, the results identify chemical differences between groundwater from Santa Fe Group deposits in Colorado and the Taos Plateau volcanic field in New Mexico and distinguish four sources of water to the Taos Plateau aquifer.

Groundwater from Colorado wells is calcium-bicarbonate (Ca-HCO_3)—unique in the study area—and is identical in ion chemistry to the Rio San Antonio, indicating the stream is a source of recharge to the Santa Fe Group. Groundwater from the Taos Plateau in New Mexico contains noticeably higher amounts of sodium (Na), magnesium (Mg), and dissolved solids, and locally high sulfate (SO_4) and chloride (Cl). Chemical and isotopic characteristics of New Mexico well water also have a consistent geographic distribution, influenced by recharge, residence time, and geologic strata and structures.

The four sources of groundwater inflow and recharge contribute water to the Taos Plateau aquifer are: 1) underflow from the Tusas Mountains; 2) infiltration and recharge from precipitation on the lava-capped plateau and volcanic domes; 3) upwelling of a deep source of mineralized, thermal water near the Red River fault zone; and 4) influent seepage from the Rio San Antonio and the Rio Grande north of Ute Mountain.

Underflow from the Tusas Mountains**—**Groundwater underflow from the Tusas Mountains, entering the western margin of the plateau through the Hinsdale Formation and Santa Fe Group, is chemically unique. These waters are elevated (relative to the central plateau) in dissolved solids, carbonate alkalinity, calcium (Ca), magnesium (Mg), fluoride (F) and lithium (Li). The water originated from high altitude recharge, as indicated by ^{2}H depletion (<-105 ‰), and circulated to significant depth as indicated by anomalously warm temperatures (>19 ºC). The water displays a positive isotopic shift in ^{18}O of about 0.5 to 1.0 ‰ and elevated dissolved SiO_2 (>60 mg/L) indicative of isotopic exchange between the recharge water and silicates in the reservoir rock, which is accelerated by high water temperatures. This groundwater underflow is the oldest water in the study area, with an apparent ^{14}C age of about 5500 to over 8000 radiocarbon years before present. These waters become progressively younger as they flow eastward into the Servilleta Basalt and mix with local recharge. The extent of ^{2}H depleted water beneath the Taos Plateau shows that underflow from the Tusas Mountains persists as a traceable component of regional groundwater nearly to the Taos Plateau horst.

***Recharge from Precipitation*—**Substantial recharge originates from precipitation and infiltration on the lava-capped plateau and volcanic domes. Most of the plateau consists of closed drainage basins with active playas. Perched aquifers or recharge mounds in the regional aquifer are associated with San Antonio Mountain, Ute Mountain, No Agua Peaks, and Cerro de la Olla. Carbon-14 and ^{3}H composition and CFC-12 recharge ages demonstrate mixing of older underflow from the Tusas Mountains with tritium- and CFC-bearing recent recharge beneath the closed surface basins of the central plateau. Stable isotope composition demonstrates a common recharge source for San Antonio Mountain perched groundwater and regional groundwater beneath the central and eastern regions of the Taos Plateau.

***Upwelling of Thermal, Mineralized Groundwater near the Red River Fault Zone*—**The inferred Taos Plateau horst, or a fault boundary of the horst, appears to control groundwater flow from the Taos Plateau aquifer to the west as well as from the Taos graben to the east. West-to-east groundwater flow on the western half of the Taos Plateau is deflected southeast and south along the inferred eastern margin of the horst, just west of the Rio Grande gorge. Combinations of elevated groundwater temperatures and anomalously high concentrations of dissolved solids, sodium, sulfate, chloride, bromide, fluoride, boron, lithium, and arsenic are measured in wells and springs aligned with the Red River fault zone and the inferred Taos Plateau horst. Chemical and temperature anomalies in the vicinity of the Taos Plateau horst demonstrate a structural control for upwelling thermal, mineralized waters. Calcium, mixed cation, bicarbonate water from the Taos Plateau aquifer mixes with deep sourced $Na\text{-}HCO_3\text{-}Cl\text{-}SO_4$ thermal water and discharges to local wells and springs aligned with the structure. An ion-based mixing model estimates that discharge to the warm Bear Crossing spring in the Rio Grande gorge represents a mixture of about 20% fault-zone water and 80% Taos Plateau groundwater. Mineralized thermal waters may originate from deep groundwater circulation through the Taos graben, which is forced upward by the Taos Plateau horst and/or Red River fault zone, or from upflow of deep thermal fluids along the horst-bounding basement faults. Either or both deep sources may contribute to elevated groundwater temperatures and chemical anomalies in the southeastern corner of the Taos Plateau.

***Seepage from the Rio San Antonio and the Rio Grande*—**Local mounds and ridges in the surface of the Taos Plateau aquifer demonstrate the effects of local topography and recharge superimposed on regional flow. Groundwater mounds exist beneath the Rio Grande in the Ute Mountain reach and the Rio San Antonio near Antonito, Colorado, indicating that channel infiltration locally recharges the regional aquifer. The groundwater mound beneath the Rio Grande is constrained to the Ute Mountain reach upstream of the accretion zone and the Ute Mountain spring zone. Waters that discharge from the Ute Mountain spring zone in the Rio Grande gorge have a unique isotopic signature and appear to be unrelated to the Taos Plateau regional aquifer. The data suggest a recharge source from east of the Rio Grande gorge, from precipitation on Ute Mountain, the Sunshine Valley or the Sangre de Cristo Mountains. We find no evidence to support the notion that groundwater from Alamosa Valley flows beneath the Taos Plateau to discharge into the Rio Grande.

I. INTRODUCTION

Background

In addition to containing the Rio Grande's entry point into New Mexico, Taos County is also host to most of the river's perennial tributaries, as well as a 19-mile reach between Ute Mountain and the Red River that gains more than 80 cubic feet per second (~58,000 acre-feet per year) through the combined flow of more than 160 springs and seeps.

Both sides of the Rio Grande in Taos County are characterized by relatively flat plains that grade into high mountain ranges. East of the Rio Grande gorge, the Costilla Plains lead to the Sangre de Cristo Mountains. West of the gorge, the Taos Plateau transitions to the Tusas Mountains.

Within Taos County, all perennial tributary streams to the Rio Grande originate on the east side in the Sangre de Cristo Mountains. Several of these tributaries are deeply incised into the plateau. In contrast, the northern Taos Plateau is devoid of an integrated surface drainage system, and in fact contains large areas of hydrologically closed surface basins, in spite of the high mountain range to the west. The northern Taos Plateau also lacks deeply incised canyons.

An excellent study of the groundwater conditions of the Sunshine Valley area of the Costilla Plains was done in the 1950s (Winograd, 1959). No such hydrogeologic study has been attempted on the Taos Plateau. A recent inventory of the springs in the Rio Grande gorge reported many large springs on both the east and the west sides of the river (Bauer et al., 2007). This observation has led to questions about the nature of the groundwater system under the Taos Plateau, and its connections to the Rio Grande.

This is not the first time that such questions have arisen. In a U.S. Geological Survey (USGS) report on the geology and water resources of the San Luis Valley in Colorado, Siebenthal (1910) wrote "... the flow of the Rio Grande below the Embudo Canyon [archaic term for the Rio Grande gorge] will always be largely independent of the flow at the head of the canyon. Thus the sands and gravels of the San Luis Valley act as a natural reservoir with lasting benefit to the Rio Grande valley below." Without having collected any hydrogeologic data on the Taos Plateau or the gorge springs, Siebenthal was arguing that aquifer storage in the San Luis Valley in Colorado was directly feeding the springs in the Rio Grande gorge of New Mexico by underflow beneath the Taos Plateau.

This notion was rebutted by Bryan (1928), who wrote "The fact that invisible gain in flow takes place in Rio Grande Canyon, both above and below the Cerro Chiflo Barrier, leads to the assumption that this flow is local in origin and not derived from any distant source. Thus ... the losses and gains in flow of the Rio Grande in Rio Grande Canyon, except for the visible inflow of surface waters, are due to the local underground movement of water without regard to the underground movement of water in the San Luis Valley." Bryan's argument was based solely on inferences related to the geography and geology of the region.

Thus, the origin and characteristics of the west-side Rio Grande gorge springs has remained unstudied and undetermined, even though it represents a significant portion of the base flow of the upper Rio Grande in New Mexico. To our knowledge, our study is the first comprehensive assessment of the groundwater conditions of the Taos Plateau. Our approach is to integrate new and existing geologic, geophysical, hydrologic, and geochemical data in order to develop a conceptual model of the hydrogeologic system of the northern Taos Plateau.

Previous Work

Studies of the geology of the Taos County region have been reported in a variety of formats. A series of geologic quadrangle maps has been produced by the New Mexico Bureau of Geology & Mineral Resources (http://geoinfo.nmt.edu/publications/maps/geologic/ofgm/home.cfm), including recent maps of the Guadalupe Mountain quadrangle and quadrangles to the south (Fig. 1). A great variety of geologic and hydrogeologic topics are covered in the 2004 New Mexico Geological Society Guidebook (Brister et al., 2004), and by references therein. The 2007 Friends of the Pleistocene Field Trip Guidebook examined parts of the northeastern Taos Plateau (Machette et al., 2007). Grauch and Keller (2004) and Bankey et al. (2006) provided updated interpretations of regional geophysical studies of the southern San Luis Basin. USGS scientists are currently working on a major revision of the gravity model for the entire San Luis Basin.

Published literature on regional water resources includes a report on the water availability and water quality of Taos County (Wilson et al., 1978), a general water resource inventory of Taos County (Garrabrant, 1993), a surface water assessment of Taos County (Johnson, 1998), a summary of the groundwater geology of Taos County (Benson, 2004), a regional groundwater flow model related to the Taos Pueblo water rights settlement (Burck et al., 2004), a summary of the hydrology and water supply of the Taos valley (Shomaker and Johnson, 2005), and the Taos County Regional Water Plan (Daniel B. Stephens and Assoc., 2007).

Our current understanding of the geology of the Taos Plateau area is mostly based on the pioneering studies of the Taos Plateau volcanic field by Lipman and Mehnert (1975, 1979), Peterson (1981), Dungan et al. (1984, 1989), and recent unpublished geologic mapping by Ren Thompson of the USGS.

Previous published hydrogeology of the northern Taos Plateau area includes the following. Bliss and Osgood (1928) performed a seepage study on the Rio Grande between the Lobatos Bridge in Colorado and the Embudo gage. Bryan (1928) investigated possible groundwater connections between the San Luis Valley and the Rio Grande in New Mexico. Bryan (1938) summarized the geology and hydrogeology of the San Luis Basin, including a short section on the Taos Plateau. Winograd (1959) completed a major study of groundwater of the Sunshine Valley area, including an eastern strip of the northern Taos Plateau. Summers and Hargis (1984) reevaluated the work of Winograd (1959), and proposed an alternative hydrogeologic conceptual model. Coons and Kelly (1984) proposed a regional hydrogeologic conceptual model for groundwater/surface water flow in the San Luis Basin of New Mexico. Hearne and Dewey (1988) published a regional hydrologic analysis of the San Luis Basin of Colorado and New Mexico, including the Taos Plateau. Benson (2004) compiled water levels from drillers' records, and created a regional, contoured groundwater map of Taos County. Bauer et al. (2007) inventoried the springs of the Rio Grande gorge in Taos County.

Due to the importance of the aquifers, and the agricultural industry that depends on them, numerous geologic, hydrogeologic, and hydrologic studies have been published for the San Luis Valley of Colorado. Of particular interest to this study is the early USGS report by Siebenthal (1910) which suggested that the water gained by the Rio Grande above Embudo originates in the San Luis Valley and flows beneath the Taos Plateau until discharging as springs in the Rio Grande gorge. Therein, it was argued that increased irrigation in the San Luis Valley would actually increase the delivery of Colorado water into New Mexico.

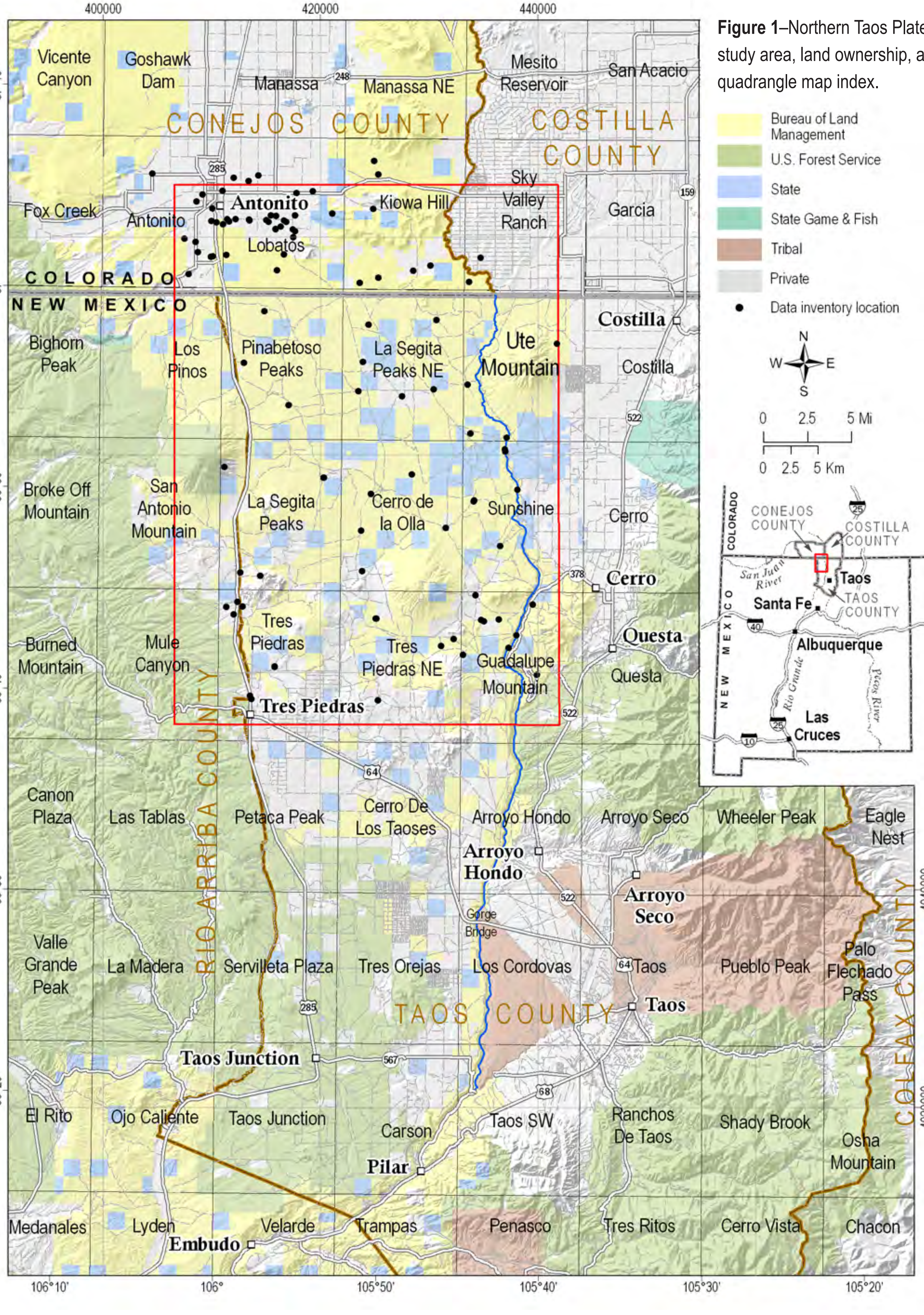

Figure 1–Northern Taos Plateau study area, land ownership, and quadrangle map index.

Purpose and Scope of the Current Study

The principle objective of this study was to characterize and interpret the shallow three-dimensional geology and hydrogeology of the northern Taos Plateau area and the Rio Grande gorge. It was beyond the scope of work to perform new geologic mapping of the Taos Plateau. Rather, the focus of this report was to compile existing hydrologic and geologic data, collect new hydrologic and geochemical data, and interpret it all in a geologic context.

Field work on the Taos Plateau was conducted by staff of the New Mexico Bureau of Geology & Mineral Resources between October 2007 and October 2009. Field data collection included locating all water wells in the study area, surveying their locations, and measuring water levels and sampling water from as many as possible (Fig. 2). The second phase of work included compiling geologic maps, interpreting existing geophysical data, and drawing hydrogeologic cross sections. During the final phase of the project, we analyzed the hydrologic and geochemical data, integrated these data with the geologic model, and developed a conceptual model of groundwater flow for the northern Taos Plateau.

The report contains seven detailed geologic cross sections and a regional geologic map, maps of surface drainages and closed basins, locations of inventoried wells, and data tables of well characteristics, water-level measurements, and results of geochemical sampling and laboratory analyses of well-water chemistry. It also contains interpretive maps of a regional potentiometric surface, the physical, chemical and isotopic characteristics of groundwater including temperature, distribution of dissolved ions and elements, and apparent ^{14}C, tritium (^{3}H), and chlorofluorocarbon groundwater ages. Interpretive plots of groundwater geochemistry provide additional insight into controlling hydrogeochemical processes, sources of groundwater, and groundwater flow paths. When integrated, these multiple data sets support a conceptual hydrogeologic model of the groundwater flow system.

This study has been undertaken in parallel with a major investigation of the springs in the Rio Grande gorge of northern New Mexico (Bauer et al., 2007). These studies advance understanding of the groundwater system in the northern Taos Plateau, and the interconnection of groundwater and surface water along the Rio Grande in northern Taos County.

Description of the Study Area

Geography—The Taos Plateau is a physiographic subdivision of the San Luis Basin of northern New Mexico and southern Colorado (Upson,

Figure 2–A typical water well location in the remote northern Taos Plateau.

1939). The plateau consists of the largely volcanic landscape south of the San Luis Hills that lies between the Rio Grande and the Tusas Mountains (Fig. 3). The Tusas Mountains represent the western flank of the Rio Grande rift, with peaks that exceed 11,000 feet in elevation. Near Antonito, the Taos Plateau physiographic province grades northward into the southwestern San Luis Valley.

The northern Taos Plateau study area (677 mi^2, 1753 km^2) extends northward from the line of large Pliocene volcanoes (Cerro Chiflo, Cerro de la Olla, Cerro del Aire, and No Agua Peaks) that lie between the Red River confluence and the village of Tres Piedras (Fig. 2). The eastern boundary is approximately the Rio Grande gorge, a steep-sided canyon that deepens from the state line southward to the Red River confluence. The western boundary of our area is approximately the west edge of the plateau, where the Tusas Mountains begin to rise. The northern boundary is just north of the town of Antonito, Colorado, and includes the southernmost San Luis Hills.

The San Luis Hills are a set of moderate-relief hills and mesas that trend northeastward across the middle of the San Luis Valley. The Rio Grande occupies a canyon cut through the San Luis Hills about 14 miles north of the state line. In New Mexico, the Rio Grande gorge separates the Taos Plateau from the piedmont slopes of the Costilla Plains, which rise gently eastward to join the Sangre de Cristo Mountains. Three named Rio Grande tributaries cross the Costilla Plains in the study area (Costilla Creek, Latir Creek, and the Red River). Both Costilla Creek and the Red River have carved deep canyons that are graded to the Rio Grande, although due to irrigation diversions on Costilla Creek, only the Red River exhibits perennial flow.

The Taos Plateau is a low-relief landscape that is punctuated by broad, high-relief volcanoes. The northern Taos Plateau is separated from the southern Taos Plateau by an impressive line of volcanic hills (Cerro Chiflo 8978 ft, Cerro de la Olla 9464 ft, Cerro Montoso 8655 ft, Cerro del Aire 9023 ft, and No Agua Peaks 9150 ft). The only other major peak in the study area is San Antonio Mountain (10,908 ft), which occupies the west-central part of the plateau. Most of the study area is a broad volcanic plain that slopes eastward from an elevation of about 8200 ft near highway 285 to about 7550 ft along the Rio Grande gorge rim, for an average topographic gradient of approximately 50 ft/mi.

Basin Geomorphology**—**The northern Taos Plateau is geomorphically remarkable due to the complexity of surface drainages and the scarcity of drainage integration of this 3 million-year-old landscape. This is well illustrated in a map of the surface-water drainage basins (or catchment areas) of the study area (Fig. 4). The catchment map was created by tracing the drainage divides between second-order streams, with the first-order stream being the Rio Grande. East of the Rio Grande, second-order streams such as the Red River and Costilla Creek have large watersheds and well-integrated systems of third-order streams. The geomorphology of the Taos Plateau is dramatically different. Two second-order stream systems do exist along the north and south edges of the study area: the Conejos River drainage to the north and the Arroyo Aguaje de la Petaca drainage to the southwest. Most of the study area (453 mi^2) consists of closed basins and poorly developed surface drainage systems. These basins can be divided into three types:

1) Closed basins such as the two large basins in the center of the plateau, and two small closed basins near No Agua Peaks and Punche Arroyo, cover 128 mi^2 of the study area. Both of the large basins originate on San Antonio Mountain. Along the eastern sides of the closed basins, there are areas near the gorge rim that actually drain westward, away from the Rio Grande. The closed basins only display running water during major rainstorms or extreme snowmelt events. Both of the large closed basins contain numerous, large playas, primarily in their eastern ends, which typically contain standing water following large rainstorms and local snowmelt events (Fig. 5).

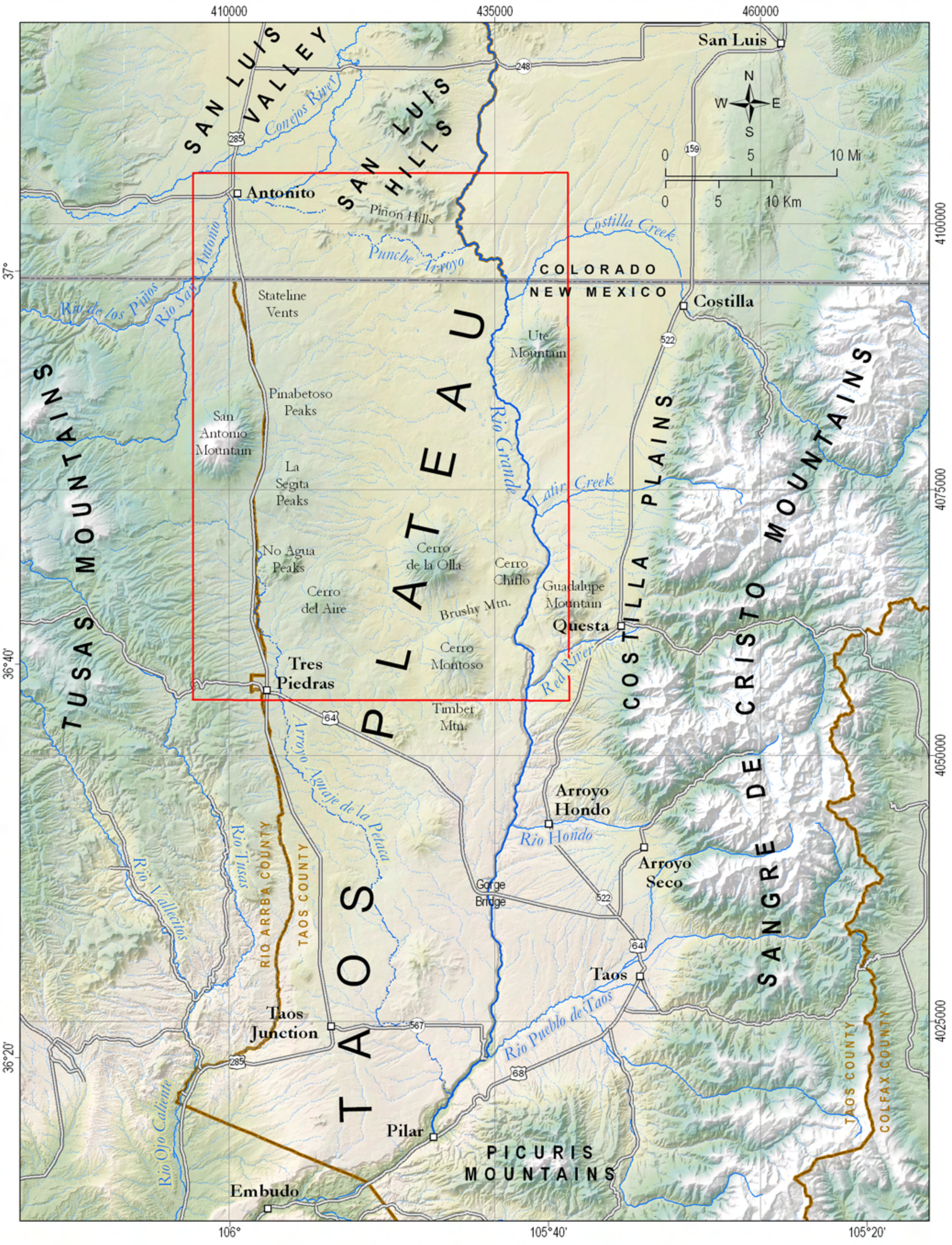

Figure 3–Physiographic features of the southern San Luis Basin, with study area outlined in red.

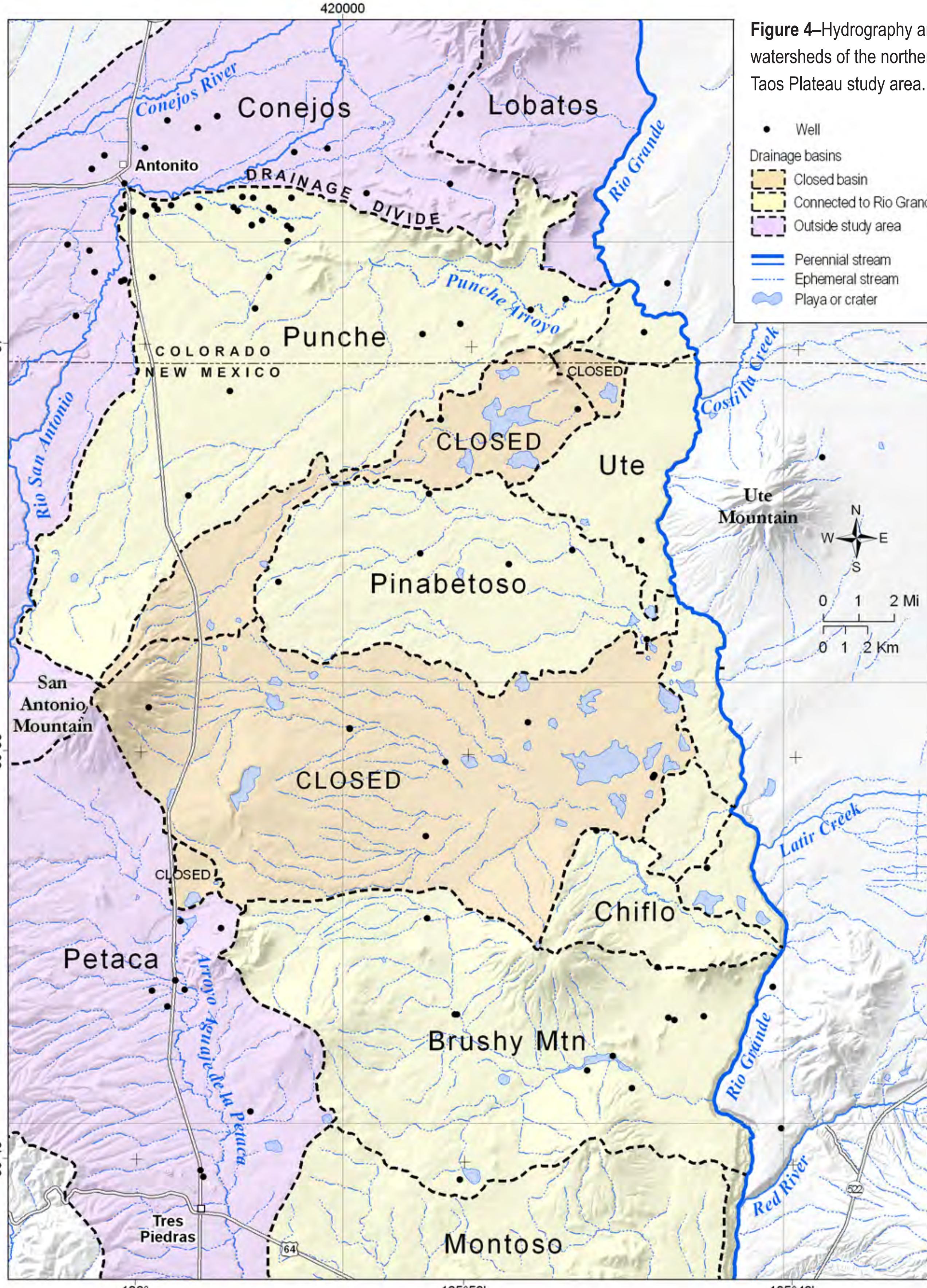

Figure 4–Hydrography and watersheds of the northern Taos Plateau study area.

2) Large basins with narrow outlets to the Rio Grande gorge cover 278 mi^2. From north to south, these catchments are labeled Punche, Pinabetoso, Chiflo, Brushy Mountain, and Montoso. The northern three basins taper dramatically to narrow, shallow canyons where they intersect the Rio Grande gorge. In all cases, the outlets are small canyons that hang well above the Rio Grande, in most cases hundreds of feet above the river. All are incised from 40 to 80 feet into the gorge rim. The Brushy Mountain drainage shares a 6-mile-wide border with the Rio Grande gorge, but the surface water outlet is a narrow canyon that is incised about 120 feet into the gorge rim. The open basins only display running water during major rainstorms or extreme snowmelt events. All of the open basins contain some small playas that typically contain standing water following large storm and melt events.

3) Small riverside catchments encompass 52 mi^2. Five relatively small second-order basins exist along the rim of the Rio Grande gorge. The largest of these, labeled Lobatos and Ute, are located to the north. Three smaller catchments are located to the south. These basins have poorly developed drainage systems. They contain some small- to medium-sized playas that contain standing water after large storm and/or melt events.

The Rio San Antonio, the only perennial stream in the study area, flows from the Tusas Mountains northward into Colorado in the northwestern corner of the study area, then joins the Conejos River in the San Luis Valley. The transition between the Taos Plateau and the San Luis Valley physiographic provinces is approximately coincident with a subtle, but highly significant, surface drainage divide that separates the Rio San Antonio drainage to the north from the Punche Arroyo drainage to the south (Fig. 4). From the Rio Grande, the drainage divide snakes westward along the Pinon Hills, with high relief to the north and south. At the western end of the South Pinon Hills, the divide plunges down to the low-relief valley floor along the southern perimeter of the Rio San Antonio watershed, then trends due west toward Antonito. At Antonito, the divide swings sharply south, paralleling Highway 285 until heading southwestward between the Rio San Antonio and San Antonio Mountain. The most remarkable aspect of this drainage divide is the extremely low relief between the two watersheds where it parallels the Rio San Antonio. According to the Lobatos 7.5-minute USGS topographic

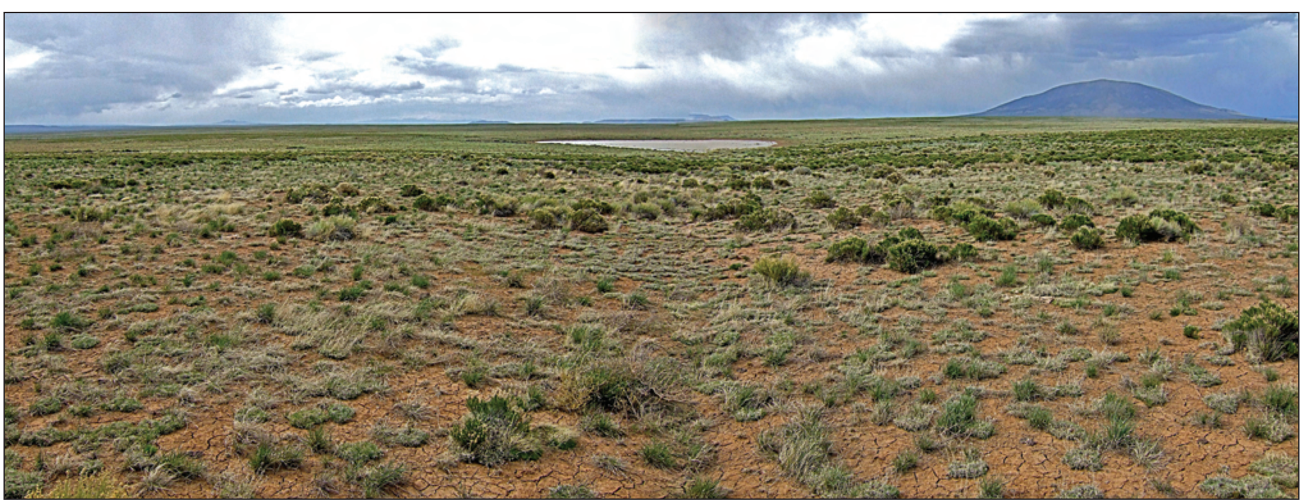

Figure 5–Small playa lake in a large closed basin north of Cerro de la Olla. Notice mud cracks in dry sediments in foreground, indicative of recent wetting. Ute Mountain is on the right skyline.

map, at Antonito the drainage divide separates the channel of the Rio San Antonio from the headwaters of Punche Arroyo by less than 10 feet of elevation.

In a qualitative sense, the Punche Arroyo drainage system is much better developed than it should be, considering its small, low-elevation watershed. We suspect that at some time in the recent geologic past, Punche Arroyo was attached to a considerably larger headwaters area, most likely the modern Rio San Antonio system. In such a scenario, the Rio San Antonio flowed down Punche Arroyo to the Rio Grande. Perhaps a delta or sediment plug in Pleistocene Lake Alamosa, combined with headward erosion of Punche Arroyo, resulted in the temporary capture of the Rio San Antonio. At some point, the Rio San Antonio was recaptured by the Conejos River system, creating the modern, ephemeral Punche Arroyo.

Land Status and Accessibility—The study area is composed mostly of BLM land with a checkerboard pattern of state-owned and private sections (Fig. 1). Private lands occupy much of the northern and southern borders of the area. Forest Service lands cover most of San Antonio Mountain, the Tusas Mountains near Tres Piedras, and the southeastern corner of the plateau. Most of the field area is accessible only by high-clearance vehicle along primitive BLM roads. Access from the south is provided by a dirt road north from just west of the Dunn Bridge near Arroyo Hondo. Access from the west is available on rough roads east of Highway 285 near San Antonio Mountain. Access from the north is provided by a good gravel road from Antonito through the San Luis Hills. Many of the roads on the northern Taos Plateau are difficult to traverse when wet, and when dry the roads are rough due to jagged volcanic rocks in great abundance.

II. METHODS

Data Used in This Investigation

The data used in this investigation include: published geologic map data, subsurface geologic data from water-well records and lithologic logs, depth-to-water and water quality data collected from Taos Plateau wells by the NMBGMR in 2008 and 2009, water quality data collected from local streams and Rio Grande gorge springs by NMBGMR in 2006 through 2009, and historical depth-to-water and water quality data from published and unpublished sources. Details about data sources, data measurement and analysis methods, site characteristics, sample collection, and sample analysis for these data are described below.

Geologic Maps and Cross Sections

The geologic map used in this study is a digital combination of the 7.5-minute quadrangles of the NMBGMR STATEMAP program, and where no quadrangle coverage exists, the geologic map in the 2004 NMGS Guidebook (Brister et al., 2004, Plate 2) or the 1:500,000 digital geologic map of New Mexico (Green and Jones, 1997) was used. The USGS has more detailed, preliminary quadrangle maps of the northern part of the study area, but they are not yet published.

We created seven new hydrogeologic cross sections for this study. The locations of sections were chosen to optimize hydrogeologic insights and maximize the number of measured wells that could be incorporated into the section lines. The topographic profiles were generated by ArcGIS software. All cross sections are vertically exaggerated by a factor of eight to better illustrate hydrologic and geologic details.

The surface geology was picked off of the geologic map, and geologic contacts that are hidden by surficial deposits were interpolated. Lithologic picks of volcanic rock versus sediment at each well were made using the lithologic logs on the available drillers' well records on file with the New Mexico Office of the State Engineer (NMOSE). The volcanic intervals were used as approximate guides for drawing the geologic units. In some cases, it was clear that the driller had generalized the minor lithologic variations encountered in the hole.

The configurations of the volcanic edifices were drawn based on a conceptual model of the geologic evolution of the Taos Plateau volcanic field. Most of the volcanic units in the study area have well-constrained radiometric ages, allowing us to portray their subsurface relationships with other volcanic units. Although the volcanic vents are shown with feeder dikes, it is likely that the numbers of dikes are greatly underestimated and their geometries are greatly oversimplified.

None of the drillers' logs differentiated between Servilleta Basalt and older volcanic units such as the Hinsdale Basalt. Although the depictions of these two units on the cross sections are based on the geologic maps and an understanding of the volcanic and sedimentary systems and geologic processes of the area, it is possible that the thicknesses of Servilleta and Hinsdale units are not accurately represented. For example, the upper basalt sequence shown as Servilleta basalt could actually represent both the Servilleta and Hinsdale units. Furthermore, the drillers' logs do not distinguish basalt from any of the dacitic or andesitic flows that make up most of the volcanic cones. It is certainly possible that unrecognized buried volcanoes exist in the study area.

The cross sections utilize all of the mapped faults known in the study area. However, due to the difficulty of mapping faults in such a volcanic landscape, we have certainly underrepresented the rift-related faults in the cross sections. Subsurface geologic structures were inferred in several places where surface geologic features and geophysical data (gravity and magnetic maps) were suggestive of buried faults and features.

Water Level Data

A major component of this study was measuring water levels in all accessible wells located on the northern Taos Plateau. A total of 40 wells were visited, field located with a handheld GPS device, and numbered with a TC-### designation (Table1). Between May 2008 and June 2009, water-level measurements were made in 21 wells using a 500–foot steel tape for pump-equipped wells, and a 650–foot electric meter for clear wells. Of these 21 wells, 19 are located in New Mexico and 2 are in Colorado. Two additional wells located east of the Rio Grande in the Bureau of Land Management Wild Rivers Recreation Area were measured in November 2010. Measurements were made to a repeatable accuracy of 0.01 feet. Water levels could not be measured at 17 of the 40 wells for one the following reasons: the well was abandoned and the casing had collapsed or had filled in with debris; the well casing was welded or locked shut; or the well was more than 500 feet deep and contained a pump. Five of these 17 wells had high-precision water-level measurements previously made by the USGS. Another 10 of the 17 wells had static water levels recorded on the NMOSE record, and two of the 17 wells had no water-level data of any type.

In addition to the 40 visited wells, other wells and well records were used along the southern and northern boundaries of the study area to add subsurface geologic and hydrologic control. All well records were evaluated for quality control. Some of the 10 southern water wells were previously inventoried by the Taos Soil & Water Conservation District (TSWCD) during their Taos County water well inventory (Benson, 2004). They are included in Table 1 with published TSWCD well numbers and located on figures with published coordinates. In all cases, well depth, water level, and screen interval were compiled from original well records. Although the GPS locations recorded by TSWCD staff are considered to be accurate, the static water level entries from driller's records are considered to be approximate.

Water levels from 26 northern wells were selected from the online databases of the Colorado Division of Water Resources (CDWR) and Colorado's Decision Support Services (CDSS). Because most of these wells are located in the San Luis Valley alluvial aquifer, rather than the Taos Plateau aquifer, they were selected with the following criteria: 1) total depth and water level are known; 2) total depth is more than 100 feet; and 3) the screened interval totals less than 60 feet in length.

Elevations of all wells were calculated in ArcGIS using the 10–meter DEM coverage and GPS-derived coordinates. Well and site information are presented in Table 1 for Taos Plateau wells, and in Table 2 for Colorado wells. Well and spring locations are shown in Figure 6, and original well records and field photos are attached in Appendix A. Well construction information, including well depth, screened (perforated) interval(s), and estimated yield are summarized in Table 1. Some wells are shown on the geologic cross sections. Several measured wells are of unknown construction, as the well records are unavailable.

Measured Versus Recorded Water Levels—Some measured water levels differed significantly from the static water level recorded by drillers on NMOSE well records (Table 1). In the 16 wells that yielded precise water levels and had recorded static water levels, the discrepancies with the recorded level ranged from -45 feet (measured level was lower than recorded level) to +120 feet (measured level was higher than recorded level). Water levels in 4 of the measured wells differed by more than 30 feet with those

Figure 6–Measurement and sample locations of wells and springs.

Table 1A–Taos Plateau well and site information.

Well number	Well name	NMOSE or CDWR well number	TSWCD well number	USGS site ID	Location UTM (m) Northing NAD83	Easting NAD83	Northing NAD27	Easting NAD27	Surface elevation (ft asl)	Use	Date drilled	Well depth (ft bls)	Sceen top (ft bls)	Sceen bottom (ft bls)	Yield (gpm)	Lith log	Site visit	Water level	Water sample	Well notes
TC-201	Cerrito Negro	RG-36732	TP-20		4064954	425081	4064747	425130	7661	STK	1956	354	335	345	10	x	x	x	x	Well log from Red Top Drilling.
TC-202	Abeyta	RG-36733	TP-16		4062420	431099	4062213	431149	7605	STK	1960	550					x	x		
TC-203	Brushy Mtn mine		TP-17		4063085	432249	4062878	432298	7579	IND	U	U					x	x		Inactive well in wellhouse on abandoned perlite mine at Brushy Mtn.
TC-204	Ezequiel	RG-51763	WG-16		4064876	436395	4064670	436444	7618	STK	1990	500	440	490	30	x	x	x	x	BLM file #5995.
TC-205	Ruil Brothers		WG-18	364812105460101	4073307	431521	4073100	431570	7641	ABAN	1955	345				x	x	x		No OSE record. Open hole 100 ft NW of WG-17. 3" pipe cut at ground level. Winograd 30/11/27/333.
TC-206	Abandoned		WG-12		4061619	433132	4061413	433181	7664	ABAN	1970	640					x			TSWCD info from owner. No records.
TC-207	Chiflo test hole 9-A		WG-14	364450105440801	4067094	434292	4066888	434342	7667	STK	1947	554				x	x	x		ACE, US Army, Chiflo dam-site test hole 9-A. Current owner Robert Ortega (Questa).
TC-208	Moeller/Rael		WG-15		4071608	436530	4071402	436580	7608	STK	1973	340	305	335	30	x	x	x	x	BLM file #4491. Drawdown test data on record. Re-entered by driller in late 1990s.
TC-209	Abeyta/Rael	RG-38563	WG-21b		4075717	434090	4075511	434140	7661	STK	1982?	400	355	400	10	x	x	x	x	BLM file #2222. Redrilled WG-21a in 1982 and again in 1992 to 400 ft. Cavern at 295 ft.
TC-210	Abeyta/Moeller abandoned		WG-21a	364940105442701	4075814	434137	4075608	434186	7661	STK	1955	370			30	x	x	x		BLM file #2222: open hole. USGS water level.
TC-211	Chiflo test hole R-11		WG-28	365504105465201	4086025	430411	4085818	430460	7608	STK	1947	323				x	x			USGS TSTHOL-R11. BLM allotment 590. ACE Chiflo dam-site test hole R-11. Open hole.
TC-212	Middlemist (Punche)	RG-45204	WG-20		4078218	428405	4078011	428454	7703	STK	1986	422	389	419	20+	x	x	x	x	BLM file #5815. Working well with big white tank on hilltop.
TC-213	Maestas (Ute Mtn test 2)		WG-34	365258105443701	4081974	433797	4081769	433846	7569	STK	1937	303				x	x	x	x	Probably same as Winograd 31/11/34/400. BOR Ute Mtn dam-site test hole 2.
TC-214	Blain Bagwell		WG-27	365524105445201	4086472	433556	4086266	433605	7589	STK	1989	U					x	x		USGS water level
TC-215	McGregor solar	RG-68500	WG-22		4076425	424662	4076220	424711	7677	STK	1926	400			20		x	x		May be same as Winograd 30/10/14/400 (TD=440' SWL=350').
TC-216	Moeller (new)	RG-85494			4073057	423767	4072852	423816	7720	STK	2005	540	520	540	60	x	x	x	x	
TC-217	Alire abandoned		WG-23	365038105533501	4077925	420318	4077720	420367	7923	STK	1953	616				x	x			Lith logs in Garrabrant (1993), BLM file #588, BLM file #1181.
TC-218	Alire (Bagwell S)				4077934	420310	4077729	420359	7923	STK	U	630					x		x	
TC-219	Sowards	RG-43600	WG-30	365830105464701	4092411	430675	4092204	430725	7671	STK	1954 2001	358 501	335	356	25	x x	x	x	x	Lith log in BLM file #2144 and Garrabrant (1993). Deepened in 2001 from 358 to 501 ft (well went dry)
TC-220	Llano	RG-89492			4091963	424450	4091756	424500	7720	STK	2007	430	402	422	18+	x	x	x	x	Well completion information from owner
TC-221	No Agua perlite mine		TP-37	364543105572901	4068880	414471	4068674	414521	8383	IND	1971	1160	906	>1005		x	x	x	x	Perlite mine. Well log derived from down-hole camera. USGS water level
TC-222	Bagwell N		WG-25	365623105583501	4088493	412989	4088288	413038	8114	STK	1955	685				x	x	x	x	BLM file #1967. Deepened from 655' to 685'.
TC-223	Stateline	RG-50361	WG-32		4093238	414876	4093031	414926	7989	STK	1990	500	450	490	30	x	x	x	x	
TC-224	Shawcroft west	RG-75708	WG-31		4084584	417086	4084379	417135	8123	STK	U	900					x		x	Drilled under permit RG-31444 in wrong place. Existing well has new #. Pump ~900 ft.
TC-225	Chiflo test hole 7-A		WG-13	364336105434701	4064807	434773	4064607	434832	7594	TEST	1946	362				x	x			ACE Chiflo dam-site test hole 7-A. Open 2" casing that sticks up in pit near log cabin.
TC-226	Shawcroft east		WG-33	365458105510301	4085871	423516	4085666	423565	7746	STK	U	410					x		x	Winograd well 31/10/23/110 (TD=410' SWL=390'). To be redrilled in 2010.
TC-227	Harborlite perlite mill, CO	CO-03286F			4101396	410470	4101191	410519	7897	IND	2002	228	202	228	70	x	x		x	Colorado Well Permit #3286F.
TC-229	Crow	RG-37144	WG-29	365444105484701	4085394	427538	4085189	427587	7638	STK	1951	363			100		x	x	x	BLM allotment 578.
TC-230	Little Page	RG-37146	WG-26	365624105511301	4088577	423928	4088372	423977	7749	STK	1961	480			100?	x	x	x		Well serviced in 2007. Lith log from owner.
TC-231	Twin Lakes, CO	CO-44477			4096284	425330	4096078	425379	7642	STK	1971	254	239	254	2.5	x	x	x		CO well permit #44477.
TC-232	Lobatos, CO				4095908	433672	4095702	433721	7583	STK	1971	350					x	x		Inactive well on BLM Riverside Allotment, near Rio Grande, south of Punche Arroyo. Large tan vertical tank on concrete pad.
TC-233	San Antonio Mtn	RG-24777			4078883	411193	4078678	411242	9246	DOM	1920	50					x	x	x	Hand-dug well at last house at development on east side of San Antonio Mtn.
TC-234	Schofield	RG-34987	TP-02		4069187	412641	4068982	412690	8220	STK	1980	650	600	645		x	x		x	Warm water well.
TC-235	Punche Valley, CO				4097420	430130	4097214	430179	7574	IND	U	U					x			Inactiave well on large abandoned farm complex with concrete footings.
TC-236	Chiflo test hole R-12A, CO				4096932	428536	4096726	428585	7580	TEST	1946	305				x	x			Corps of Engineers, U.S. Army, Chiflo dam-site test hole R-12A.
TC-237	Saritas, CO	CO-112858A			4096990	416015	4096785	416064	7865	STK	1982	337	297	337	20	x	x	x		CO well permit #112858A. Well head in locked steel box. USGS water level
TC-238	Alta Lake, CO	CO-112859A			4098418	411370	4098213	411419	7941	STK	1982	333	313	333	15	x	x	x		CO well permit #112859A. Well head in locked steel box. USGS water level
TC-239	West of Twin Lakes, CO	CO-44478			4095838	423625	4095633	423674	7687	STK	1971	280	265	280	20	x	x			CO well permit #44478.
TC-240	BLM Chiflo CG	RG-17985	CER-24		4066219	439516	4066014	439565	7500	GOV	1972	415	391	410	56	x	x	x	x	
TC-241	Tom Bradley	RG-27193			4066042	411336	4065837	411385	8276	DOM	1976	730	700	730	15	x				
TC-242	Quinlan Ranches	RG-37145	TP-19	364603105511101	4069322	423829	4069117	423878	7739	STK	1967	463			17			x		USGS water level
TC-243	Sherri Anderson	RG-63610	TP-21		4060566	415803	4060361	415852	8062	DOM	1996	960	900	920	1	x		x	x	Water sample collected by TSWCD 9/28/2002
TC-244	George Smith	RG-66248	TP-04		4066076	412834	4065871	412883	8207	DOM	1997	700	630	690	20	x				
TC-245	Jack Kessler	RG-71541			4064718	435048	4064513	435097	7596	STK	2003	430	400	430	7	x				
TC-246	Carl Bradley	RG-72733	TP-03		4066506	412397	4066301	412446	8201	DOM	2000	860	800	860	35	x			x	Water sample collected by TSWCD 11/30/2004
TC-247	Harold Hartell	RG-80377			4065328	412039	4065123	412088	8210	DOM	2004	800	760	800	25	x				
TC-248	Jessie Medina	RG-83402			4057470	425315	4057265	425364	7861	DOM	2005	880	760	880	20	x				
TC-249	BLM Wild Rivers VC		CER-23	364057105401701	4059803	439907	4059598	439956	7590	GOV	1972	546	513	536			x	x	x	
TC-250	Ken Schwartz	RG-50184	TP-10		4057896	413544	4057691	413593	8117	DOM	1989	780							x	Water sample collected by TSWCD 11/11/2005
TC-251	Ken Schwartz	RG-54393	TP-11		4057596	413673	4057391	413722	8087	DOM	1991	780							x	Water sample collected by TSWCD 11/30/2004
TC-252	RC Starks	RG-66404			4090235	441775	4090029	441824	7719	STK	1997	362								WATERS database download

Table 1B—Taos Plateau well and site information

Well number	Well name	Well depth (ft bls)	Measured depth to water				Driller's static water level			Aquifer information			
			Depth (ft bls)	Date	Elevation (ft asl)	Measured by	Depth (ft bls)	Date	Elevation (ft asl)	Water bearing formation	Water bearing interval (ft bls)	Aquifer description	Aquifer notes
TC-201	Cerrito Negro	354	340.73	05/12/08	7320	NMBGMR	335	1956	7326	Tao	335-340	andesite	Well was blowing air when visited on 5/12/08.
TC-202	Abeyta	550	299.63	05/12/08	7305	NMBGMR	400	1960	7205	Tam	>300		
TC-203	Brushy Mtn mine	U	425.06	06/05/09	7154	NMBGMR		unk		Th	>425		Water bearing formation inferred from regional geology
TC-204	Ezequiel	500	435.20	05/12/08	7183	NMBGMR	390	1990	7228	Tb	435-495	basalt	
TC-205	Ruil Brothers	345	310.56	08/16/55	7330	USGS	310	1955	7331	Tao	310-330	andesite	Winograd stated that water rose 23 ft in hole.
TC-206	Abandoned	640						1970					
TC-207	Chiflo test hole 9-A	554	347.85	05/13/08	7319	NMBGMR	342	1947	7325	Tao	366-485	andesite, locally fractured	
TC-208	Moeller/Rael	340	293.20	05/13/08	7315	NMBGMR	302	1973	7306	Tb	310-335	fractured basalt	Drawdown test data on record.
TC-209	Abeyta/Rael	400	348.68	05/13/08	7312	NMBGMR	355	1982?	7306	Tb	355-380	basalt cavern	Driller hit cavern at 295 ft; no cuttings return 295-400 ft.
TC-210	Abeyta/Moeller abandoned	370	333.02	01/11/55	7328	USGS	333	1955	7328	Tb	345-350	basalt	Water in crevices at 345-350 ft, water rose, blowing air. (Winograd)
TC-211	Chiflo test hole R-11	323					276	1947	7332	Tb	276-323	basalt	
TC-212	MIddlemist (Punche)	422	390.51	05/14/08	7312	NMBGMR	387	1986	7316	Tb	400-410	fractured basalt	
TC-213	Maestas (Ute Mtn test 2)	303	246.02	05/14/08	7323	NMBGMR	247	1937	7322	Tb			
TC-214	Blain Bagwell	U	257.75	10/20/89	7331	USGS	258	1989	7331	Tb			
			257.87	12/01/88	7331	USGS							
TC-215	McGregor solar	400	357.14	05/14/08	7320	NMBGMR	380	1926	7297	Tb			Lost circulation 280-540'
TC-216	Moeller (new)	540	401.10	05/14/08	7319	NMBGMR	440	2005	7280	Tb?	400-540		
TC-217	Alire abandoned	616					584	1953	7339	Tsf	585-616	black sand, conglomerate	
TC-218	Alire (Bagwell S)	630					600		7323	Tsf			TD and SWL from owner
TC-219	Sowards	501	348.62	06/03/09	7322	NMBGMR	340	1954	7331	Tb or Th	≥350	basalt	Logs and SWL from BLM file #2144
			346.26	05/15/08	7325	NMBGMR							
TC-220	Llano	430	389.94	05/15/08	7330	NMBGMR		2007		Tsf	402-422	brown clay-sand	Log from owner
TC-221	No Agua perlite mine	1160	727.00	06/14/04	7656	USGS				Th, Tsf			Water level from 2004 during driller's work on well casing.
TC-222	Bagwell N	685	599.40	05/15/08	7515	NMBGMR	640	1955	7474	Th	630-635 640-655	cinders, sand	
TC-223	Stateline	500	436.30	05/16/08	7553	NMBGMR	435	1990	7554	Tb	440-490	fractured basalt	
TC-224	Shawcroft west	900								Th?			Blowing air strongly when visited on 5/16/08.
TC-225	Chiflo test hole 7-A	362					310	1946	7284	Th	321-362	fractured volcanic and silt/sand	
TC-226	Shawcroft east	410					390		7356				
TC-227	Harborlite perlite mill, CO	228					202	2002	7695	Tsf	202-228	gravel, boulders	Driller's SWL used as control (Fig. 15)
TC-229	Crow	363	315.40	06/04/08	7323	NMBGMR	337	1951	7301	Tb			Reportedly hit water at 330 ft.
			311.00	01/01/51	7327	USGS							
TC-230	Little Page	480	411.44	06/04/08	7338	NMBGMR	400	1961	7349	Tsf	430-440	cinders	USGS measured WLs in 1988 and 1989. Poorly performing well.
			414.40	10/20/89	7335	USGS							
TC-231	Twin Lakes, CO	254	240.86	06/03/09	7401	NMBGMR	231	1971	7411	Tb	240-254	basalt	
TC-232	Lobato, CO	350	265.77	06/04/09	7317	NMBGMR				Tsf	265-350		Water bearing formation inferred from regional geology
TC-233	San Antonio Mtn	50	19.23	06/04/09	9227	NMBGMR	45	1920	9201	Td	20-50	dacite flow and talus	Perched aquifer on San Antonio Mountain; sample taken with bail bucket.
TC-234	Schofield	650					570	1980	7650	Tr	585-645	perlite	Driller's SWL used as control (Fig. 15)
TC-235	Punche Valley, CO	U					dry			Th			When visited in 2008, well was dry and blowing cold air.
TC-236	Chiflo test hole R-12A, CO	305					204	1946	7376	Th		basalt, sand, clay	Perched water tables at 99 ft and 107 ft; 1946 water level used as control (Fig. 15)
TC-237	Saritas, CO	337	293.74	10/01/82	7571	USGS	297	1982	7568	Tsf Tb	297-337	sand, basalt	
TC-238	Alta Lake, CO	333	262.08	10/01/82	7679	USGS	269	1982	7672	Tsf	269-333	sand, gravel	
TC-239	West of Twin Lakes, CO	280					265	1971	7422	Tb	265-280	basalt	
TC-240	BLM Chiflo campground	415	342.09	11/12/10	7139	NMBGMR	344	1972	7156	Tdg	365-395	fractured dacite	Guadalupe Mtn dacite
TC-241	Tom Bradley	730					700	1976	7576	Th	720-730	volcaniclastic	
TC-242	Quinlan Ranches	463	415.75	12/02/88	7323	USGS	418	1967	7321	Tv?		unknown volcanics	
TC-243	Sherri Anderson	960					560	1996	7502	X	900-910	alteration or fault zone	In Precambrian granitic basement rocks
TC-244	George Smith	700					619	1997	7588	Tr	630-650	perlite	
TC-245	Jack Kessler	430					400	2003	7196	Tsf	400-430	sand	Sediment underlying Tb, Servilleta Basalt
TC-246	Carl Bradley	860					687	2000	7514	Th	800-860	basalt and cinders	
TC-247	Harold Hartell	800					661	2004	7549	Th	760-800	basalt	
TC-248	Jessie Medina	880					620	2005	7220	Tb	700-880	basalt	
TC-249	BLM Wild Rivers visitor center	550	485.35	11/12/10	7103	NMBGMR	487	1972	7103	Tv?	487-546	unknown volcanics	
TC-250	Ken Schwartz	780								X			
TC-251	Ken Schwartz	780								X			
TC-252	RC Starks	362					250	1997	7469	Tdu	<362	Ute Mountain dacite	

Table 2–Colorado well and site information.

Site information									Location UTM (m)									Measured depth to water				Driller's static water level			
Well number	Well name	CO DWR ID	RGDSS ID	USGS site ID	Use	Date drilled	Well depth (ft bls)	Surface elevation (ft asl)	Northing NAD83	Easting NAD83	Northing NAD27	Easting NAD27	Screen top (ft bls)	Screen bottom (ft bls)	Yield (gpm)	Lith log	Water quality	Depth (ft bls)	Date	Elevation (ft asl)	Meas. by	Depth (ft bls)	Date	Elevation (ft asl)	Well and aquifer notes
CO-01	ADAMSON GERALD K	95443A			DOM	1977	110	7927	4103321	408616	4103116	408665	90	110	15	x						94	1977	7833	Replaced 80' well drilled in 1920
CO-02	RAEL MIKE A	97665A			STK	1979	110	7795	4102046	415459	4101840	415508	100	110	15	x						91	1979	7704	Replaced 20' well.
CO-03	CASIAS JASPER	245050			STK	2003	120	7766	4102019	417671	4101814	417720	100	120	60	x						45	2003	7721	
CO-04	MONDRAGON FRED M	33191			DOM	1965	125	7910	4103935	409188	4103730	409237	90	125	20	x						45	1965	7865	
CO-05	PEREA FRED	103329			DOM	1979	136	7789	4102009	415947	4101804	415996	126	136	15	x						107	1979	7682	
CO-06	CO BOARD OF LAND COMMISSIONERS	40794			STK	1970	140	7808	4102212	421083	4102007	421132	128	140	5	x						128	1970	7680	
CO-07	T-BONE RANCH & HAMILTON W B	252RN	NA03301020CCB	370453105543401	DOM	1952	161	7743	4104245	419309	4104039	419358	82	161	30			60.12	01/22/82	7683	CDWR	49	1952	7694	
CO-08	DEHERRERA PETE L	213769A			DOM	1993	162	7766	4100040	417505	4099834	417554	122	162	15	x						98	1993	7668	
CO-09	COLORADO WATER CONSERVATION BOARD	229399	RGDSSP12		MON	2000	183	7828	4101627	413435	4101422	413484	153	173		x		160	01/01/07	7668	CDWR				NA03300934CB
CO-10	SCIVALLY KENNETH EUGENE	266464			DOM	2006	200	7805	4102645	424864	4102440	424913	160	200	15	x						117	2006	7688	
CO-11			NA03200901BBB	370300105564501	U	U	222	7789	4100778	415871	4100573	415920					x	102.59 90.28	01/22/82 02/17/70	7686 7698	USGS				Confined (USGS).
CO-12	BROYLES DAVID E	53472A			DOM	1980	223	7848	4101670	412215	4101465	412264	213	223	25	x						178	1980	7670	
CO-13			NA03200912ACC	370142105561101	U	U	230	7782	4098427	416662	4098222	416711					x	216.30 216.06	01/22/82 12/14/81	7566 7566	USGS				Confined (USGS).
CO-14	GREFCO INC/GREAT LAKES CARBON CORP	2726F			IND	1960	235	7887	4101499	409965	4101293	410014	200	235	80	x						200	1960	7687	
CO-15	BUREAU OF LAND MANAGEMENT	40223			STK	1970	250	7936	4107020	424945	4106814	424994	233	250	20	x						200	1970	7736	
CO-16	HAMILTON W B & T BONE RANCH	11509R	NA03301019CCD	370440105553001	IRR	1952	251	7756	4104082	417799	4103876	417848	220	251	900			62.90 61.3	01/20/69 02/17/70	7693 7695	USGS	67	1952	7689	Confined (USGS).
CO-17			NA03300914CCC	370538106574901	U	U	255	7799	4105724	414315	4105519	414364						107.87 107.88	01/22/82 12/16/81	7691 7691	USGS				Confined (USGS).
CO-18	CASIAS JOE E	37857			STK	1969	265	7976	4099894	407519	4099689	407568	235	265	10	x						40	1969	7936	
CO-19	BARELA LUCINDA	250323			DOM	2005	275	7920	4099612	408512	4099407	408561	255	275	7	x						215	2005	7705	
CO-20	COLORADO AGGREGATE COMPANY	170577			COM	1993	277	7881	4101198	411061	4100993	411110	232	272	15.78	x						190	1993	7691	
CO-21			NA03300922ACC	370520105582501	U	U	278	7815	4105179	413420	4104974	413469						117.00	02/21/70	7698	CDWR				Confined (USGS).
CO-22			NA03300921CCC	370450106000201	U	U	293	7867	4104279	411016	4104074	411065						181.10 181.75	01/22/82 12/03/81	7686 7686	USGS				Confined (USGS).
CO-23	DURAN ALBERT P	34869			DOM	1968	304	7966	4096650	407898	4096445	407947	264	304	10	x						260	1968	7706	
CO-24			NA03300814CCC	370540106042501	U	U	325	7986	4105891	404540	4105686	404589						117.50 123.5	02/19/70 06/24/69	7868 7862	USGS				Confined (USGS).
CO-25	US BUREAU LAND MGMT	121934	NA03301014DDD	370542105501501	STK	1982	337	7838	4105812	425335	4105607	425384	284	337	20	x		136.00	10/20/82	7702	CDWR				Confined (USGS).
CO-26	DEHERRERA PETE	10472F	NA03201066BBB	370257105553901	IRR	1966	225	7766	4100599	417661	4100393	417710	120	225	2200	x	x	84.56	01/22/82	7681	CDWR	100	1966	7666	Confined (USGS).
CO-27a	BROYLES TOLIBER B	9490F	NA03300933CAB	370326105594301	IRR	1965	279	7858	4101475	411594	4101269	411643	60	279	1300	x		174.38 174.7	01/22/82 12/15/81	7683 7683	USGS	170	1965	7688	Confined (USGS).
CO-27b	BROYLES TOLIBER B	9490F	NA03300933CAB2	370326105594302	U		235	7858	4101475	411594	4101269	411643					x								2nd well at same location: CO-28a, [illegible]
CO-28	POTTS RICHARD & POTTS BETTY J	10153F	NA03300935DBB	370324105571801	IRR	1965	225	7799	4101426	415239	4101221	415288	75	225	2200	x	x	116.68 117.1	01/22/82 12/14/81	7682 7681	USGS	64	1965	7735	Confined (USGS).
CO-29	DEHERRERA PETE	6747F	NA03300936DBB	370324105561201	IRR	1965	223	7776	4101415	416863	4101210	416912	80	223	2000	x	x	93.45 93.83	01/22/82 12/15/81	7682 7682	USGS	90	1965	7686	
CO-30				370323105582201	U		259	7825	4101570	413507							x								
CO-31	PETER MIDDLEMIST	10550F			IRR	1969	430	7841	4105514	412036	4105309	412085	80	280	2500	x						80	1969	7761	
CO-32	MEDINA RAY	33587			DOM	1968	50	7923	4098648	408729	4098442	408778	35	50	20	x						18	1968	7905	
CO-33	MONTOYA ALFREDO	254624			DOM	2004	300	7946	4098276	410096	4098070	410145	280	300	15	x						240	2004	7706	
CO-34	SANDOVAL AVELINO	25724			DOM	1965	250	7930	4098215	409938	4098009	409987	230	250	15							234	1965	7696	
CO-35	CRAVEN WELL		CB00107524CCA	370130105442501	STK	<1965	310	7560	4098143	434733								233.00	7/1/05	7327	USGS				Water-level record 1968-2009

noted on the well record. Possible reasons for these discrepancies include seasonal variations in water levels, long-term changes reflecting differences in recharge between wet and dry cycles, or inaccurate measurement or recording by the well driller. The latter may be due to measuring the water level before a static water level was reached in a newly drilled well. There are no obvious geographic patterns in the variations between water levels measured in this study and those recorded by the well drillers.

Contouring Water Levels—ArcGIS software was used to plot the well locations and water-level elevations. Contours of groundwater elevation data were drawn by hand and digitized. The density of water-level control points was insufficient to statistically interpolate elevation contours. Inherent in the contouring of regional water-level measurements are the assumptions that groundwater flow is horizontal, the measurements are from a single aquifer, and the hydraulic head does not vary with depth. In general, these assumptions were met by the regional water-level data collected in this study.

Some water-level elevations are from wells with multiple screened intervals, and thus are not point measurements of hydraulic head. Such data represent a vertical average of the hydraulic head over some aquifer interval rather than at a discrete point in the aquifer. With these facts, and the variation in data quality, in mind, water-level elevation contours were controlled primarily by measured water levels rather than recorded and were not forced to fit every water-level control point.

The 21 water levels measured between May 2008 and June 2009, and in November 2010 were used as point control for water-level elevation contours on the Taos Plateau in New Mexico. Static water levels from well records did not provide adequate control for the contoured surface in New Mexico. In Colorado, we used 2 measured water levels from wells located south of the San Luis Hills, and 26 recorded water levels from files of the Colorado Division of Water Resources. Ten of these water levels are high-precision measurements made by the USGS in the month of January between 1969 and 2007. The remaining 16 measurements are static water levels from driller's records, taken between 1960 and 2005. Contours are dashed where approximate and queried where inferred.

Geochemical Methods

Groundwater samples were collected by NMBGMR from 21 wells on the northern Taos Plateau, six springs in the Rio Grande gorge, and stream flow from the Rio San Antonio and the Rio Grande. Samples were analyzed for major and minor ion and trace element chemistry, oxygen and hydrogen isotopes, and field measurements of specific conductance, dissolved oxygen, pH and temperature. Select sites were also sampled for measurement of carbon isotopes (^{14}C and $^{13}C/^{12}C$ ratio), tritium (^{3}H), and chlorofluorocarbon (CFC) recharge ages. Six tributary streams flowing from the northern Sangre de Cristo Mountains were sampled for oxygen and hydrogen isotopes ($^{18}O/^{16}O$, $^{2}H/H$ and ^{3}H). Data for ion and trace element chemistry from four wells on the Taos Plateau were compiled from the TSWCD database. Limited major ion data from seven wells in southern Colorado near the New Mexico border were also compiled from the USGS National Water Information System (NWIS) database. Well locations and information are provided in Figure 6, Table 1 (wells sampled during this study), and Table 2 (data compiled for Colorado wells). Details about site characteristics, sample collection, and sample analysis for these data are discussed below.

Sample Collection and Analysis—Groundwater samples were collected from wells on the Taos Plateau in May-June 2008 and June 2009. Two wells east of the Rio Grande were sampled in November 2010. Sampled well types include stock and industrial wells equipped with dedicated submersible pumps. One bailed sample was collected from a shallow, hand-dug, domestic well on San Antonio Mountain. Sample depths ranged from 34 to over 950 feet with a median of 390 feet. Grab samples of stream flow from the Rio San Antonio and Rio Grande were taken in June 2008 and September 2009.

During the fall and spring of 2006-2007, water samples were collected from six springs that discharge from the Taos Plateau aquifer along the west side of the Rio Grande gorge. These sample events were conducted as part of a study of the gorge springs, but chemical data are interpreted here in the context of discharge from the Taos Plateau aquifer. Site and sample information for stream and spring samples are provided in Table 3. Chemical data for all well, spring and stream samples are presented in Table 4. Hydrogen, oxygen and carbon isotope data for well, spring, and stream waters are provided in Table 5. CFC data and recharge ages for wells and springs are presented in Table 6. Sample collection forms and laboratory data are given in Appendix B. The following sections describe the sampling and analytical methods performed.

Field Parameters—Groundwater discharge temperature, specific conductance (SC), pH and dissolved oxygen (DO) were measured prior to sampling using a YSI 556 multi-probe system. The probe has a rated accuracy of 0.15 °C for temperature, 0.5 percent for SC, 0.2 units for pH, and 2 percent for DO. The probe was calibrated prior to each field deployment according to the manufacturer's instructions. For springs, field parameters were measured in the spring pool. For wells, field parameters were monitored continuously during the well purge in a bucket filled with discharge water. Sample collection was initiated following parameter stabilization. Between three and six bore-hole volumes of water were extracted during purge and sample collection.

Table 3–Site and sample information for springs and streams of the Taos Plateau region.

Site and sample information			Location UTM (m)					Chemistry Data Collected					
Site number	Spring or stream name	Site description	Elev (ft asl)	Northing NAD83	Easting NAD83	Northing NAD27	Easting NAD27	Field	General chem	SI	^3H	CFC	^{14}C
TS-8	Bear Crossing	Large spring in zone that discharges beneath boulder field on west bank.	7136	4063426	438022	4063219	438072	x	x	x	x		
TS-14	Cow Patty W	Small spring discharging beneath fractured basalt, just above river, west bank, downstream from Cow PattyTrail.	7388	4081577	437135	4081370	437184	x	x	x	x		x
TS-16b	North Big Arsenic 2	Largest spring set in North Big Arsenic zone; large discharge well above east bank	6818	4059853	438429	4059647	438478	x	x	x	x		
TS-17	Little Arsenic	Small spring near path above east bank	6732	4058447	438678	4058240	438728	x	x	x	x		
TS-61	Felsenmeere	Very large spring discharging from 2-m wide zone from under basalt boulders.	7057	4062267	437309	4062062	437358	x	x	x			x
TS-71	Sunshine	Large spring discharging from river gravels at base of boulders on west bank	7282	4080507	436962	4080300	437011	x	x	x	x	x	x
TS-72	Sunshine Trail W	Small spring discharging from base of basalt at top of river terrace, west bank	7282	4076798	438133	4076592	438183	x	x	x	x		x
TS-113	Lava Tube	Very large spring discharging from from crater in river bed.	7285	4080326	437001	4080120	437052	x	x	x	x	x	x
TS-114	Rio Grande above Lava Tube spring	Sample site along east bank of river 20 m above	7285	4080366	437000	4080160	437048	x	x	x			
TC-228	Rio San Antonio at Antonito	Sample site upstream of Hwy 285 bridge, north bank; collected grab sample from current, beneath surface	7887	4102657	410091	4102452	410140	x	x	x	x		
Cost-2	Rio Costilla	Under NM-196 bridge near Amalia.	8179	4086028	460238	4085822	460287			x	x		
Latir	Latir Creek	Above head gate on Latir Creek, on Latir Ranch.	8245	4076023	451073	4075817	451122			x	x		
Cabr	Cabresto Creek	In canyon, at head gate near road.	7753	4065042	449551	4064836	449600			x	x		
Red	upper Red River	Above Ranger Station and gage where tailings pipes cross river at head gate.	7484	4061947	449698	4061741	449747			x	x		
Hondo	Rio Hondo	50 m above gaging station where Hondo Canyon exists mountain fromt.	7661	4044202	450186	4043997	450235			x	x		
Seco	Rio Seco	Near headgate of Temporalis ditch, in Seco Canyon past the mountain front.	8222	4041619	452076	4041414	452125			x	x		

Table 4A—Taos Plateau chemistry data.

Site and sample information								Field parameters					General chemistry						
Site number	Site name	Site type	Analyzing lab	Lab number	Sample date	Sample depth* (ft bls)	Mean surface temperature (°C) **	Temp (°C)	Temp (°F)	SC (µS/cm)	DO	pH	Lab pH	Lab SC (µS/cm)	TDS	Total Anions (meq/L)	Total Cations (meq/L)	Charge balance (% diff)	Water Type
TC-201	**Cerrito Negro**	well	NMT		5/12/08	348	U	12.9	55.2	205	3.6	7.8	U	U	U			U	U
TC-204	**Ezequiel**	well	NMBGMR	08-0650	5/13/08	465	6.8	17.0	62.6	236	3.4	8.4	7.8	255	173	2.44	2.40	-0.7	Na-Ca-HCO3
TC-208	**Moeller/Rael**	well	NMBGMR	08-0651	5/13/08	320	6.8	15.0	59.0	340	3.5	8.5	8.1	375	231	3.43	3.31	-1.7	Na-HCO3-Cl
TC-209	**Abeyta/Rael**	well	NMBGMR	08-0652	5/14/08	378	6.6	18.0	64.4	315	2.6	8.6	8.2	345	216	3.15	3.08	-1.1	Na-HCO3-Cl
TC-212	**Middlemist**	well	NMBGMR	08-0653	5/14/08	404	6.5	15.2	59.4	184	2.9	8.5	8.0	250	146	2.01	1.95	-1.5	Ca-Mg-Na-HCO3
TC-213	**Maestas**	well	NMBGMR	08-0733	6/3/08	274	6.9	15.3	59.5	226	5.4	8.2	8.0	240	174	2.41	2.39	-0.4	Ca-Mg-Na-HCO3
TC-216	**Moeller**	well	NMBGMR	08-0654	5/14/08	530	6.5	17.7	63.9	186	3.2	8.3	8.0	230	158	2.05	1.96	-2.2	Ca-Mg-Na-HCO3
TC-218	**Alire**	well	NMBGMR	08-0734	6/3/08	600	5.9	19.8	67.6	212	4.7	8.1	8.1	220	169	2.25	2.32	1.5	Mg-Ca-Na-HCO3
TC-219	**Sowards**	well	NMBGMR	09-0404	6/3/09	345	6.6	18.1	64.5	166	7.6	8.1	8.2	175	148	1.79	1.85	1.7	Ca-Na-Mg-HCO3
TC-220	**Llano**	well	NMBGMR	08-0656	5/15/08	412	6.5	15.2	59.4	158	3.0	8.5	8.1	200	132	1.70	1.62	-2.4	Ca-Na-HCO3
TC-221	**No Agua Mine**	well	NMBGMR	08-0657	5/15/08	956	4.6	31.0	87.8	236	2.6	7.3	7.4	260	196	2.43	2.41	-0.5	Ca-Mg-HCO3
TC-222	**Bagwell N**	well	NMBGMR	08-0735	6/3/08	642	5.4	19.5	67.1	240	5.3	8.1	7.9	245	202	2.53	2.56	0.7	Ca-Na-Mg-HCO3
TC-223	**Stateline**	well	NMBGMR	08-0658	5/16/08	470	5.7	12.8	55.0	164	3.5	8.1	7.7	190	132	1.76	1.70	-1.7	Ca-Na-HCO3
TC-224	**Shawcroft W**	well	NMBGMR	08-0659	5/16/08	880	5.4	19.0	66.2	200	3.1	8.4	8.0	250	172	2.15	2.13	-0.4	Ca-Na-HCO3
TC-226	**Shawcroft E**	well	NMBGMR	08-0660	5/16/08	390	6.4	14.5	58.1	263	2.9	8.5	8.1	290	198	2.75	2.65	-1.8	Na-Ca-Mg-HCO3-SO4
TC-227	**Perlite Mill**	well	NMBGMR	08-0736	6/3/08	215	6	11.4	52.5	588	7.7	8.4	8.3	605	413	5.97	5.90	-0.6	Na-HCO3-SO4
TC-229	**Crow**	well	NMBGMR	08-0738	6/3/08	339	6.7	15.0	59.0	184	5.3	8.2	8.1	195	149	1.96	1.94	-0.4	Ca-Na-Mg-HCO3
TC-233	**San Antonio Mtn**	well	NMBGMR	09-0406	6/4/08	34	2.2	6.6	43.9	139	10.5	6.5	7.8	145	146	1.50	1.59	2.7	Ca-Mg-Na-HCO3
TC-234	**Schofield**	well	NMBGMR	09-0407	6/5/09	622	5.1	26.7	80.1	381	2.4	7.7	8.0	395	233	4.03	4.20	2.1	Ca-Mg-HCO3
TC-240	**BLM Chiflo CG**	well	NMBGMR	10-0896	11/12/10	380	7.1	17.4	63.3	259	7.2	8.3	8.3	335	177			-2.4	Ca-Na-HCO3-SO4
TC-243	**Anderson**	well	NMBGMR	02-2671	9/28/02	910	5.5	U	U	U	U	U	7.7	385	380			2.6	Ca-Mg-HCO3
TC-246	**Bradley**	well	NMBGMR	04-1607	11/30/04	830	5.1	U	U	U	U	U	6.5	230	121			-3.1	Ca-Mg-Na-HCO3
TC-249	**BLM Wild Rivers VC**	well	NMBGMR	10-0897	11/12/10	518	6.8	17.8	64.0	248	7.2	8.3	8.3	310	171			-1.6	Ca-Na-HCO3-SO4
TC-250	**Schwartz, TP-10**	well	NMBGMR	05-0799	11/11/05	750	5.4	U	U	U	U	U	7.9	340	229			-1.9	Ca-Mg-HCO3
TC-251	**Schwartz, TP-11**	well	NMBGMR	04-1605	11/30/04	U	5.5	U	U	U	U	U	7.3	335	186			-1.8	Ca-HCO3
TS-8	**Bear Crossing**	spring	NMBGMR	06-0762	8/29/06		8.1	16.5	61.7	222	7.8	8.3	8.3	210	173			0.3	Na-Ca-Mg-HCO3
TS-14	**Cow Patty W**	spring	NMBGMR	06-0763	8/29/06		7.4	12.9	55.2	133	7.3	7.8	7.9	170	130			0.4	Ca-Mg-Na-HCO3
TS-16b	**Big Arsenic**	spring	NMBGMR	06-0764	8/31/06		9.0	17.5	63.5	249		8.2	8.2	235	175			-0.1	Ca-Na-Mg-HCO3-SO4
TS-17	**Little Arsenic**	spring	NMBGMR	06-0765	8/31/06		9.2	15.4	59.7	224	7.0	8.2	8.2	210	159			-1.8	Ca-Na-Mg-HCO3
TS-61	**Felsenmeere**	spring	NMBGMR	07-1078	5/9/07		8.3	16.8	62.2	U	6.6	U	8.3	190	149			2.2	Ca-Na-Mg-HCO3
TS-71	**Sunshine**	spring	NMBGMR	08-1125	9/25/08		7.7	14.9	58.8	202	9.3	8.2	8.3	210	124			-1.1	Ca-Mg-Na-HCO3
TS-72	**Sunshine Trail W**	spring	NMBGMR	08-1124	9/25/08		7.7	12.5	54.5	183	9.3	7.9	7.9	190	115			-2.5	Ca-Mg-Na-HCO3
TS-113	**Lava Tube**	spring	NMBGMR	09-0662	9/2/09		7.7	15.2	59.4	214	7.3	8.0	8.3	225	162			-0.6	Ca-Na-Mg-HCO3
TC-228	**Rio San Antonio**	stream	NMBGMR	08-0737	6/3/08		U	7.7	45.9	49	5.9	7.5	7.9	57	50			-2.5	Ca-HCO3
TS-114	**Rio Grande above Lava Tube spring**	stream	NMBGMR	09-0663	9/2/09		U	15.9	60.6	329	7.3	8.6	8.7	345	212			0.5	Na-Ca-HCO3-SO4
CO-11	**370300105564501**	well	USGS	U	8/17/81	162	6.3	11.5	52.7	179	U	U	U	U	145			U	U
CO-13	**370142105561101**	well	USGS	U	6/4/82	223	6.3	14.5	58.1	172	U	7.9	U	U	136			0.07	Ca-HCO3
CO-26	**370257105553901**	well	USGS	U	6/4/82	172	6.4	11.5	52.7	190	U	7.9	U	U	140			-2.85	Ca-HCO3
CO-27	**370326105594302**	well	USGS	U	6/4/82	<235	6.1	10.5	50.9	247	U	8.4	U	U	184			1.63	Ca-Mg-Na-HCO3
CO-28	**370324105571801**	well	USGS	U	6/4/82	150	6.3	10.5	50.9	164	U	8.2	U	U	135			-0.66	Ca-HCO3
CO-29	**370324105561201**	well	USGS	U	6/4/82	152	6.3	10.5	50.9	202	U	8.0	U	U	148			1.74	Ca-Mg-HCO3
CO-30	**370323105582201**	well	USGS	U	6/4/82	<259	6.2	10.5	50.9	218	U	7.6	U	U	168			0.83	Ca-Mg-HCO3

All concentrations in mg/L (ppm); results for Ag, Be, Cd, Co, Ni, Se, Sb, Sn, Th, and Tl are below detection limits (not shown)
* Sample depth is the mid-point of screen interval, or where well screen is unknown, the mid-point of the water column
Mean surface temperatures estimated for each site from temperature-elevation regression of regional climate data: MST (°C) = -0.0091* Elev(m) + 27.9
U = undetermined; BD = below detection

Table 4B—Taos Plateau chemistry data.

Site		Major and minor ions													Trace elements															
Site number	**Site type**	**Ca**	**Mg**	**Na**	**K**	**HCO_3^-**	**CO_3^{2-}**	**SO_4^{2-}**	**Cl^-**	**Br**	**F^-**	**Fe**	**Mn**	**NO_3^-**	**Al**	**As**	**B**	**Ba**	**Cr**	**Cu**	**Li**	**Mo**	**Pb**	**Si**	**SiO_2**	**Sr**	**Ti**	**U**	**V**	**Zn**
TC-201	well	U	U	U	U	U	U	U	U	U	U	U	U	U	U	U	U	U	U	U	U	U	U		U	U	U	U	U	U
TC-204	well	16	5.9	24	3.3	110	0	13	9.9	0.060	0.89	BD	BD	2.3	0.003	0.005	0.060	0.012	0.002	0.001	0.040	0.003	BD	20	43	0.161	0.002	0.002	0.012	0.016
TC-208	well	9	6.0	53	3.4	120	0	26.0	28	0.117	2.10	BD	BD	1.20	0.001	0.009	0.142	0.008	0.002	0.002	0.093	0.007	BD	20	42	0.106	0.002	0.001	0.013	0.019
TC-209	well	10	4.8	48	3.9	115	0	21.0	24.0	0.108	2.30	BD	BD	1.6	0.003	0.009	0.132	0.006	0.001	0.001	0.113	0.006	BD	20	43	0.120	0.002	0.002	0.008	0.039
TC-212	well	18	6.3	11	2.6	105	0	7.8	2.2	0.039	0.31	0.05	BD	3.1	0.003	0.002	0.023	0.006	0.001	0.002	0.007	0.001	0.001	20	42	0.178	0.002	0.002	0.009	0.015
TC-213	well	21	8.1	14	3.0	120	0	11.0	4.5	0.055	0.39	0.05	0.017	4.0	0.002	0.002	0.028	0.008	0.002	0.001	0.007	0.002	0.001	22	48	0.191	0.002	0.002	0.010	0.007
TC-216	well	19	5.6	11	3.2	110	0	6.7	1.8	0.023	0.30	BD	BD	2.3	0.002	0.003	0.022	0.046	0.003	BD	0.008	0.001	BD	25	53	0.166	0.002	0.002	0.012	0.10
TC-218	well	16	11	13	2.4	115	0	9.0	3.0	0.065	0.34	0.008	BD	4.8	0.005	0.002	0.024	0.040	0.004	0.002	0.006	0.001	BD	24	52	0.153	0.002	0.001	0.015	0.017
TC-219	well	16	5.3	12	2.7	97	0	5.1	1.7	0.022	0.29	BD	BD	1.9	0.001	0.004	0.024	BD	0.002	0.002	0.007	0.001	BD	23	54	0.167	0.002	BD	0.013	0.013
TC-220	well	18	3.3	9	2.5	94	0	4.4	1.1	0.021	0.24	BD	BD	1.6	0.001	0.003	0.018	0.026	0.002	BD	0.005	0.001	BD	21	44	0.154	0.002	0.001	0.011	0.009
TC-221	well	26	6.3	11	5.2	135	0	3.6	2.4	0.041	0.52	BD	BD	3.2	0.001	0.003	0.011	0.021	0.001	0.002	0.013	0.001	BD	33	70	0.186	0.003	0.001	0.011	0.017
TC-222	well	23	6.7	17	5.4	135	0	8.9	2.7	0.049	0.38	0.006	BD	2.1	0.001	0.003	0.028	0.008	0.002	0.001	0.010	0.002	BD	32	68	0.256	0.002	0.004	0.012	0.010
TC-223	well	18	4.3	9	2.3	94	0	7.3	1.2	0.020	0.19	BD	BD	1.4	0.001	0.002	0.021	0.035	0.001	0.001	0.004	0.001	BD	19	41	0.141	0.001	0.001	0.007	0.024
TC-224	well	20	5.1	14	4.5	120	0	3.9	1.9	0.040	0.33	BD	BD	1.9	0.001	0.003	0.021	0.008	0.001	0.001	0.009	0.001	0.001	28	60	0.184	0.002	0.002	0.012	0.10
TC-226	well	17	7.3	26	2.8	105	0	37.0	5.8	0.120	0.42	0.197	0.027	4.4	0.001	0.003	0.055	0.035	0.003	0.001	0.008	0.002	BD	21	44	0.177	0.001	0.002	0.013	0.013
TC-227	well	11	3.6	115	2.1	190	0	66.0	25.0	0.481	3.00	0.01	BD	38.0	BD	0.068	0.351	BD	BD	BD	0.020	0.005	BD	25	53	0.202	BD	0.017	0.244	0.038
TC-229	well	17	5.7	13	2.7	99	0	11.0	1.8	0.034	0.29	0.030	BD	2.4	0.003	0.003	0.028	0.009	0.001	0.001	0.005	0.001	BD	21	46	0.149	0.001	0.002	0.010	0.006
TC-233	well	14	5.1	8.5	3.9	78	0	4.6	3.5	0.023	0.20	0.053	BD	BD	0.067	0.001	0.013	0.087	0.001	0.010	0.001	BD	BD	26	67	0.101	0.009	BD	0.004	0.031
TC-234	well	48	13	13	6.6	205	0	19	8.3	0.117	0.20	BD	0.072	2.3	BD	BD	0.016	0.019	0.001	0.003	0.013	BD	0.001	22	53	0.372	0.003	0.004	0.002	0.267
TC-240	well	21	6.0	21	2.6	105	0	26	8.0	0.086	1.30	BD	BD	4.9	0.004	0.001	0.025	0.024	0.002	BD	0.022	0.003	BD		34	0.180	0.002	0.003	0.005	0.023
TC-243	well	80	18	25	5.5	372	0	7.8	2.7	U	0.31	0.073	0.006	11.0	BD	BD	U	0.023	0.001	0.024	0.050	0.002	0.033		45	0.590	U	0.021	BD	5.3
TC-246	well	17	8.6	13	6.1	135	0	3.1	2.5	BD	0.58	0.058	0.001	2.4	BD	0.003	0.012	0.029	0.007	0.001	0.016	0.001	BD		100	0.160	0.002	BD	0.046	0.002
TC-249	well	20	5.7	21	2.4	100	0	25.0	8.6	0.082	1.20	BD	BD	4.0	0.005	0.002	0.030	0.015	0.002	BD	0.026	0.003	BD		32	0.180	0.002	0.003	0.005	0.035
TC-250	well	40	9.6	16	2.1	190	0	12	8.9	0.170	2.50	0.370	0.013	3.3	BD	0.001	0.022	0.021	0.002	0.011	0.029	0.010	0.007		38	0.290	0.001	0.026	0.001	4.2
TC-251	well	46	8.6	11	1.2	180	0	14	8.1	0.120	0.78	0.160	0.001	6.4	BD	BD	0.017	0.120	0.003	0.001	0.013	0.001	BD		39	0.300	0.001	0.005	0.004	0.017
TS-8	spring	17	6.3	21	3.1	110	0	11	8.0	0.042	0.77	BD	BD	2.6	0.003	0.004	0.047	0.016	0.003	0.001	0.029	0.002	BD		48	0.158	0.002	0.002	0.013	BD
TS-14	spring	17	6.5	10	2.4	93	0	10	3.1	0.037	0.40	1.2	0.002	1.6	0.035	0.001	0.019	0.026	0.003	BD	0.004	0.001	BD		32	0.139	0.002	0.002	0.007	BD
TS-16b	spring	21	6.9	20	2.4	105	0	25	7.9	0.070	1.10	0.04	<0.001	4.1	0.010	0.001	0.023	0.023	0.002	0.001	0.021	0.003	BD		34	0.180	0.001	0.003	0.006	BD
TS-17	spring	17	6.0	19	2.5	100	0	18	6.6	0.070	1.30	0.12	<0.001	2.7	0.012	0.002	0.029	0.025	0.003	0.001	0.021	0.005	BD		36	0.150	0.001	0.002	0.008	BD
TS-61	spring	18	6.5	13	2.9	100	0	8	3.1	0.040	0.40	BD	BD	2.7	0.001	0.003	0.027	0.018	0.002	0.001	0.01	0.001	BD		44	0.160	0.003	0.002	0.011	BD
TS-71	spring	18	7.3	13	2.3	105	0	13	4.1	0.052	0.48	BD	BD	2.7	0.004	0.001	0.030	0.077	0.003	0.008	0.006	0.002	BD		36	0.176	0.001	0.002	0.008	0.015
TS-72	spring	16	7.6	11	2.5	105	0	10	3.3	0.035	0.48	BD	BD	1.9	0.017	0.002	0.028	0.089	0.003	0.027	0.006	0.001	0.001		35	0.132	0.002	0.002	0.009	0.024
TS-113	spring	19	7.4	14	2.6	110	0	13	4.2	0.055	0.48	BD	BD	2.9	0.004	0.002	0.033	0.079	BD	0.006	0.008	0.002	BD		43	0.180	0.002	0.002	0.009	0.015
TC-228	stream	6	1.0	2	1.2	33	0	1	BD	0.010	BD	0.13	0.008	BD	0.160	BD	BD	0.018	BD	0.006	0.004	BD	BD		21	0.049	0.006	BD	0.002	0.002
TS-114	stream	23	7.4	33	4.6	130	0	36	9.9	0.089	0.56	BD	0.008	1.0	0.023	0.003	0.069	0.079	0.001	0.006	0.008	0.004	BD		28	0.230	0.002	0.002	0.007	0.010
CO-11	well	24	4.3	7	2.4	U	U	U	U	U	U	U	U	0.8	U	U	U	U	U	U	U	U	U			U	U	U	U	U
CO-13	well	22	3.8	7	2.9	97	U	6	2.0	U	0.20	0.02	0.020	0.6	U	U	U	U	U	U	U	U	U		42	U	U	U	U	U
CO-26	well	24	4.1	6	2.9	108	U	5	2.1	U	0.20	U	BD	1.1	U	U	U	U	U	U	U	U	U		38	U	U	U	U	U
CO-27	well	27	7.6	13	3.0	138	U	6	2.3	U	0.90	U	BD	2.0	U	U	U	U	U	U	U	U	U		47	U	U	U	U	U
CO-28	well	21	3.9	6	2.3	93	U	BD	2.0	U	0.20	0.01	U	0.7	U	U	U	U	U	U	U	U	U		37	U	U	U	U	U
CO-29	well	27	5.1	6	3.1	111	U	5	2.4	U	0.20	U	U	1.3	U	U	U	U	U	U	U	U	U		39	U	U	U	U	U
CO-30	well	28	5.8	9	2.9	128	U	BD	1.6	U	0.20	0.04	U	1.4	U	U	U	U	U	U	U	U	U		37	U	U	U	U	U

All concentrations in mg/L (ppm); results for Ag, Be, Cd, Co, Ni, Se, Sb, Sn, Th, and Tl are below detection limits (not shown)
* Sample depth is the mid-point of screen interval, or where well screen is unknown, the mid-point of the water column
Mean surface temperatures estimated for each site from temperature-elevation regression of regional climate data: MST (°C) = -0.0091* Elev(m) + 27.9
U = undetermined; BD = below detection

Major Ions and Trace Elements—Samples were collected in 125-mL (trace elements) or 500-mL (ions) polypropylene bottles that were triple-rinsed with purge water prior to filling. All samples were stored on ice and in the dark and transported to the laboratory within 24 to 36 hours of collection. Samples were filtered upon arrival at the NMBGMR water quality laboratory using a 0.45 micron filter and acidified to pH less than 2 by the addition of MerckTM ultra-pure nitric acid (5 ml 6 N HNO3). Alkalinity was determined by titration within 36 hours of sample collection. Major anions were analyzed by ion chromatography (IC), major cations by inductively coupled plasma-optical emission spectroscopy (ICP-OES), and trace elements by inductively coupled plasma-mass spectrometry (ICP-MS). The quality of the chemical analyses was inspected by analyzing blanks, duplicate samples, and checking ion balances. Analytical error for major ions and trace elements is generally less than 10 percent using IC, ICP-OES, and ICP-MS.

Table 5–Isotopic data for well, spring, and stream waters.

	Site and sample information			Stable isotopes		Tritium		Carbon isotopes				
	Site number	Site name	Sample date	δ^2H (‰)	$\delta^{18}O$ (‰)	Tritium (TU)	Error (TU)	$\delta^{13}C$ (‰)	^{14}C Activity (pmC)	1 σ ^{14}C error (pmC)	^{14}C Apparent Age (RCYBP)	^{14}C Apparent Age Error (RCYBP)
WELLS	TC-201	Cerrito Negro	5/12/08	-102.6	-15.1	0.04	0.09	-11.5	46.95	0.23	6070	40
	TC-204	Ezequiel	5/13/08	-95.2	-14.6	0.22	0.09	-10.7	54.31	0.27	4900	40
	TC-208	Moeller/Rael	5/13/08	-94.8	-14.5	0.03	0.09	-9.8	55.27	0.28	4760	40
	TC-209	Abeyta/Rael	5/14/08	-95.6	-14.6	0.02	0.09	-10.0	52.13	0.26	5230	40
	TC-212	Middlemist	5/14/08	-97.1	-14.7	1.25	0.09	-11.5	64.01	0.32	3580	40
	TC-213	Maestas	6/3/08	-96.2	-14.5	0.36	0.09	-10.2	52.71	0.26	5140	40
	TC-216	Moeller	5/14/08	-100.6	-15.0	0.19	0.09	-11.5	49.29	0.25	5680	40
	TC-218	Alire	6/3/08	-101.6	-15.2	0.04	0.09	-11.3	36.79	0.23	8030	50
	TC-219	Sowards	6/3/09	-100.3	-15.1	50.8	1.70	-10.2	47.42	0.24	5990	40
	TC-220	Llano	5/15/08	-107.2	-14.8	0.00	0.09	-12.3	55.82	0.28	4680	40
	TC-221	No Agua Mine	5/15/08	-107.9	-14.7	0.02	0.09	-10.7	44.39	0.22	6520	40
	TC-222	Bagwell N	6/3/08	-109.0	-15.0	0.02	0.09	-11.8	50.47	0.25	5490	40
	TC-223	Stateline	5/16/08	-106.6	-15.0	0.10	0.09	-12.4	58.02	0.29	4370	40
	TC-224	Shawcroft W	5/16/08	-109.6	-15.0	-0.02	0.09	-11.5	49.16	0.31	5700	50
	TC-226	Shawcroft E	5/16/08	-107.0	-15.0	0.03	0.09	-11.1	49.04	0.31	5720	50
	TC-227	Perlite Mill	6/3/08	-97.7	-13.2	1.02	0.09	-7.9	43.09	0.21	6760	40
	TC-229	Crow	6/3/08	-108.1	-15.0	0.05	0.09	-11.7	61.59	0.31	3890	40
	TC-233	San Antonio Mtn	6/4/08	-103.3	15.4	U	U	U	U	U	U	U
	TC-234	Schofield	6/5/09	-104.8	-14.7	0.09	0.09	-5.2	36.10	0.22	8180	50
	TC-240	BLM Chiflo CG	11/12/10	-98.0	-13.6	0.84	0.09	-12.6	80.12	0.39	1780	40
	TC-249	BLM Wild Rivers HQ	11/12/10	-98.7	-13.6	0.38	0.09	-12.2	74.73	0.36	2340	40
SPRINGS	TS-8	Bear Crossing zone	8/29/06	-103.8	-14.5	0.09	0.09	U	U	U	U	U
	TS-14	Cow Patty W	8/29/06	-102.8	-14.5	-0.03	0.09	-11.3	81.50	0.41	1,640	40
	TS-16b	Big Arsenic middle	8/31/06	-99.4	-14.2	0.60	0.09	U	U	U	U	U
	TS-17	Little Arsenic	8/31/06	-100.1	-14.2	0.02	0.09	U	U	U	U	U
	TS-61	Felsenmeere Middle	5/9/07	-107.1	-15.3	U	U	-10.6	57.90	0.30	4,400	40
	TS-71	Sunshine	9/25/08	-97.6	-14.2	0.08	0.09	-10.6	69.58	0.35	2,910	40
	TS-72	Sunshine Trail W	9/25/08	-96.4	-14.4	0.02	0.09	-11.9	72.86	0.36	2,540	40
	TS-113	Lava Tube	9/2/09	-101	-14.5	0.1	0.09	-11.1	61.97	0.31	3,840	40
STREAMS	TC-228	Rio San Antonio	6/4/08	-104.3	-14.8	6.7	0.22					
	TS-114	Rio Grande	9/2/09	-89.7	-12.0	U	U					
	Cost-2	Rio Costilla	2/9/08	-102.5	-14.0	6.7	0.22					
	Latir	Latir Creek	2/8/08	-101.6	-14.3	8.3	0.27					
	Cabr	Cabresto Creek	2/8/08	-101.2	-14.1	6.1	0.2					
	Red	upper Red River	2/9/08	-99.34	-13.80	5.1	0.17					
	Hondo	Rio Hondo	2/7/08	-96.2	-13.7	8.5	0.28					
	Seco	Rio Seco	2/7/08	-95.6	-13.6	7.5	0.25					

U = undetermined

Table 6–CFC data and recharge ages.

Site and sample information				CFC water concentration corrected for stripping efficiency			Equivalent atmospheric concentration			CFC-derived recharge ages (years before sampling date)		
Site number	Site name	Sample date	Lab ID number	CFC12 pmol/Kg	CFC11 pmol/Kg	CFC113 pmol/Kg	CFC12 pmol/mol	CFC11 pmol/mol	CFC113 pmol/mol	CFC12	CFC11	CFC113
TC-204	Ezequiel	5/13/08	68.01	1.068	1.132	0.061	215.262	57.831	9.884	**33**	39	34
			68.01D	1.027	1.289	0.122	206.998	65.851	19.767	**34**	38	29
			68.01D1	0.959	1.423	0.110	193.293	72.697	17.823	**35**	37	30
TC-208	Moeller/Rael	5/13/08	70.01	0.720	1.220	0.082	145.121	62.326	13.286	**37**	38	32
			70.01D	0.812	1.245	0.061	163.664	63.604	9.884	**36**	38	34
			70.01D1 *	1.066	1.900	0.088	214.859	97.066	13.934	33	35	32
TC-209	Abeyta/Rael	5/14/08	70.02	0.163	0.244	0.012	32.854	12.465	1.944	**48**	48	40
			70.02D	0.174	0.297	0.012	35.071	15.173	1.944	**48**	46	40
			70.02D1	0.173	0.273	0.008	34.869	13.947	1.296	**48**	47	40
TC-212	Middlemist	5/14/08	68.02	0.350	0.610	0.002	70.545	31.163	0.324	**43**	42	40
			68.02D	0.357	0.588	0.023	71.956	30.039	3.727	**43**	42	39
			68.02D1	0.368	0.708	0.033	74.173	36.170	5.347	**42**	41	38
TC-213	Maestas	6/3/08	68.03	1.168	2.531	0.147	235.418	129.302	23.818	**32**	32	28
			68.03D	1.078	2.186	0.147	217.278	111.677	23.818	**33**	34	28
			68.03D1	1.148	2.329	0.152	231.387	118.982	24.628	**33**	33	27
TC-218	Alire	6/3/08	70.03	0.872	1.425	0.097	175.757	72.799	15.717	**36**	37	31
			70.03D	0.830	1.569	0.094	167.292	80.156	15.230	**36**	37	31
			70.03D1	0.851	1.637	0.099	171.524	83.630	16.041	**36**	36	31
TC-219	Sowards	6/3/09	74.01	0.487	0.936	0.068	98.158	47.818	11.018	**42**	41	34
			74.01D	0.464	0.881	0.058	93.522	45.008	9.398	**42**	41	35
			74.01D1	0.463	0.841	0.058	93.321	42.964	9.398	**42**	42	35
TC-220	Llano	5/15/08	70.04	0.017	0.187	0.000	3.426	9.553	0.000	**59**	50	40
			70.04D *	0.164	0.518	0.011	33.055	26.463	1.782	48	43	40
			70.04D1	0.011	0.103	0.000	2.217	5.262	0.000	**59**	52	40
TC-222	Bagwell N	6/3/08	70.05 *	1.379	7.649	0.164	277.946	390.766	26.572	30	-0	27
			70.05D	0.057	0.149	0.004	11.489	7.612	0.648	**56**	52	41
			70.05D1	0.084	0.596	0.006	16.931	30.448	0.972	**54**	42	40
TC-223	Stateline	5/16/08	70.06	1.445	2.338	0.209	291.249	119.442	33.863	**29**	33	25
			70.06D	1.444	2.223	0.215	291.047	113.567	34.836	**29**	33	24
			70.06D1	1.465	2.303	0.203	295.280	117.654	32.891	**29**	33	25
TC-224	Shawcroft W	5/16/08	70.07	0.023	0.128	0.000	4.636	6.539	0.000	**58**	52	40
			70.07D *	0.320	0.574	0.031	64.498	29.324	5.023	43	42	38
			70.07D1	0.013	0.171	0.000	2.620	8.736	0.000	**59**	51	40
TC-226	Shawcroft E	5/16/08	70.08	1.069	2.179	0.134	215.464	111.319	21.712	**33**	34	28
			70.08D	1.002	1.714	0.118	201.959	87.564	19.119	**34**	36	29
			70.08D1	0.999	1.853	0.116	201.355	94.665	18.795	**34**	35	29
TC-227	Perlite Mill	6/3/08	68.04	0.391	1.003	0.038	78.809	51.241	6.157	**42**	40	38
			68.04D	0.403	0.987	0.033	81.227	50.423	5.347	**42**	40	38
			68.04D1 *	1.550	9.352	0.167	312.412	477.768	27.058	28	-0	27
TC-229	Crow	6/3/08	70.09	1.457	3.047	0.213	293.668	155.663	34.512	**29**	30	25
			70.09D	1.492	2.709	0.206	300.722	138.395	33.377	**29**	31	25
			70.09D1	1.455	3.037	0.202	293.264	155.152	32.729	**29**	30	25
TC-240	BLM Chiflo CG	11/12/10	89.01	0.934	1.641	0.123	188.280	83.815	19.929	**37**	39	31
			89.01D	0.967	1.670	0.129	194.930	85.310	20.974	**37**	39	31
			89.01D2	0.935	1.671	0.124	188.518	85.376	20.011	**37**	39	31
TC-249	BLM Wild Rivers VC	11/12/10	89.02	0.792	1.211	0.114	159.644	61.842	18.482	**39**	41	32
			89.02D	0.788	1.193	0.117	158.814	60.925	18.891	**39**	41	32
			89.02D2	0.789	1.203	0.113	158.995	61.445	18.320	**39**	41	32
TS-71	Sunshine	9/25/08	61.01	1.957	1.503	0.112	394.446	76.784	18.147	**24**	37	30
			61.01D	1.268	1.421	0.105	255.573	72.595	17.013	**32**	38	30
			61.01D1	1.193	1.459	0.108	240.457	74.536	17.499	**32**	37	30
TS-113	Lava Tube	9/2/09	76.01	0.551	1.156	0.074	93.846	48.608	9.602	**42**	41	36
			76.01D	0.550	1.151	0.070	93.674	48.392	9.061	**42**	41	36
			76.01D1	0.528	0.954	0.070	89.878	40.119	9.061	**42**	42	36

Age calculations assume 2400 m recharge elevation and 6.1°C recharge temperature; TS-113 assumes 2900 m elevation and 2.0 °C temperature
*atmospheric contamination.

Hydrogen and Oxygen Isotopes—Samples for hydrogen-2 (deuterium, ^2H) and oxygen-18 (^{18}O) analyses were collected in 25 mL amber glass bottles that were triple-rinsed with purge water prior to filling, and analyzed at the New Mexico Institute of Mining and Technology, Department of Earth and Environmental Sciences stable isotope laboratory on a Thermo Finnigan Delta Plus XP isotope ratio mass spectrometer. Analytical uncertainties for δ^2H and $\delta^{18}O$ are typically less than 1 per mil (‰) and 0.1‰, respectively.

Carbon Isotopes—Carbon isotope samples were collected in one 1-L polypropylene bottle, or two 500 mL polypropylene bottles, that were tripled-rinsed with purge water. Sampling followed protocols described at www.radiocarbon.com/groundwater.htm, with the exception of the addition of NaOH . Samples were chilled and stored in a dark environment until shipment to Beta Analytic, Miami, Florida, for analysis. The ^{14}C activity and $^{13}C/^{12}C$ ratios ($\delta^{13}C$) of the water sample were derived from the dissolved inorganic carbon (DIC) by accelerator mass spectrometry. Measured $\delta^{13}C$ values were calculated relative to the PDB-1 standard. Result verification and isotopic fractionation correction using $\delta^{13}C$ were completed by Beta Analytic. Results are reported as ^{14}C activity (in percent of modern carbon (pmC)) and as the apparent radiocarbon age (in radiocarbon years before present (RCYBP), where "present" = AD 1950), with an uncertainty of one standard deviation. No corrections for geochemical effects have been completed, and the reported apparent ^{14}C ages do not exactly represent the residence time of the water within the aquifer. The ^{14}C activity and apparent ^{14}C age are used as a relational tool to interpret hydrologic differences between wells.

Tritium (^3H)—Tritium samples were collected in one 1-L polypropylene bottle, or two 500 mL polypropylene bottles, that were tripled-rinsed with purge water. Sampling followed protocols described at www.rsmas.miami.edu/groups/tritium/advice-sampling-tritium.html. Samples were shipped to University of Miami Tritium Laboratory where they were analyzed by internal gas proportional counting with electrolytic enrichment. The enrichment step increases tritium concentrations in the sample about 60-fold through volume reduction, yielding lower detection limits. Accuracy of this low-level measurement is 0.10 tritium unit (TU) (0.3 pCi/L of water), or 3.0%, whichever is greater. The stated errors, typically 0.09 TU, are one standard deviation.

Chlorofluorocarbons (CFCs)—CFC samples were collected from well and spring discharge, with no atmospheric exposure, into three 125-mL glass bottles with foil-lined caps. The bottles and caps were thoroughly rinsed with purge water or spring sample water, and were filled and capped underwater in a plastic bucket. Sampling followed stringent protocols described at www.rsmas.miami.edu/groups/tritium/advice-sampling-cfc.html. Samples were shipped to University of Miami Tritium Laboratory where they were analyzed using a purge-and-trap gas chromatograph with an electron capture detector. The limit of detection for the method is 0.001×10^{-12} moles/kg of water (pmol/kg). Precision of CFC-11, CFC-12 and CFC-113 analyses is 2% or less and the accuracy of CFC-12 derived recharge ages is 2 years or less. Calculations of CFC recharge ages assumed a recharge elevation of 2400 meters and a recharge temperature of 6.1 °C, which are the average elevation and mean annual temperature for the Taos Plateau.

Data Compilation and Data Quality—Geochemical data for four well sites in New Mexico were compiled from the TSWCD database. Data from seven well sites in southern Colorado were compiled from the USGS National Water Information System (NWIS) database, including major ions, silica (SiO_2), and field parameters of temperature, pH, and specific conductance. The data were reviewed and filtered for data quality based on several criteria including an accurate map location or geographical coordinates for the sample site and an ion balance less than ± 5.0.

III. GEOLOGY OF THE NORTHERN TAOS PLATEAU

Regional Geology

Rio Grande Rift—The study area lies within the southern San Luis Basin, the northernmost large basin of the Rio Grande rift. The 150-mile-long San Luis Basin is bordered by the Sangre de Cristo Mountains on the east and the Tusas and San Juan Mountains on the west. The basin is roughly divided into two major provinces, the broad San Luis Valley of southern Colorado and the Taos Plateau of northern New Mexico (Fig. 3). At the southern end of the basin, near Taos, the rift is about 20 miles wide and filled with a thick section of sediments and volcanic rocks.

Unlike the rift basins to the south, the San Luis Basin is relatively undissected. That is, the sedimentary material that fills the basin has not yet been extensively exposed by the action of rivers and streams. Instead, the Rio Grande and its major eastern tributaries have cut several deep, narrow canyons through the volcanic rocks that cap most of the area. The river canyons provide the only good exposures of the rocks in the basin.

The San Luis Basin is asymmetric, with a deep, narrow structural trough east of the gorge, known as the Taos graben in New Mexico, and a shallow bedrock ramp west of the gorge. The seismically active east rift border is the Sangre de Cristo fault, a complex system of west-down normal faults (Fig. 7). In detail, the northern half of the rift basin is structurally complex, with a number of sub-basins and structural highs, including the Alamosa and Taos-Costilla sub-basins and the San Luis Hills and Brushy-Timber Mountain horsts.

Taos Plateau Volcanic Field—The Pliocene to Pleistocene Taos Plateau volcanic field of northern New Mexico and southern Colorado is the largest and compositionally most diverse volcanic field of the Rio Grande rift. Nearly all of the isolated, rounded mountains scattered across the Taos Plateau are extinct volcanoes that erupted between 6 and 1 million years ago (Lipman and Mehnert, 1979; Appelt, 1998). At least 35 discrete volcanic vents have been identified on the plateau (Dungan et al., 1984; Appelt, 1998), and the number of buried volcanoes is unknown but probably large.

The volcanoes of the Taos Plateau occur in a variety of sizes and shapes. Cinder cones (such as the cone exposed in the gorge in Wild Rivers Recreation Area) are small, steep-sided features constructed from cinders and bombs ejected from a central vent. Shield volcanoes (such as the vents of La Segita Peaks) are shallow-sloped and constructed of successive lava flows that can flow long distances. Lava domes (such as San Antonio Mountain, Ute Mountain, Cerro Chiflo, PNo Agua Peaks, Cerro del Aire, Cerro de la Olla, and Cerro Montoso) are large, steep-sided volcanoes that were formed from numerous eruptions of thick, sticky lava. Flood or plateau basalts (such as the Servilleta Basalt) are fluid lava flows erupted out of low-relief vents, and can travel for many miles before solidifying.

The volcanoes that flank the Rio Grande gorge span a wide variety of compositions. Although most are mafic to intermediate in composition (basalts, andesites, dacites), rhyolites are not uncommon. Cerro de la Olla (4.97 Ma), Cerro Montoso (5.88 Ma), and Cerro de los Taoses (4.84 Ma) are all andesite volcanoes. Ute Mountain (2.7 Ma), San Antonio Mountain (3 Ma), and Guadalupe Mountain (5.3 Ma) volcanoes are all composed of dacite. Cerro Chiflo volcano (5.3 Ma) is also composed of dacite, but is chemically different from any other dacite

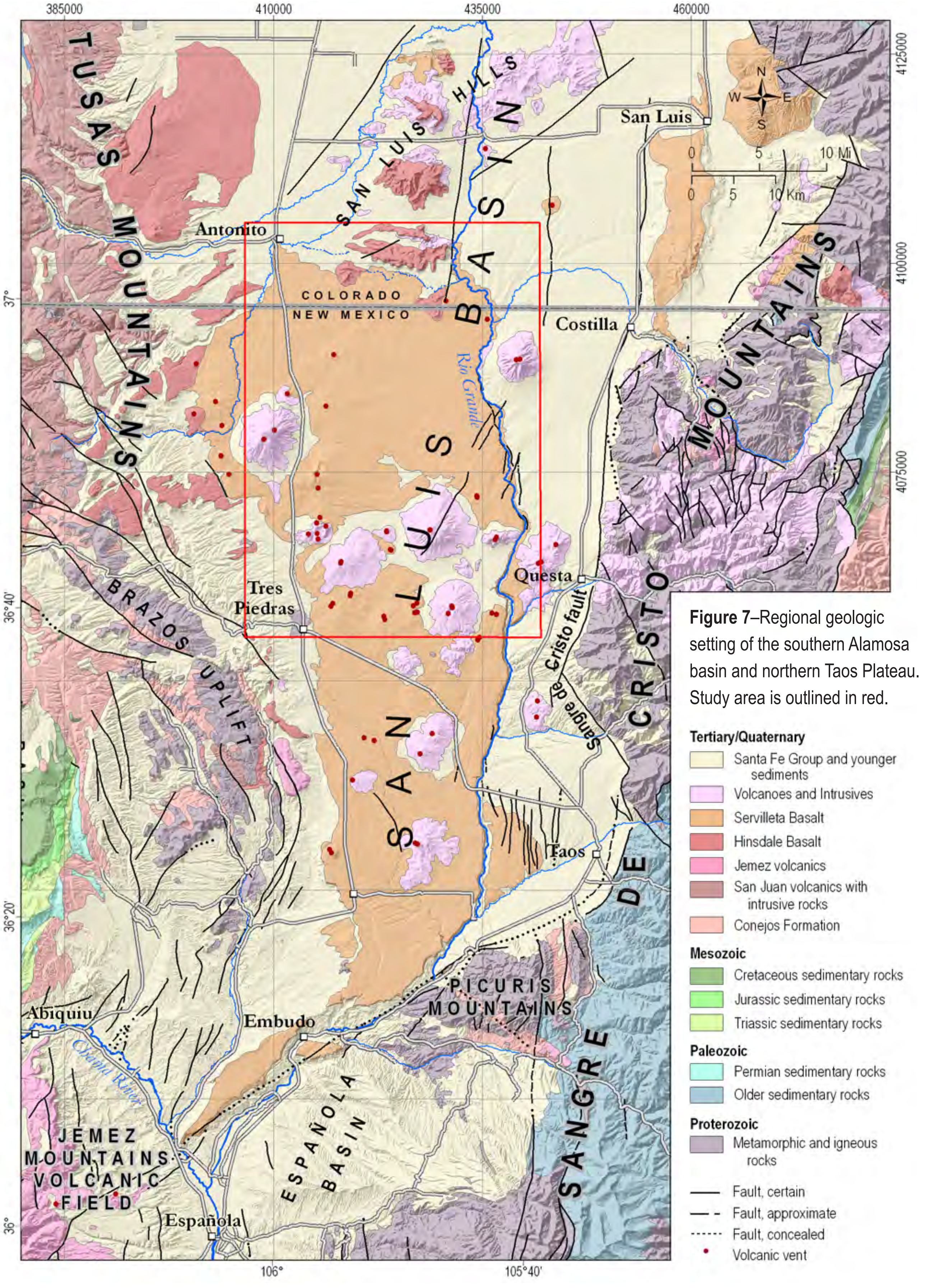

Figure 7–Regional geologic setting of the southern Alamosa basin and northern Taos Plateau. Study area is outlined in red.

volcano on the plateau. The principal rhyolite volcano, No Agua Peaks (4 Ma), is of special interest because of its valuable perlite deposits and the fascinating view of its internal workings provided by an active mining operation.

San Luis Hills—The San Luis Hills form a topographic and structural high between the Taos Plateau and the Alamosa sub-basin. They consist of an elongate series of flat-topped mesas and eroded hills that trend northeasterly from the state line 28 miles into Colorado (Fig. 8). They represent the surface expression of a large intrarift horst (the San Luis Hills horst) in the San Luis Basin. Several small outliers of similar-aged rocks exposed to the south at Brushy and Timber Mountains define a similar intrarift horst. The San Luis Hills, Brushy Mountain and Timber Mountain are mostly composed of middle Tertiary volcanic rocks with local exposures of interlayered sedimentary strata. It is likely that similar rocks underlie the Pliocene volcanic rocks of much of the Taos Plateau. The San Luis Hills and similar horsts are flanked by rift basin-fill sediments.

Rio Grande Gorge—Upon exiting the San Juan Mountains, the Rio Grande turns southward, transects the San Luis Basin, and flows south through successive rift basins toward the Gulf of Mexico. The river follows the topographically lowest part of the rift, carving several spectacular canyons along the way. Beginning in southern Colorado, the Rio Grande has cut a steep-sided basalt canyon known as the Rio Grande gorge. The gorge deepens southward to 850 feet at the Wild Rivers Recreation Area near Questa (Fig. 9), and then gradually shallows as the Rio Grande flows through the southern San Luis Basin and into the Española Basin. The Rio Grande occupies a canyon through the San Luis Hills that represents the spillway of Pleistocene Lake Alamosa. The canyon was initially cut when the lake overtopped a saddle between the Fairy Hills and Brownie Hills approximately 440,000 years ago (Machette et al., 2007-Chapter G).

Geologic Units of the Northern Taos Plateau Study Area

The rocks and deposits exposed in the study area consist of: 1) surficial deposits of Quaternary age; 2) the Pliocene Servilleta Basalt; 3) other Pliocene lavas of the Taos Plateau volcanic field; 4) sediments of the Santa Fe Group; 5) mid-Tertiary (Oligocene) volcanic rocks of the Hinsdale Formation (and related units); and 6) Proterozoic crystalline basement rocks. These units are

Figure 8–The flat-topped San Luis Hills are predominantly composed of pre-rift volcanic units.

Figure 9–View upstream of Rio Grande gorge with Cerro Chiflo on left horizon.

shown on the geologic map (Fig. 10) and on a series of east-west and north-south geologic cross sections (Figs. 11a and 11b).

***Surficial Deposits*—**Surficial sedimentary deposits occur throughout the study area, but most are too thin to show on the geologic map and cross sections. Thin sheets of eolian sand and silt (Holocene) exist throughout the area. Thicknesses are generally less than 2 meters. Fine-grained pond deposits (Holocene to upper Pleistocene) have accumulated in closed depressions (playas and craters) on basalts and other lava flows. Thicknesses are unknown, but could be as much as 5 meters. Some of the principal drainages contain mappable thicknesses of channel alluvium (Holocene) that consists of fluvial sand, gravel, and silt deposits. All of the moderate- to steep-sided volcanoes, and much of the San Luis Hills, are ringed by poorly sorted, fine- to coarse-grained, nonstratified colluvial deposits of Holocene to Pleistocene age. These gravitationally driven deposits are derived locally, and include extensive talus eroded from the bedrock highs and probably some small debris flows.

***Servilleta Basalt*—**A single type of volcanic rock volumetrically dominates the Taos Plateau, the olivine tholeiite flood basalts of the Servilleta Basalt. The gorge walls chiefly consist of thin, near-horizontal layers of this dark gray, pahoehoe, vesicular lava. The basalts were erupted from low-relief shield volcanoes, traveling as thin, molten sheets for tens of miles before solidifying. Prominent vent locations include Pinebetoso Peaks, La Segita Peaks, State Line vents, a cluster

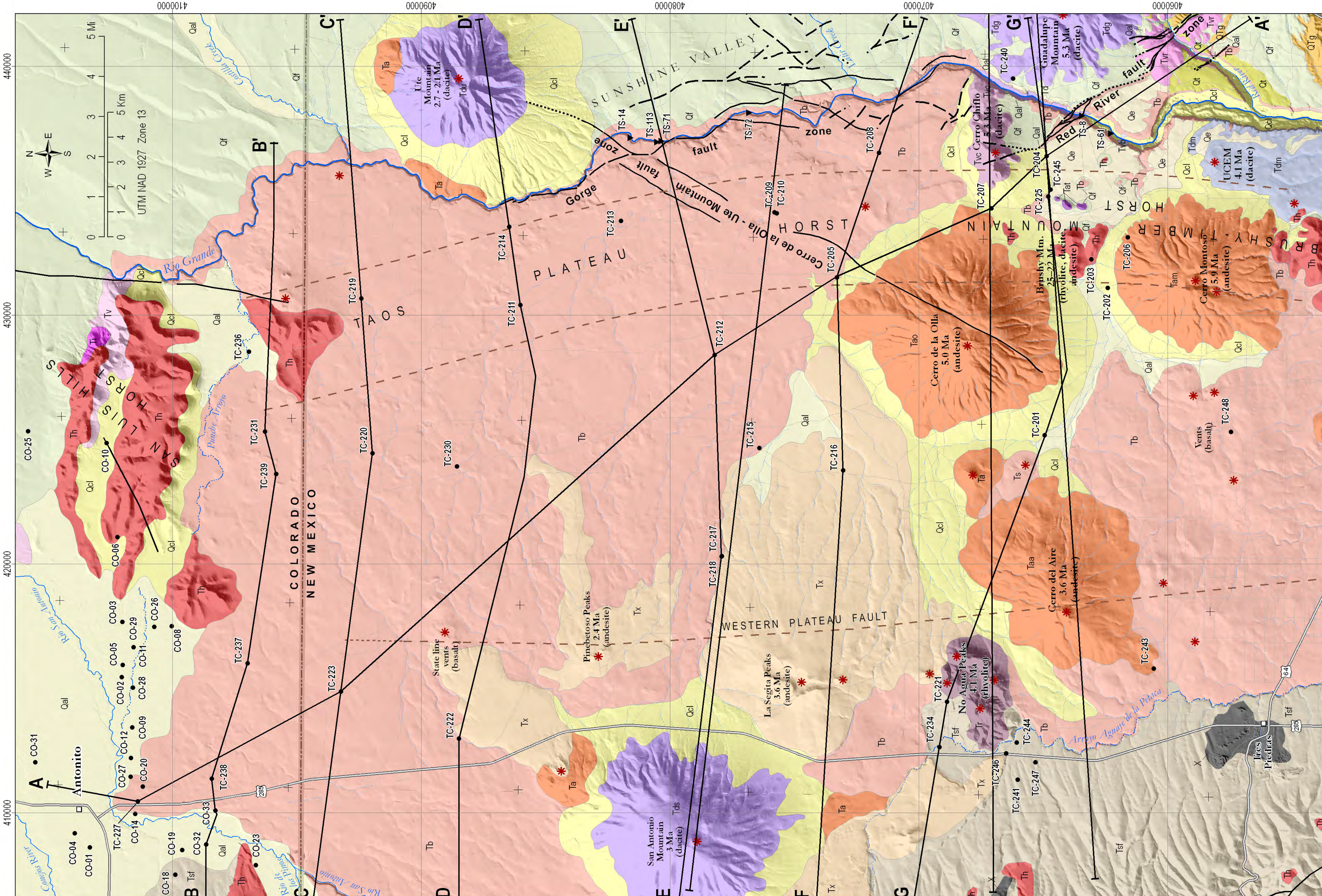

Figure 10—Geologic map of the northern Taos Plateau, New Mexico and Colorado.

of three low shields west of Cerro Montoso, and unnamed vents northwest of San Antonio Mountain. Over 600 feet of basalt were locally stacked up during about 2 million years of episodic eruptions, between about 4.8 and 2.8 million years ago. These rocks can be seen from any location along the gorge, and over much of the plateau surface in the study area.

Servilleta Basalt ranges in thickness across the Taos Plateau. Flows taper down to zero where they onlap preexisting volcanoes and other highlands. Basalts thin into the northwestern study area, and feather out to zero near Antonito. Gorge exposures in the southeastern map area, near the Red River confluence, demonstrate Servilleta thicknesses of at least 800 feet. The variable thickness and monolithic nature of these basalts make them poor stratigraphic markers that cannot be convincingly correlated in the subsurface using well data alone. These fluid lavas clearly flowed around topographic obstructions, and appear to have flowed around the east edge of the southern San Luis Hills and northward into the Alamosa Valley.

Servilleta basalts are extensively fractured, especially by columnar joints that tend to vertically penetrate entire basalt flows (Fig. 12). Many of the columnar fractures are open. Such basalt fracturing formed as each lava flow cooled, thus we expect the buried basalt units to also be extensively fractured, and therefore exceedingly permeable in the vertical dimension. In addition, the flow tops are typically characterized by highly vesicular ropy structures that create porous and permeable horizontal zones between flows.

Other Pliocene Lavas of the Taos Plateau Volcanic Field—Although volumetrically less important, the Taos Plateau also contains a wide compositional range of volcanoes, from rhyolite domes to andesitic and dacitic domes. Some of the volcanoes predate the 2.8-4.8 Ma Servilleta basalts, some overlap in time with the basalts, and some post-date the basalt eruptions. Where known, the latest, published, high-precision radiometric ages of the volcanoes are shown on the geologic map (Fig. 10).

The large lava domes of the study area are each composed of many small lava flows that have collectively built each volcanic edifice. Each volcano probably contained multiple vents, and all are therefore highly complex in three dimensions. Although each individual lava flow is composed of relatively dense, fine-grained rock of very low porosity, the flows do contain extensive fractures and rubble zones around their edges, which create local high-permeability horizons. Columnar joints are also common in some of the thinner flows. In addition, the dacite flows, such as on Cerro Chiflo, are mantled by extremely fractured rubble zones that formed as the lava cooled. Furthermore, the buried bases of the volcanoes may contain interlayered zones of clastic sediments. These volcanoes therefore contain complicated three-dimensional networks of high porosity and permeability zones intermingled with dense, low- or zero-permeability zones.

Santa Fe Group—Although some of the sediment that fills the rift basin was deposited by the Rio Grande, most of the clay, silt, sand, gravel, and cobbles were eroded from the nearby mountains during the past 25 million years. The San Luis Basin is surrounded by alluvial fans (and related deposits) that have slowly advanced from the mountains into the basin. In the Rio Grande rift, these deposits are called the Santa Fe Group. Over much of the basin, we can only see the youngest basin fill at the surface. However, glimpses of Santa Fe Group sediments exist in the gorge, commonly as red or tan layers sandwiched between basalt or dacite lava flows in the gorge walls. The youngest of these alluvial fans and ancestral Rio Grande river deposits overlie the Servilleta basalts along the perimeter of the basin and along the rim of the gorge.

The Santa Fe Group deposits in the study area can be roughly divided into two horizontal zones: 1) deep sedimentary deposits that are stratigraphically below the oldest Servilleta Basalt (i.e., older than about 5 million years); and 2) intermediate-depth sediments that are interbedded with the Servilleta Basalt units (i.e., between about 4.8 and 2.8 million years). In

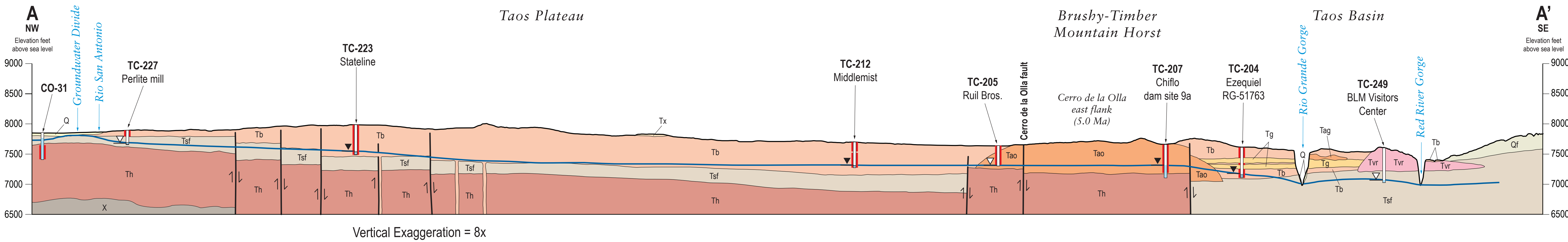

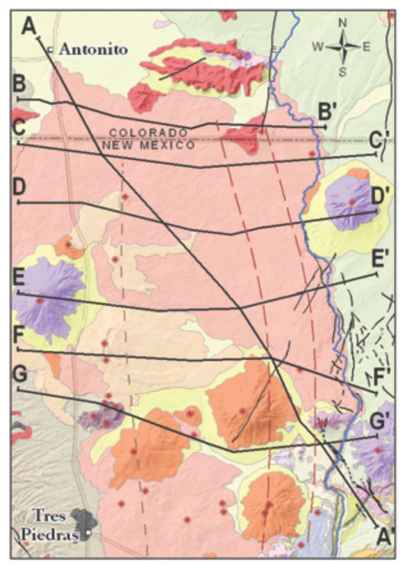

Figure 11A–(A) North-south and (B) east-west hydrogeologic cross sections through the northern Taos Plateau, showing approximate elevation of the water table for the regional aquifer.

Geologic Units

- Q — *Alluvium, undivided (Pleist. to Holocene)*
- Qf — *Alluvial fan deposits (mid-Pleist. to Holocene)*
- Tb — *Servilleta basalt (Pliocene)*
- Tg — *Servilleta interbasalt gravel (Pliocene)*
- Tsf — *Santa Fe Group (Miocene to Pliocene)*
- Tdu — *Dacite of Ute Mtn (Pliocene)*
- Tds — *Dacite of San Antonio Mtn (Pliocene)*
- Tx — *Xenocrystic basaltic andesite (Pliocene)*
- Taa — *Andesite of Cerro del Aire (Pliocene)*
- Tr — *Rhyolite of No Agua Peaks (Pliocene)*
- Tvr — *Volcanic rocks of Red River (Pliocene)*
- Tao — *Andesite of Cerro de la Olla (Pliocene)*
- Tdg — *Dacite of Guadalupe Mtn (Pliocene)*
- Ta — *Older andesites (Miocene or Pliocene)*
- Tat — *Amalia Tuff (Oligocene)*
- Th — *Hinsdale Formation and related rocks*
- X — *Proterozoic (Paleo- and Mesoproterozoic)*

Fault – Arrows show sense of vertical movement

Well Key

RG-63022 — OSE well file number
Chiflo — Well name (*Table 1*)

Well head (*actual elevation, if projected*)
Volcanic intervals, Tv (*from well record*)
Measured water-level
Recorded water-level
Screened interval

Aquifer Symbols

Water table surface in regional aquifer

0 1 Mi
0 1 Km

HYDROGEOLOGIC CROSS SECTIONS

We constructed seven detailed cross sections through the study area that depict the subsurface distribution of geologic and hydrostratigraphic units, faults, well data, rivers, streams and playas, and depth to water. A north-south cross section (A-A') is constructed generally perpendicular to regional groundwater flow and extends from Antonito north of the Rio San Antonio southeast across the Taos Plateau to the Rio Grande gorge and the Red River. East-west cross sections (B-B', C-C', D-D', E-E', F-F' and G-G') are constructed generally parallel to regional groundwater flow and extend from the western limit of the study area eastward across the Taos Plateau to the Rio Grande. Several cross sections dissect large volcanoes, including San Antonio Mountain (E-E'), La Segita Peaks (F-F'), Cerro de la Olla (F-F', G-G'), and No Agua Peaks (G-G'). Wells are rarely deep enough to penetrate the early Tertiary Hinsdale Formation and older rocks. In addition, available interpretations of gravity and aeromagnetic geophysical studies are inadequate for defining the shallow geology and geologic structures in the study area. Consequently, much of the subsurface geology shown on these cross sections is conceptual, based mainly on surface mapping, limited well data, and a consideration of the geologic history of the region. The cross sections therefore represent our current understanding of the subsurface distribution, location, and extent of hydrogeologic units of the northern Taos Plateau.

both cases, the sedimentary layers contain extensive vertical and horizontal compositional and textural variations due to the complex depositional environments found in the rift basin. A younger unit of Santa Fe Group is exposed east of the gorge as a vast piedmont slope deposit that represents large, coalescent alluvial fans derived from the major drainages in the Sangre de Cristo Mountains. Westward, these fans are interlayered with flows of the Taos Plateau volcanic field.

The characteristics of the deep sedimentary deposits are not well known, as they are not exposed in the basin, and few wells in the study area are drilled that deep. The sediments probably belong to the lower Chamita and Tesuque Formations of the Santa Fe Group. These lower Santa Fe Group alluvial deposits are typically composed of well-consolidated layers and lenses of clay, silt, sand, gravel, and cobbles.

Some of the intrabasalt sediments are exposed in the Rio Grande gorge. In general, these deposits are layered alluvial fan and fluvial deposits that are dominated by clay, silt, sand, and pebble- to cobble-sized clasts of Tertiary volcanic and Proterozoic metamorphic rock. Typically, these deposits are altered to a brick red color where overlain and baked by basalt flows.

Hinsdale Formation and Older Volcanic Units—Eruption of Oligocene lavas related to the San Juan volcanic field predated the formation of the structural Rio Grande rift. In the study area, these rocks are known as the Conejos Formation (ca. 30-29 Ma) and the Hinsdale Formation (ca. 26 Ma), which are separated by a major unconformity. Hinsdale rocks were deposited on a deeply eroded Conejos surface that had considerable topographic relief (Thompson and Machette, 1989). In the San Luis Hills, the unconformity is locally marked by discontinuous conglomerates of the Los Pinos Formation, a sediment that was derived from nearby Conejos Formation lavas (Thompson and Machette, 1989).

The Conejos Formation consists of andesite and dacite lava flows, flow breccias, lahar or mudflow breccias, and vent-facies pyroclastic rocks erupted or derived from local sources. Conejos rocks are locally intruded by hypabyssal andesite and dacite porphyry dikes that are apparently related to cogenetic quartz monzonite plutons and diorite stocks (Thompson and Machette, 1989).

The Hinsdale Formation consists of basaltic lava flows, associated breccia, and near-vent pyroclastic deposits (Thompson and Machette, 1989). These units typically cap the flat-topped mesas of the San Luis Hills near the state line. Locally, the Hinsdale contains layers of fine-grained eolian sediments interlayered with basalt flows.

For the purposes of this report, and the figures herein, the Conejos Formation and Los Pinos Formation rocks are lumped in with the Hinsdale Formation. This was done because no information on the subsurface extent and thickness of either of these units exists. It is possible that Conejos and Los Pinos rocks are locally shallow enough to be involved in the shallow regional

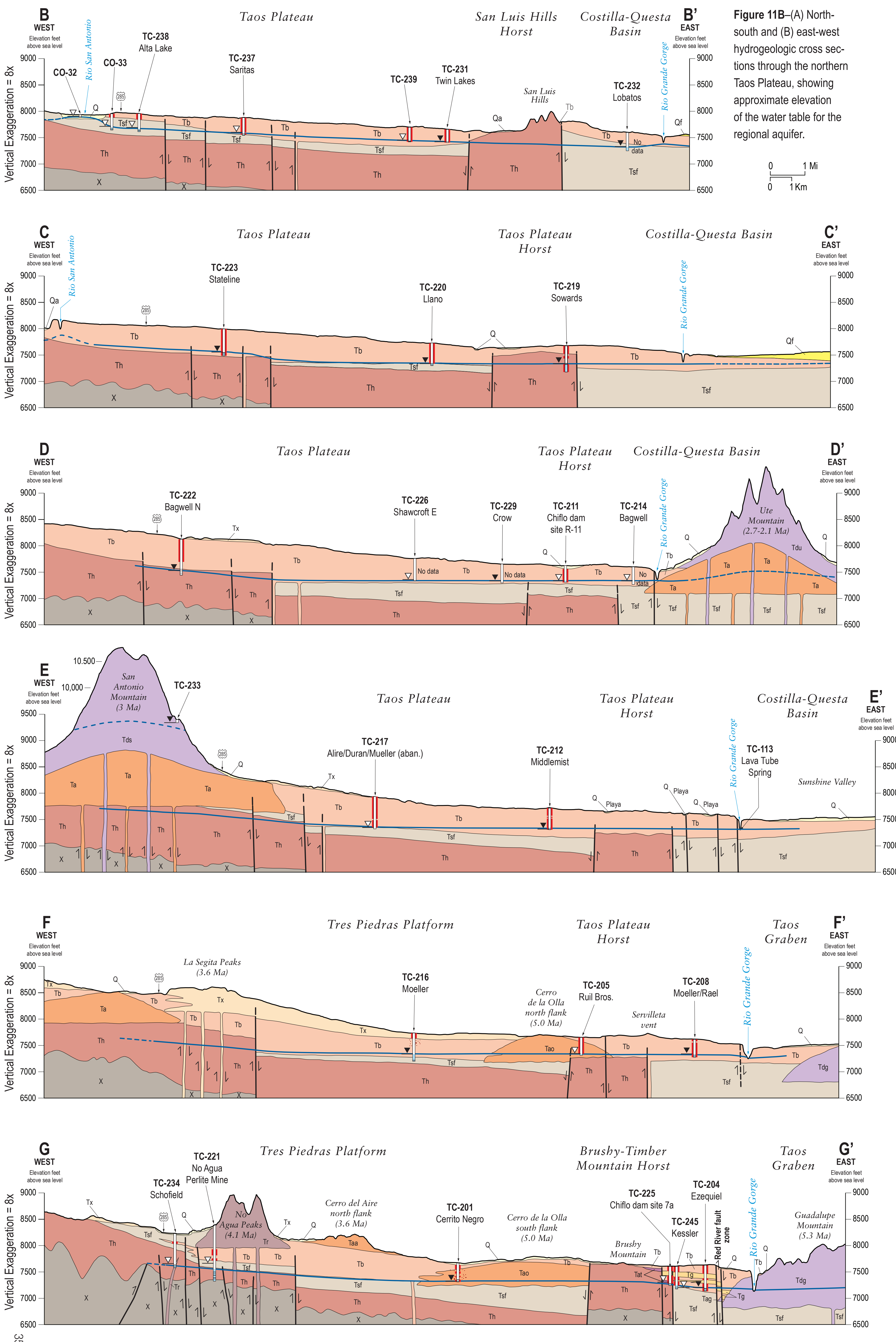

Figure 11B–(A) North-south and (B) east-west hydrogeologic cross sections through the northern Taos Plateau, showing approximate elevation of the water table for the regional aquifer.

Figure 12–Dense columnar jointing of Servilleta Basalt in the Rio Grande gorge.

aquifer along the western edge of the study area and along the San Luis Hills, Taos Plateau, and Brushy-Timber Mountain horsts.

Erosional remnants on Timber Mountain and Brushy Mountain display a small volume of post-caldera volcanism of the Latir volcanic field (Thompson et al., 1986). The rocks are predominantly dacitic lavas, but include flows of andesite and rhyolite lavas, and ash flow tuffs.

Even though the Hinsdale Formation rocks are considerably older than the Pliocene rocks of the Taos Plateau volcanic field, the basalt-dominated Hinsdale can be quite similar in appearance to the younger Servilleta Basalt, and where the two formations are contiguous, they could be easily mistaken in lithologic logs from drill holes.

Basement Rocks—In the study area, Pre-Tertiary rocks are exposed in several erosional windows of Proterozoic granite near Tres Piedras, where they form a shallow east-tilted platform between the Tusas Mountains and the Brushy-Timber Mountain horst. The granite occurrences represent basement topographic highs that were onlapped and covered by Tertiary units. These ancient hills indicate that the pre-rift landscape probably had considerable topographic relief. Proterozoic rocks certainly underlie all of the study area, but appear to be shallow enough to interact with the top of the Taos Plateau regional aquifer only in the southwest corner of the study area.

Geologic Structures of the Northern Taos Plateau Study Area

Faults and Related Structures—The study area contains the following fault zones or inferred fault zones: 1) the Red River fault zone; 2) the Gorge fault zone; 3) the Cerro de la Olla-Ute Mountain fault zone; 4) the San Luis Hills horst; 5) the Brushy/Timber Mountain horst; 6) the inferred Taos Plateau horst; and 7) the inferred Western Plateau fault.

The Red River fault zone (Peterson, 1981; Dungan et al., 1984; Kelson et al., 2008) is an east-dipping rift fault system that transects the Red River and Rio Grande gorges in the south-eastern map area (Fig. 13). The faults are well exposed in the gorge where they form open, brittle fracture zones in the Servilleta basalts. The fault zone consists of several steeply dipping, east-down, normal, en echelon fault segments that offset Pleistocene gravels in the Wild Rivers Recreation area. The faults strike northwesterly from near Lama to Cerro Chiflo, whereupon their surface expressions are lost. We suspect that they exist in the subsurface, where they merge northward with the eastern limb of the northern extension of the proposed Taos Plateau horst.

The Gorge fault zone is a complex swarm of small normal faults that are shown on USGS maps of the Sunshine and Ute Mountain 7.5-minute quadrangles (Machette et al., 2007). The faults are generally north striking and clustered along the Rio Grande gorge. These faults were determined by a combination of field mapping and preliminary interpretation of high-resolution aeromagnetic data by USGS mappers. They are similar to gorge-parallel faults mapped to the south, such as the Dunn fault (Kelson and Bauer, 2006), and may represent the surface expression

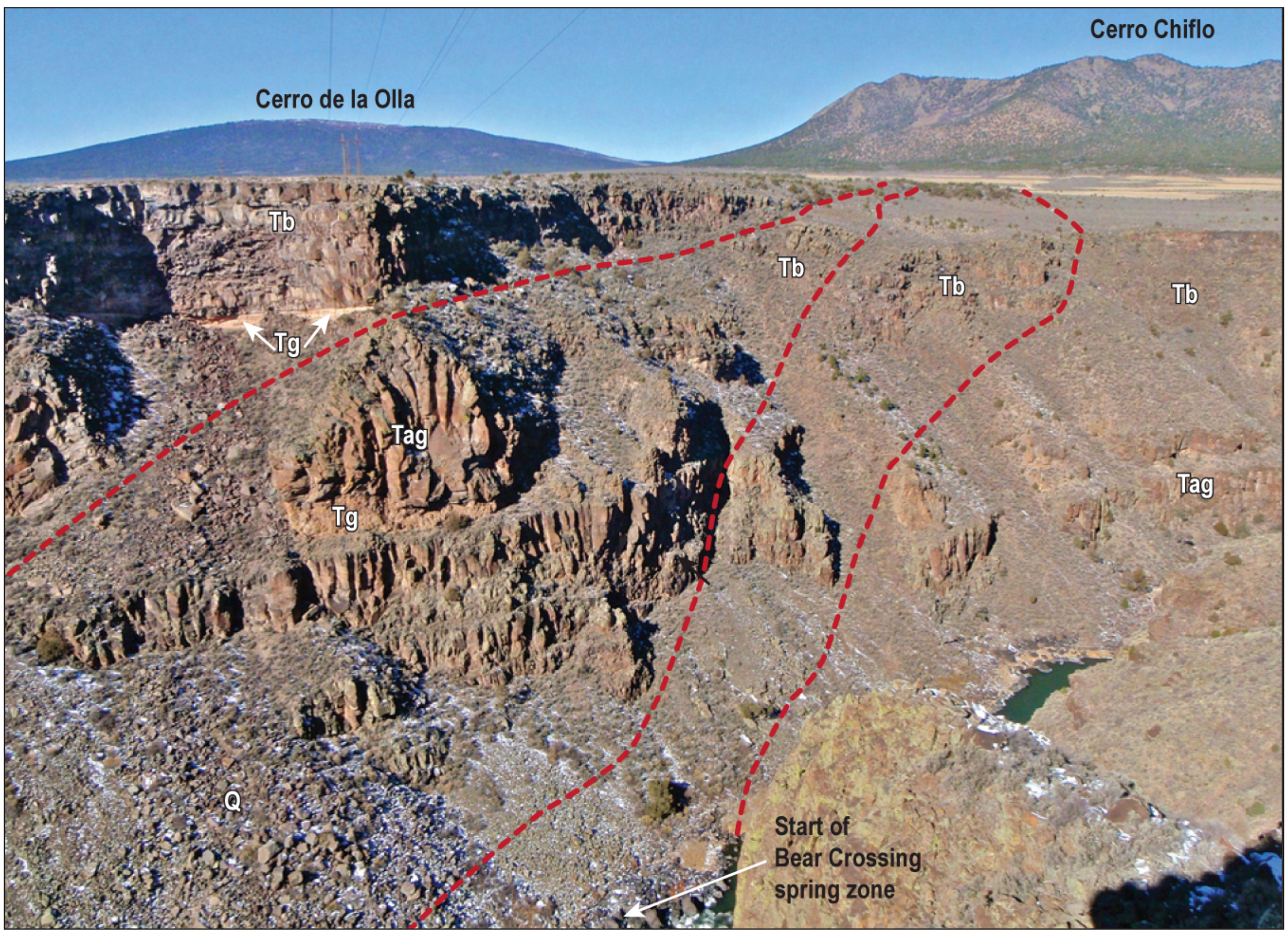

Figure 13–View northwest across the Rio Grande gorge along the Red River fault zone. Three en echelon, east-down fault splays offset Servilleta Basalt (Tb) and overlying Quaternary gravel. The youngest basalts show about 100-130 feet of vertical separation across the fault (Kelson et al., 2008). Thicknesses of basalts and intra-flow sediments (Tg) change abruptly across the faults. Volcanic rocks are extensively fractured along the faults, and the large, west-side springs of the Bear Crossing spring zone are coincident with the fault zone.

of the Gorge fault mapped to the south, which is the western structural boundary of the Taos graben (Kelson and Bauer, 2003). We have shown these USGS-mapped faults between Ute Mountain and Cerro Chiflo on the geologic map (Fig. 10).

The Cerro de la Olla-Ute Mountain fault zone is expressed as a zone of topographic lineaments that strike northeastward from Cerro de la Olla to the base of Ute Mountain (Fig. 10). USGS workers reported that the linears represent "late-middle Pleistocene to Holocene fault scarps" (Machette et al., 2007). However, due to the volcanic landscape and a lack of Quaternary surficial deposits, it is difficult to find direct field evidence (e.g., slickenlines, fault striations, breccia zones, and fault offsets) of these features.

The San Luis Hills are the northernmost surface expression of a major intrarift horst (San Luis Hills horst) within the central part of the San Luis basin. Two Oligocene igneous sequences are exposed in the San Luis Hills, an older intermediate-composition volcanic-intrusive assemblage and unconformably overlying basaltic rocks of the Hinsdale Formation (Thompson et al., 1991). Brister and Gries (1994) concluded that much of the structural relief observed in the subsurface of the northern San Luis Valley, including the San Luis Hills horst, predates rifting and is probably due to Laramide deformation. The geologic map of the southern San Luis Hills by Thompson and Machette (1989) shows no faults along the flanks of the hills, although the regional geologic map included in the 2004 NMGS Guidebook on page 114 (Brister et al., 2004) shows a fault along the east edge of the horst in southernmost Colorado. We have included this fault on our geologic map (Fig. 10). In geologic cross section B-B' (Fig. 11b), we have drawn high-angle, north-striking faults along both the east and west flanks of the southern San Luis Hills. Although we suspect that such horst-bounding faults do exist, their geometries and kinematic histories are unknown.

Two sets of hills north (Brushy Mountain, Fig. 14) and south (Timber Mountain) of Cerro Montoso contain Oligocene volcanic rocks that are similar to the San Luis Hills exposures (Thompson et al., 1991). Previous workers have concluded that they represent the eroded surface expression of an intrarift horst. We refer to this structural high as the Brushy-Timber Mountain horst (Fig. 10). Although the actual horst-bounding faults are buried by rift-fill sediments and younger lava flows, we have drawn one permissible fault geometry in cross section G-G' (Fig. 11b).

Similar volcanic units of the Hinsdale Formation are thus exposed at Brushy Mountain-Timber Mountain in the southern study area and in the San Luis Hills in the northern study area. On the geologic map, we show the trace of

Figure 14–View northwest of the cluster of hills, including Brushy Mountain, that expose older Tertiary volcanic rocks of the Brushy-Timber Mountain horst. Cerro de la Olla looms in the background.

an inferred, buried, continuous, structural high connecting these horsts beneath the eastern Taos Plateau (Fig. 10). In cross sections C-C', D-D', E-E', and F-F' this herein informally named Taos Plateau horst is shown to be bordered by steep, north-striking, normal faults (Fig. 11b). The Red River fault, which is well mapped in the Guadalupe Mountain quadrangle, is inferred northward from Cerro Chiflo to merge with the eastern fault zone of the Taos Plateau horst. We believe that an ongoing study of gravity and magnetic geophysical data from the Taos Plateau by USGS scientists will help to evaluate our proposed structural geometry for this part of our study area.

To the south and west of our field area, the western flank of the rift is marked by many north-striking normal faults and fracture zones (Fig. 7). Although no such faults have been mapped and published in our study area, there is a north-trending alignment of volcanic vents extending from south of Cerro del Aire northward to the State Line vents. We postulate a series of buried, rift-related faults and fractures approximately coincident with these vents, as conceptualized on the cross sections (Fig. 11b). These buried faults could have provided conduits for ascending magma. One of the inferred faults, labeled "Western Plateau fault" on the geologic map (Fig. 10), is shown as the largest displacement fault on the geologic cross sections (Fig. 11b). This fault zone was drawn to roughly coincide with the easternmost alignment of volcanic centers in the western study area. The Western Plateau fault is also coincident with an anomaly in the regional groundwater gradient.

Hydrogeologic Cross Sections

Many observations and interpretations of the Taos Plateau groundwater flow system were made from an analysis of geologic cross sections, well and water-level data. Based on an analysis of 58 lithologic logs from water well records (Appendix A, Tables 1 and 2) and the geologic maps (Figs. 7 and 10), we constructed seven detailed cross sections (Figs. 11A and 11B) through the study area that depict the subsurface distribution of geologic and hydrostratigraphic units, faults, well data, and hydrologic features and characteristics including rivers, streams, springs, playas, and depth to groundwater. These cross sections illustrate the distribution, location, and extent of aquifers in the context of both the geologic framework and surface water features. Integrating geologic and hydrologic information on the cross sections provides insight regarding distribution of aquifers and the geologic controls on groundwater flow.

IV. HYDROLOGIC SYSTEMS OF THE NORTHERN TAOS PLATEAU

Hydrostratigraphic Units

The distribution of hydrostratigraphic units is best understood through examination of the geologic maps and cross sections (Figs. 10, 11). Five major hydrogeologic units exist beneath the northern Taos Plateau: 1) Tertiary Servilleta Basalt and thinly interlayered sediments (Tb); 2) Pliocene lava domes composed of dacites (Td), andesites (Ta), and rhyolites (Tr); 3) Tertiary Santa Fe Group alluvial deposits (Tsf) that lie below the oldest Servilleta Basalt and other lava flows and domes; 4) Oligocene-Miocene Hinsdale Formation and older volcanic and volcaniclastic units (Th); and 5) Proterozoic granitic bedrock (X).

Servilleta Basalt (Tb) and Santa Fe Group Alluvial Fill (Tsf)—Regional groundwater beneath the Taos Plateau occurs primarily within the Servilleta Basalt and the Santa Fe Group alluvial deposits that lie below the oldest basalt layer. This groundwater reservoir, which we call the "Taos Plateau aquifer" or the "regional aquifer", generally exists under unconfined conditions. Most wells on the Taos Plateau in New Mexico draw groundwater from the Servilleta Basalt, whereas virtually all Colorado wells tap Santa Fe Group alluvium (Table 1, Fig. 11). Lithologic logs on well records indicate that basalts are thick, continuous, and interbedded with thin sedimentary layers of clay, silt, or sandy clay. Fractured basalt, caverns, lost circulation, and blowing holes are common notations in drillers' logs and geologic field notes, implying locally high (in some cases extreme) vertical and horizontal permeability and high anisotropy. The uppermost layers of the Santa Fe Group alluvial fill that underlie Servilleta Basalt are reported to include sand, sandstone, clay and sandy clay with minor gravel and conglomerate.

South of the state line in New Mexico and east of the Western Plateau fault, wells are completed primarily within the Servilleta Basalt, with water depth ranging from 241 to 620 ft and yields ranging from 2.5 to 100 gallons per minute (gpm). The average yield is 29 gpm. Servilleta Basalt progressively thins to the northwest and pinches out along the south bank of the Rio San Antonio, just south of Antonito, Colorado. Between the state line and the Rio San Antonio, thin Servilleta Basalt is generally unsaturated and lies above saturated Santa Fe group alluvium (cross section A-A' Fig. 11a, cross section B-B' Fig. 11b). In wells southeast of Antonito (TC-237, TC-239, TC-231), groundwater is first encountered in the basal portion of the Servilleta Basalt or the underlying Santa Fe Group alluvium. From the Rio San Antonio north into Colorado, all wells are completed in the Santa Fe Group. In the Colorado wells catalogued for this study, depth to water in the Santa Fe Group alluvium ranges from 18 to 294 ft. The average well yield is 375 gpm. For wells completed in the Santa Fe Group in New Mexico, depth to water ranges from 390 to 660 ft.

Pliocene Lava Domes (Td, Ta, Tr, Tv)—Pliocene lava domes with various volcanic compositions (dacite, andesite and rhyolite) comprise a significant portion of the shallow subsurface in the vicinity of the large volcanoes situated on the plateau. Nine wells are located on or near the flanks of these volcanic domes (Table 1), and in most cases the wells have water levels elevated slightly or significantly above the regional aquifer. For wells completed in a volcanic dome, the depth to water ranges from 300 to 619 ft below land surface and yields range from 10 to 56 gpm.

In some cases, an elevated water level in or near a volcanic dome indicates the presence of a localized perched aquifer, which is disconnected from the regional aquifer. For example, a shallow, hand-dug well high on the east flank of San Antonio Mountain (TC-233) has a water level elevation of 9227 ft, over 1600 ft above the surface of the regional aquifer at the base of the mountain, and taps a perched aquifer within the dacite dome (cross section E-E' Fig. 11b). Downward migration of groundwater from the perched zone, through fracture and rubble zones in the dacite, is believed to recharge the regional aquifer with groundwater sourced from precipitation at higher elevations on San Antonio Mountain. We observed rapid water flow through the open hole of well TC-233, which suggests a high rate and volume of localized recharge. The isotopic and chemical characteristics of the San Antonio Mountain perched volcanic aquifer will be discussed in later sections of the report. Well TC-202 on the north flank of Cerro Montoso and well TC-252 on the north flank of Ute Mountain both show water levels elevated more than 100 feet above those measured in nearby wells.

Elevated water levels beneath or adjacent to a volcanic dome can also signify a recharge mound in the regional aquifer. For example, wells at the base of Cerro de la Olla (TC-205 and TC-207) (cross section F-F' Fig. 11b) have water levels elevated by 20 ft above the surface of the regional aquifer in adjacent or underlying Servilleta and older Tertiary units. Wells completed in the regional aquifer in Santa Fe Group or Hinsdale sediments (TC-221) or rhyolitic rocks (TC-234) that underlie No Agua Peaks (cross section G-G' Fig. 11b) also have elevated water levels. Based on these water-level data, we propose that Cerro de la Olla and No Agua Peaks are recharge zones for the adjacent and underlying regional aquifer.

Hinsdale Formation and Older Volcanic Units (Th)—South of the state line in New Mexico and west of the Western Plateau fault, the Hinsdale Formation and older volcanic and volcaniclastic rocks comprise the primary hydrogeologic units (cross sections D-D', E-E', F-F' and G-G' Fig. 11b). Near the state line, Servilleta Basalt directly overlies Hinsdale basalts (cross section C-C' Fig. 11b). Both units may produce water, but only a thin basal section of Servilleta is likely saturated and the Hinsdale Formation forms the principal aquifer. Progressing southward, and west of the Western Plateau fault, Hinsdale and older Tertiary units contain the regional aquifer (cross section D-D', E-E', F-F' Fig. 11b). Although thin intervals of Santa Fe Group alluvium and localized rhyolitic feeder dikes form part of the aquifer beneath No Agua Peaks, these are limited in extent and the Hinsdale Formation forms the regional aquifer (cross section G-G' Fig. 11b). Depth to water in the Hinsdale Formation west of the Western Plateau fault ranges from 600 to 727 ft. The Hinsdale Formation also forms part of the Taos Plateau aquifer where it is uplifted along the San Luis Hills and Brushy-Timber Mountain horsts. Depth to water over the horst ranges from 200 to 400 ft. Well yields from the Hinsdale Formation range from 15 to 35 gpm.

Proterozoic Granitic Rocks (X)—Proterozoic granite forms a shallow east-tilted platform between the Tusas Mountains and the Brushy-Timber Mountain horst. Near Tres Piedras, these granitic rocks are exposed at the surface and comprise the only available aquifer. Three wells catalogued in this study are completed in these basement rocks near Tres Piedras. The wells range in depth from 780 to 960 feet. Minimal well yields of 1 gpm are reported.

Taos Plateau Regional Aquifer

A contoured water table surface for the regional aquifer beneath the Taos Plateau, based on 39 measured and 22 reported static water levels (Tables 1 and 2), is shown in Figure 15. The

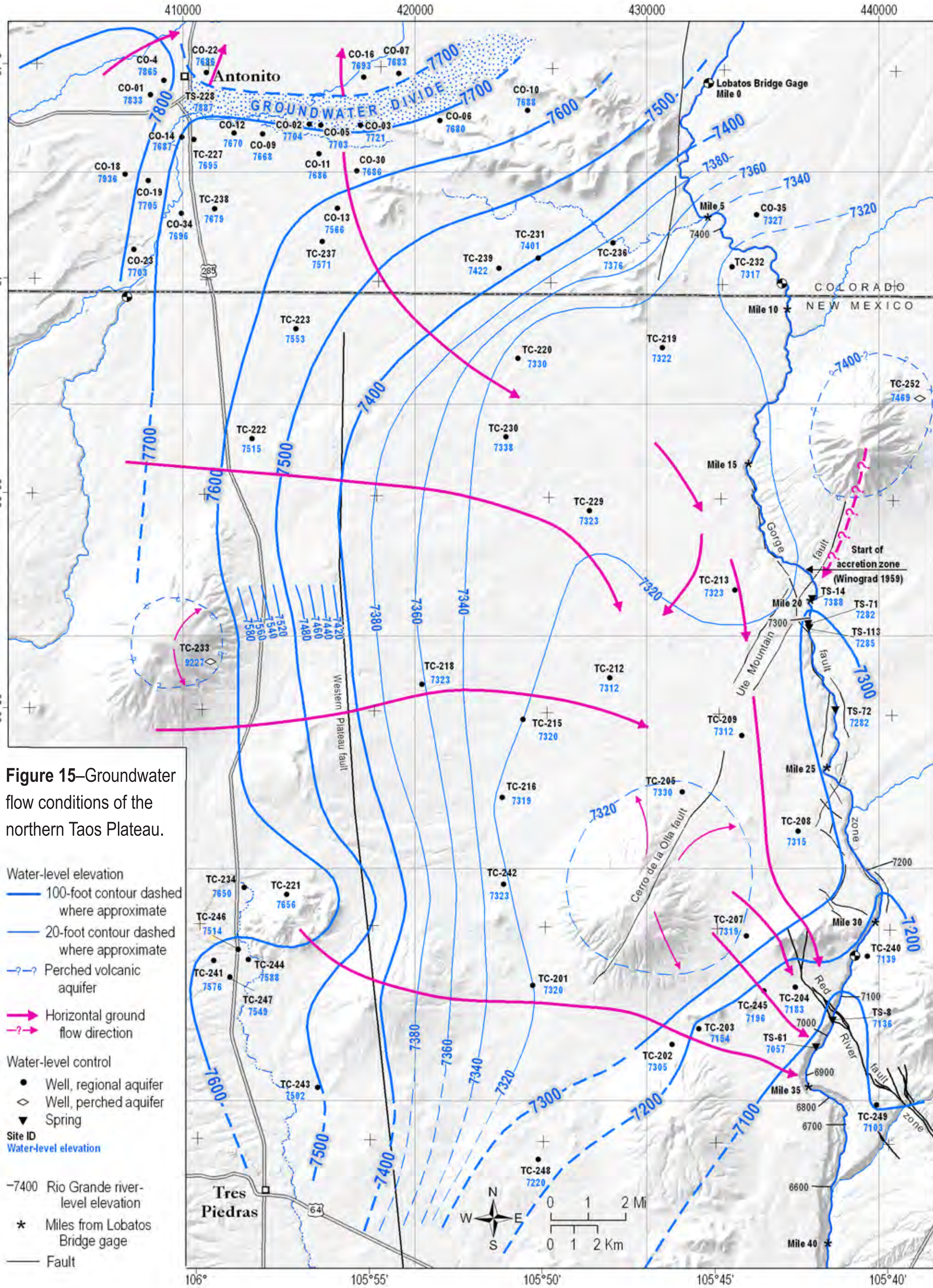

Figure 15–Groundwater flow conditions of the northern Taos Plateau.

water table surface defines a regional groundwater flow system driven by a hydraulic gradient from the Tusas Mountains to the west. Groundwater flow is generally eastward toward the Rio Grande gorge. West of the Western Plateau fault near the county boundary, the magnitude of the hydraulic gradient is about 70 ft/mi. East of the Western Plateau fault, we show a hydraulic gradient ranging from as little as 2.5 ft/mi up to 13 ft/mi. Winograd (1959) estimated a hydraulic gradient of 4 ft/mi over this area. The decrease in gradient likely reflects a contrast in aquifer permeability between the Hinsdale Formation (relatively low permeability) to the west and the Servilleta Basalt (relatively high permeability) to the east, which we believe are juxtaposed across the fault (cross sections C-C', D-D' and E-E' Fig. 11b). A hydraulic gradient of 70 ft/mi is also observed in Hinsdale basalts in the San Luis Hills to the northeast. Previous studies (Winograd, 1959; Benson, 2004) also note a flattening of the water table under the eastern half of the plateau. Local conditions causing or contributing to the flat gradient include high permeability in the fractured-basalt aquifer, flat topography, and high infiltration and recharge rates through the lava-capped plateau.

Just west of the Rio Grande gorge, the water table surface (Fig. 15) demonstrates a southerly and southeasterly flow direction flanking the inferred eastern boundary of the Taos Plateau horst, and also indicates a possible recharge mound beneath the Rio Grande in the Ute Mountain reach, upstream of river mile 19. However, the groundwater flow direction is poorly constrained because of minimal water-level data and the flat hydraulic gradient. Additional water-level data, particularly east of the Rio Grande and near Ute Mountain, are required to better define the direction of groundwater flow in this region. We also note, as did Winograd (1959), that southeast of Cerro de la Olla and east of the Brushy-Timber Mountain horst, the water table grades steeply to the Rio Grande through thick Santa Fe Group alluvium (Figs. 11a, 15).

Local mounds and ridges in the water-table surface demonstrate the effects of local topography and recharge superimposed on regional flow. A groundwater mound beneath the Rio San Antonio near Antonito, Colorado forms a subtle groundwater divide that extends east and northeast into the San Luis Hills north of Punche Arroyo (Fig. 15). From this divide groundwater flows southeast into New Mexico and north into the San Luis Valley of Colorado. There is no hydraulic evidence of groundwater flow from the San Luis Valley north of Antonito into the Taos Plateau regional aquifer. This finding is contrary to that of Benson (2004, p. 420) who reported that "... recharge is probably mainly from the San Juan Mountains headwaters of the Rio Grande in southwest Colorado, through the Alamosa Valley, with a very long residence time."

Underflow and Groundwater Recharge

Multiple sources contribute water to the Taos Plateau aquifer. These include groundwater underflow from the Tusas highlands, recharge on large volcanic domes, precipitation and recharge through the lava-capped plateau, and stream recharge from the Rio Grande and Rio San Antonio. Winograd (1959) first suggested that recharge to the Taos Plateau "derived principally from seepage of surface-water runoff from the highlands bordering the plateau on the west." Based on hydrologic data (Fig. 15) and geochemical data discussed later in this report, we concur that groundwater underflow along the western boundary of the study area originates in the Tusas Mountains, with possible contributions from San Antonio Mountain.

Modern surface runoff from the northern Tusas highlands is through the Rio San Antonio and Rio de los Pinos, which are diverted north around San Antonio Mountain and the Taos Plateau volcanic field to join the Rio Conejos in the Alamosa Valley (Fig. 3). Modern surface runoff from the southern Tusas highlands drains to the ephemeral Arroyo Aguaje de la Petaca, which enters the Taos Plateau south of No Agua and crosses the southwest corner of the volcanic field. Groundwater mounds beneath the Rio San Antonio near Antonito, Colorado and the Rio Grande near Ute Mountain (Fig. 15) indicate that these are influent stream reaches that recharge the regional aquifer. Recharge from the Rio Grande was also noted by Winograd (1959, p. 39), who observed that the water table was below river level from about river mile 19 to 4.5 miles north of the Colorado-New Mexico line, and that water levels in nearby test holes showed an upward bulge of the water table beneath the river, indicating that the river was losing water.

There is ample geologic and hydrologic evidence of significant recharge to the Taos Plateau aquifer from precipitation directly on the surface of the lava plateau and volcanic domes. Precipitation in northern Taos County varies with elevation. In the lower elevations of the plateau, the average annual precipitation varies slightly from 12.3 inches at Taos to 13.9 inches at Tres Piedras (Appendix D, Table D1). However, the increase in precipitation with elevation is significant. Means of annual precipitation on the volcanic domes of the northern plateau, estimated from a precipitation-elevation regression of regional climate data (Appendix D, Fig. D1), range from 16.5 inches on Cerro Negro, the smallest andesite dome, to 27 inches at the crest of San Antonio Mountain (Appendix D, Table D2 and Fig. 16). The crest of Cerro de la Olla receives an estimated 21.4 inches of precipitation annually, and Ute Mountain, a large dacite dome east of the Rio Grande, accumulates up to 23.9 inches. Local perched aquifers are documented in shallow wells drilled on San Antonio Mountain (TC-233), Cerro Montoso (TC-202), and Ute Mountain (TC-252) (Fig. 15). High precipitation rates, elevated water-levels, and perched aquifers on volcanic domes indicate that these volcanic highlands are

Figure 16–View west of the eastern flanks of San Antonio Mountain with a late-spring (May 2008) snowpack engulfing the upper third of the mountain. Note that only poorly developed drainages exist on the mountain's lower slopes, indicating that surface runoff from San Antonio Mountain is not an important recharge process for the plateau.

Figure 17–Large playa located at eastern end of a closed basin in the center of the Taos Plateau was filled by snowmelt and rainwater in May of 2008. Area of the playa was estimated to be at least 5 acres.

significant sources of recharge to the Taos Plateau regional aquifer.

The lack of surficial drainage, either on the plateau or from the volcanic domes, and abundance of closed or poorly integrated drainage basins (Fig. 4) attest to rapid infiltration of rainwater, storm runoff, and snowmelt into the fractured basalt flows and volcanic edifices of the plateau. Closed surface-water basins containing numerous clay- or silt-lined craters and playas comprise about 20 percent of the study area. One such playa lake, covering an estimated 5 acres, was observed during field work in May 2008 (Fig. 17). Local recharge from closed basins and playas on the basalt plateau likely contributes to the flat water table beneath the eastern half of the Taos Plateau (Fig. 15).

Groundwater Discharge

Previous Studies—Significant gains to the Rio Grande from adjacent groundwater aquifers were first measured in seepage runs by Bliss (1928) between Lobatos gage in Colorado and the Red River confluence. Winograd (1959) described a groundwater accretion zone where the river appeared to be at a lower elevation than the water table in the Sunshine Valley to the east. The accretion zone was described as beginning "... approximately 2 miles downstream of the proposed Ute Mountain dam site ..." (Fig. 15), which corresponds to river mile 19 just south of Ute Mountain. Based on scarce water-level data from the Taos Plateau, Winograd (1959) further proposed that "this gain in the Rio Grande is from the ground-water reservoir beneath the lava-capped plateau to the west, Sunshine Valley to the east, and Colorado to the north ...". No in-depth hydrogeologic study has ever addressed the recharge and discharge characteristics of the Taos Plateau regional aquifer or how and where the aquifer may contribute to spring discharge and stream gain in the Rio Grande gorge.

Recent contributions to our understanding of the hydraulic connection between the Taos Plateau aquifer and the Rio Grande come from the spring surveys of Bauer et al. (2007) and seepage studies conducted by Kinsli et al. (2011). During spring studies of the Rio Grande gorge, several large springs and spring zones along both east and west banks and within the river channel were surveyed, described and sampled. Seepage studies defined gaining, losing, and neutral reaches of the river and the magnitudes of gains and losses between Lobatos gage in Colorado and the Red River confluence (Kinsli et al., 2011). Results of these studies are very relevant to the questions of groundwater flow and discharge from the Taos Plateau aquifer.

Spring Discharge and Stream Flow in the Rio Grande Gorge—Gains in the Rio Grande in the Taos Plateau field area are focused in two short river reaches characterized by large spring discharges (Fig. 18). These spring zones coincide with two structural features of the Taos Plateau, the Ute Mountain fault zone in the north and the Red River fault zone in the south, and are herein named the Ute Mountain spring zone and the Bear Crossing-Felsenmeere spring zone, respectively. Two small intervening spring zones, Sunshine springs and Chiflo springs, are also described.

Lobatos to Ute Mountain (river mile 0–19.5). Seepage runs by Kinsli et al. (2011) quantified a loss of about 2 cfs through the upper gorge (river mile 0 to 19.5). Water-level data, from this study and Winograd (1959), show that the surface of the regional water table lies below the channel of the Rio Grande and indicate the presence of a recharge mound. There are no springs discharging to the river channel in this reach.

Ute Mountain spring zone (river mile 19.5–21). The first seepage gains to the Rio Grande in New Mexico occur in a 1.5-mile reach beginning at river mile 19.5 south of Ute Mountain via spring discharge from both banks of the river and directly into the river channel (Fig. 18). The start of this spring zone generally correlates to the start of Winograd's (1959) accretion zone as well as the intersection of the Ute Mountain fault with the Rio Grande gorge (Fig. 10). This reach is characterized by abundant discrete springs, large spring zones, and saturated seepage faces created by small springs and seeps that commonly extend a hundred yards or more along both banks. Discharge vents are typically located 5 to 15 feet above river level and generally show a hydraulic head elevated well above the channel bottom. The river gradient is constant and relatively flat (Fig. 18). The magnitude of discharge for any given spring ranges from a gallon per minute or less to hundreds of gallons per minute. The number and discharge of springs increases downstream, culminating in a large subaqueous spring discharging approximately 13 cfs (6000 gpm) from a cavern in the river channel (Bauer and Johnson, 2010). This spring, named Lava Tube spring (TS-113), demarcates the end of the Ute Mountain spring zone and spatially coincides with the Gorge fault (Fig. 10). Geochemical data for three springs in this zone (TS-14, TS-71, TS-113 in Table 3) are discussed in later sections of this report. Seepage runs by Kinsli et al. (2011) quantified a gain of approximately 37 cfs for the Ute Mountain spring zone.

Sunshine Valley (river mile 21–31). The 10-mile river reach between the bottom of the Ute Mountain spring zone and the Cerro gage at river mile 31 aligns with the Sunshine Valley east of the gorge. This stretch of river is devoid of large springs, but does contain two zones where small springs and seeps are concentrated. The Sunshine spring zone north of Latir Creek (Fig. 18) contains several small seeps, springs, and seepage faces discharging along both east and west banks. This includes a nearly continuous, half mile-long zone of east-side seeps and springs that emerge from beneath a basalt flow at the base of the canyon wall (Bauer et al., 2007), many of which were noted to be dry during field work in September 2008. This zone also contains at least two small west-side springs, including TS-72 (Table 3). The Chiflo spring zone south of Latir Creek and north of the Cerro gage (Fig. 18) also contains a small group of east- and west-side springs in the vicinity of Cerro Chiflo. Cumulative discharge for the Sunshine and Chiflo springs estimated by Bauer et al. (2007) and other unpublished field work is approximately 50 to 60 gpm. However, Kinsli et al. (2011) measured a loss of 13 cfs for the Sunshine Valley reach (Fig. 18), suggesting that more than 13 cfs is actually lost above the Chiflo springs (river mile 29-31).

Bear Crossing-Felsenmeere spring zone (river mile 33–34). Nested within the river reach known as the Upper Taos Box (Cerro gage (river mile 31) to the Red River confluence (river mile 38)) is a 1.5 mile-long zone of springs discharging from the west canyon wall downstream of the Bear Crossing Trail (Fig. 18) (Bauer et al., 2007). The upper line of springs is known as the Bear Crossing spring zone and the lower cluster of three springs is named Felsenmeere. The Bear Crossing springs emerge 50 to 100 or more feet above

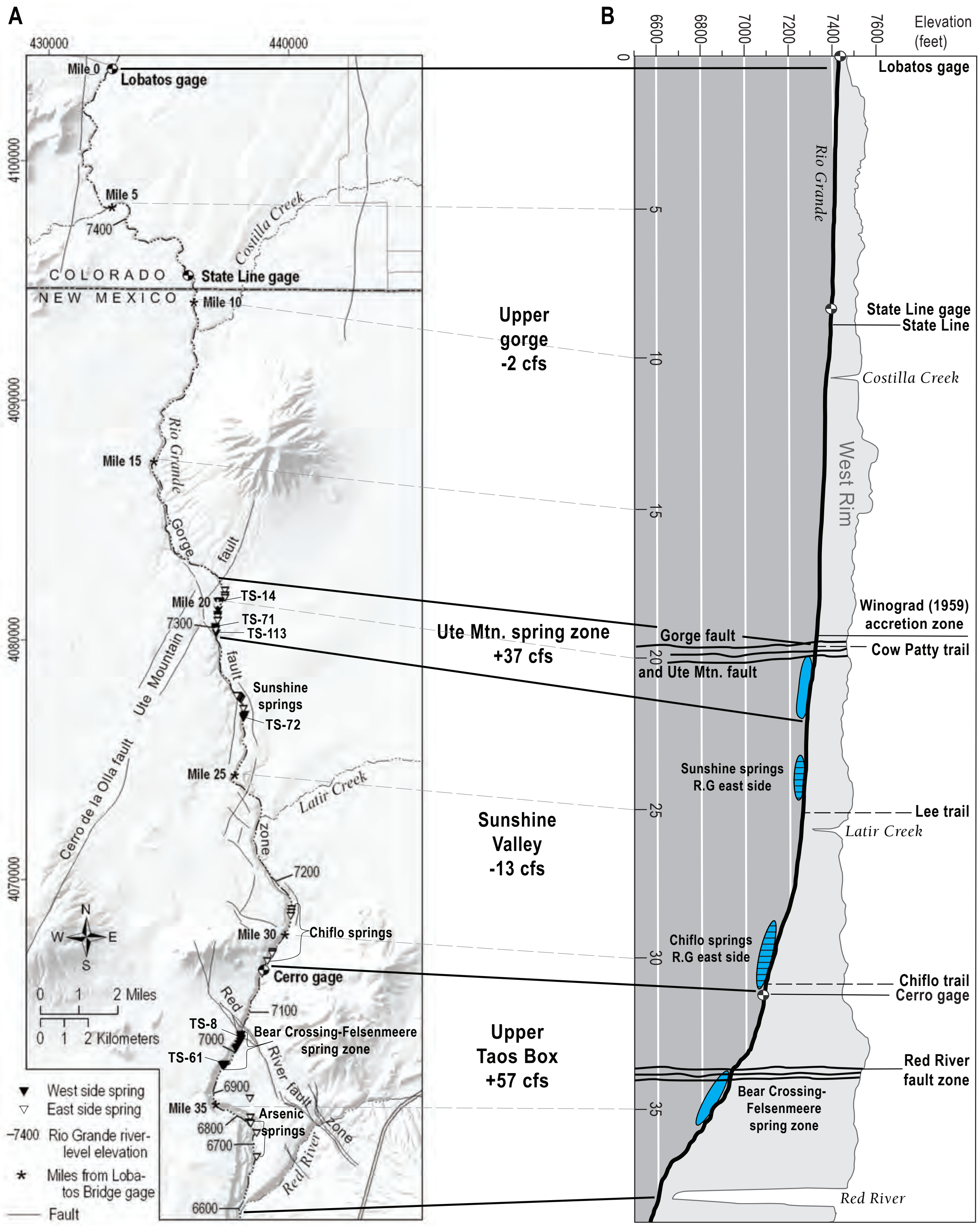

Figure 18–(A) Map of springs, spring zones and stream-flow gains and losses along the Rio Grande in northern Taos County. Spring zones and large river gains correlate with major fault zones intersecting the Rio Grande gorge. River gains and losses are summarized from Kinsli et al. (2011) and some spring locations are described in Bauer et al. (2007). (B) Topographic profile of Rio Grande and the west gorge rim showing principal spring zones and major fault zones.

the river in basalt talus starting where the Red River fault zone intersects the west wall of the Rio Grande gorge (Fig. 19). The fault zone likely enhances the fracture permeability of volcanic rocks and sedimentary deposits and behaves like a groundwater drain for the Taos Plateau aquifer, funneling groundwater flow to the spring discharge zone in the canyon wall. Bauer et al. (2007) estimated a cumulative discharge of approximately 6400 gpm (14 cfs) for the Bear Crossing spring zone. The Felsenmeere springs are visible from the eastern rim as high-velocity, high-discharge columns of water that emerge from the basalt talus about 100 ft above the river. Total minimum discharge from the three Felsenmeere springs was estimated at 9700 gpm (21.6 cfs). The large volume of groundwater discharging via springs in the west canyon wall is a response to the high gradient (84 ft/mi) and deep incision of the Rio Grande through this reach. Geochemical data from the largest spring in the center of the Bear Crossing spring zone (TS-8, Table 3) and the Felsenmeere middle spring (TS-61, Table 3) are discussed in subsequent sections. A number of other large east-side springs (such as Big Arsenic springs) exist above the Red River confluence, but are outside of the area of this study. Kinzli et al. (2011) measured

Figure 19A–View upstream of Rio Grande gorge along the Bear Crossing spring zone. Springs emerge under the talus along left river bank. Cerro Chiflo is on the skyline.

Figure 19B–One of many springs in the Bear Crossing spring zone. Springs emerge from below the basalt talus, typically with watercress.

a gain of about 57 cfs between the Cerro gage and the Red River confluence.

Groundwater and Heat Flow

For most of its length the Rio Grande rift system is characterized by high heat flow and conductive thermal gradients, extension tectonics, fault block mountains and deep sedimentary basins, Quaternary volcanism, and Quaternary faults (Reiter et al., 1975; Seager, 1975; Swanberg and Morgan, 1978; Chapin and Cather, 1994). Conductive temperature gradients in the Rio Grande rift, calculated from bottom-hole temperatures in 2-km deep wells, range from 25-55 °C/km (Goff et al., 1981). A major geothermal anomaly with heat-flow values greater than 105 milliwatts per square meter (mW/m2) coincides with the western part of the rift in northern New Mexico and intersects the western edge of the Taos Plateau (Reiter et al., 1975). In our study area, this anomaly manifests exceptionally high thermal gradients of 101 ºC/km (126 mW/m2) at No Agua and 51 ºC/km (111 mW/m2) at Tres Piedras (Reiter et al., 1975) (Fig. 20).

Such thermal anomalies are largely due to convection (the transport of heat by flowing groundwater) and are common in deep basins characterized by permeable aquifers, faulting and fracture zones, and recharge and discharge of groundwater. Many examples of local and basin-scale forced convection systems, involving deep circulation and heating of groundwater, have been described in the Rio Grande rift (Harder et al., 1980; Morgan et al., 1981; Swanberg, 1984a, 1984b; Mailloux et al., 1999; Johnson et al., 2012). Geothermal anomalies in the northern rift are generally associated with groundwater barriers and constrictions (Harder et al., 1980; Morgan et al., 1981; Witcher et al., 1992; Mailloux et al., 1999) or with upflow along rift-margin faults (Trainer and Lyford, 1979) and intrabasin faults (Plummer et al., 2004a, 2004b; Manning, 2009), where hydrogeologic conditions force heated groundwater to flow upward toward the surface. The Embudo constriction at the southern terminus of the San Luis Basin has been proposed as one setting that generates groundwater convection and thermal anomalies (Morgan et al., 1981; Swanberg, 1984a, 1984b; Coons and Kelly, 1984). Basement piercing faults and volcanic features associated with the Cerros del Rio volcanic field have been linked to upward migration of deep mantle fluids in the Española Basin (Manning, 2009). Elevated water temperatures, chloride and arsenic have been observed in close proximity to major faults in the Albuquerque basin (Plummer et al., 2004a, 2004b). In the Española Basin, spatial overlap of elevated chemical (fluoride, boron, lithium, arsenic, sulfate) and thermal anomalies with the eastern faulted margin of the Caja del Rio horst suggests that the anomalies are fault controlled (Johnson et al., 2012). Data from this study suggest that heat flow and upwelling thermal water along rift-margin structures influence both the flow and chemical characteristics of groundwater in the Taos Plateau aquifer.

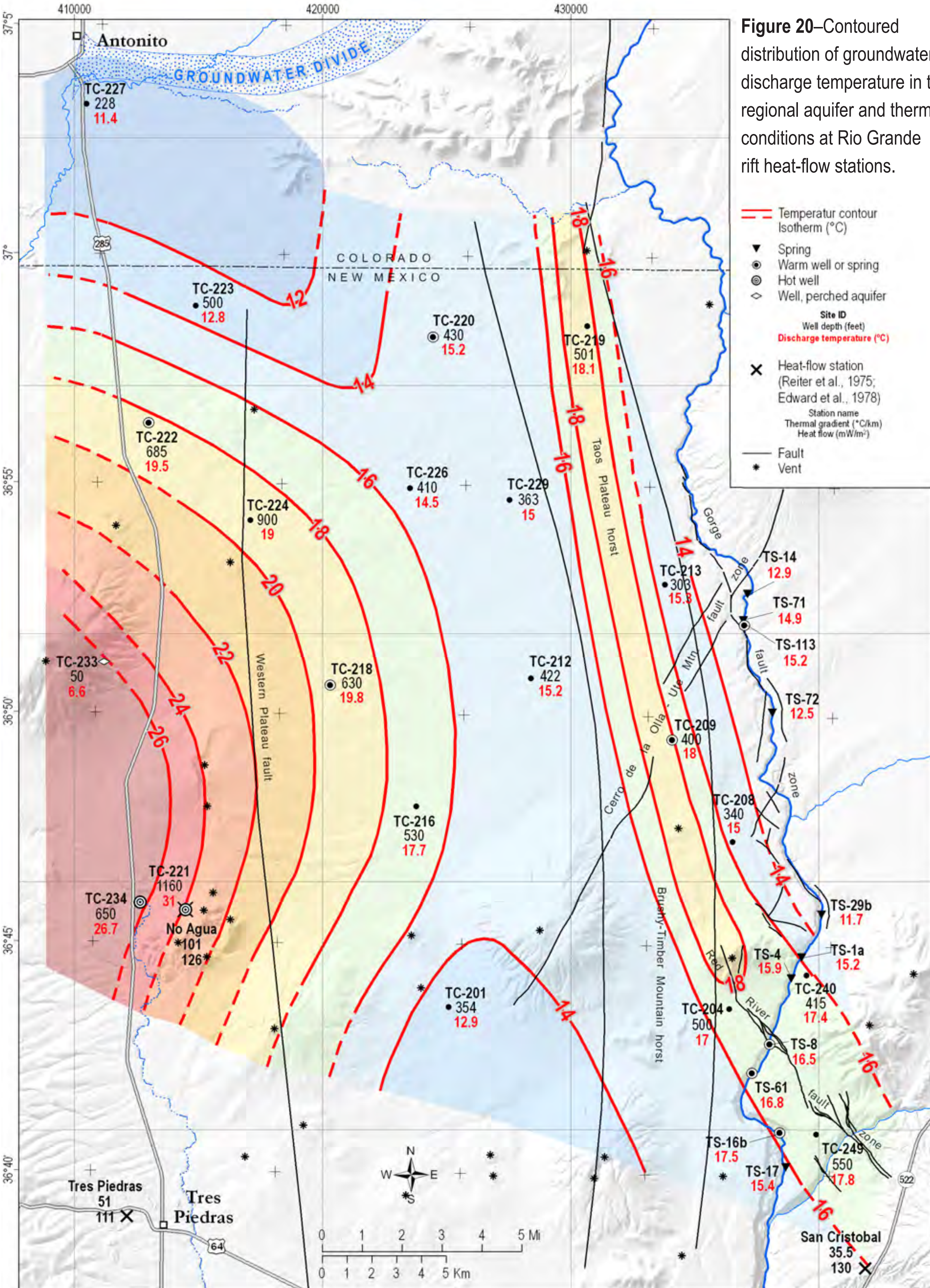

Figure 20–Contoured distribution of groundwater discharge temperature in the regional aquifer and thermal conditions at Rio Grande rift heat-flow stations.

V. THERMAL, CHEMICAL AND ISOTOPIC COMPOSITION OF GROUNDWATER

Chemical, thermal and isotopic data for groundwater from the Taos Plateau were examined for relations and spatial patterns useful in determining sources of groundwater, groundwater flow patterns, recharge and discharge zones, groundwater residence time, and active geochemical processes. We analyze groundwater discharge temperature, total dissolved solids (TDS), calcium (Ca^{2+}), sodium (Na^{+}), magnesium (Mg^{2+}), sulfate (SO_4^{2-}), chloride (Cl^{-}), bromide (Br^{-}), boron (B), lithium (Li^{+}), fluoride (F^{-}), arsenic (As), silica (SiO_2), deuterium (δ^2H) and oxygen-18 ($\delta^{18}O$). Groundwater residence time is evaluated by a combination of methods, including radiocarbon (^{14}C) dating of dissolved inorganic carbon (DIC), tritium (^3H) content, δ^2H and $\delta^{18}O$, and chlorofluorocarbons (CFCs). Contours of chemical data were constructed by interpolation of concentration values using inverse distance weighting in ArcGIS 9.3.1, followed by manual smoothing. The San Antonio Mountain well (TC-223), a shallow hand-dug well that taps a perched aquifer, was not used as a control point for contours of thermal, chemical, or isotopic data from the regional aquifer, although it does appear on figures as a point of reference. Concentrations of chemical and isotopic parameters measured in wells and springs are presented in Tables 4 and 5.

Field Parameters

***Temperature*—**Temperature measurements of groundwater discharge from shallow wells and springs are used to define temperature patterns for the Taos Plateau and identify thermally anomalous wells. Groundwater temperature data can help detect and characterize recharge and discharge zones and intermixing of deep and shallow water sources. Local and regional variations in groundwater temperatures are primarily caused by differences in depth of circulation and the local thermal gradient (Mazor, 2004). Temperatures of recharge water and shallow groundwater with circulation depths of 100 m or less are close to the local mean surface temperature. Groundwater temperatures significantly above the local mean surface temperature indicate circulation to considerable depths. The local mean annual surface temperature for the study area ranges from 2.2 ºC on San Antonio Mountain to 8.0 ºC at Bear Crossing Spring in the Rio Grande gorge, and 5.1-6.9 ºC on the basalt plateau.

The discharge temperature of groundwater beneath the Taos Plateau ranges from 10.5 to 31 ºC (50.9 to 87.8 ºF) (Fig. 20). The highest groundwater temperatures (>19 ºC) extend from the eastern flank of San Antonio Mountain south to No Agua. A zone of wells and springs along the eastern edge of the plateau has higher discharge temperatures than adjacent areas, and define a temperature high aligned with the Red River fault zone and the inferred Taos Plateau horst. Cool groundwater (<16 ºC) covers the center of the Taos Plateau from Antonito to Cerro de la Olla.

In order to recognize anomalous water temperatures for a given well depth and thermal gradient, we modify a method that uses the mean annual air temperature (MAT) as a baseline from which to define a thermal spring (Witcher, 1981; Swanberg, 1981; Steele and Wagner, 1981; Swanberg and Morgan, 1978). In Arizona, Witcher (1981) established one standard deviation above the MAT (7.5 ºC) as the quantitative criteria for defining a “warm” spring, and two

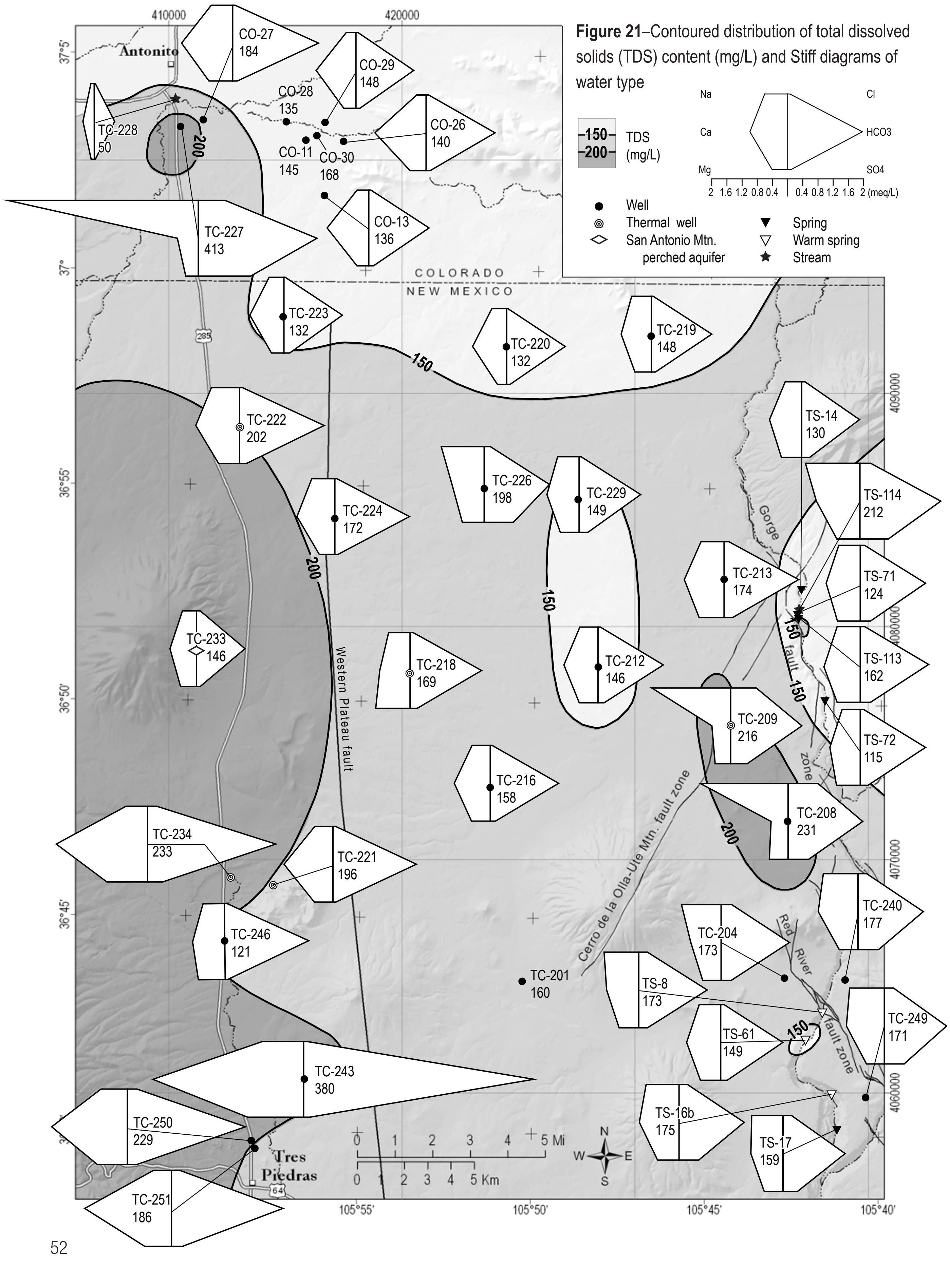

Figure 21–Contoured distribution of total dissolved solids (TDS) content (mg/L) and Stiff diagrams of water type
Na
Ca
Mg
Cl
HCO3
SO4
2 1.6 1.2 0.8 0.4 0.4 0.8 1.2 1.6 2 (meq/L)
150
200
TDS (mg/L)
Well
Thermal well
San Antonio Mtn. perched aquifer
Spring
Warm spring
Stream
410000
420000
37°5'
37°
36°55'
36°50'
36°45'
105°55'
105°50'
105°45'
105°40'
4090000
4080000
4070000
4060000
Antonito
Tres Piedras
COLORADO
NEW MEXICO
Western Plateau fault
Cerro de la Olla-Ute Mtn. fault zone
Gorge fault zone
Red River fault zone
CO-27 184
CO-29 148
CO-28 135
CO-26 140
CO-11 145
CO-30 168
CO-13 136
TC-228 50
TC-227 413
TC-223 132
TC-220 132
TC-219 148
TS-14 130
TC-222 202
TC-226 198
TC-229 149
TS-114 212
TC-224 172
TC-213 174
TS-71 124
TS-113 162
TC-233 146
TC-218 169
TC-212 146
TC-209 216
TS-72 115
TC-216 158
TC-208 231
TC-234 233
TC-221 196
TC-240 177
TC-246 121
TC-204 173
TC-201 160
TS-8 173
TS-61 149
TC-249 171
TC-243 380
TS-16b 175
TS-17 159
TC-250 229
TC-251 186
0 1 2 3 4 5 Mi
0 1 2 3 4 5 Km
N S E W
285
64

standard deviations (15 ºC) to define a "hot" spring. We extend this method to groundwater wells and estimate expected sample discharge temperatures by applying an average regional thermal gradient of 30 ºC/km (Reiter et al., 1975; Edwards et al., 1978), the sample depth, and site-specific mean surface temperatures estimated as a function of elevation (Table 4 and Fig. D2, Appendix D). Using this approach we identify two hot wells (TC-221 and TC-234) and three warm wells (TC-209, TC-218, and TC-222) with discharge temperatures ranging from 18 ºC to 31 ºC (Fig. 20). The thermal wells are located near San Antonio Mountain, No Agua, and the Red River fault zone. Two large warm springs, TS-8 (16.5 ºC) and TS-61 (16.8 ºC), discharge from the Red River fault zone on the west side of the Rio Grande gorge. A third warm spring, TS-16b (17.5 ºC), discharges from the east wall of the gorge near the fault zone. Thermal wells and springs are designated on figures presenting chemical and thermal data.

Dissolved Oxygen and pH—Groundwater in the regional aquifer is well oxygenated. Dissolved oxygen (DO) concentrations in well water range from 0.4 to 7.7 mg/L, with a mean of 3.9 mg/L. DO concentrations in spring discharge range from 7.0 to 9.3 mg/L, with a mean of 8.0 mg/L. DO concentrations generally decrease with sample depth, and one sample has a DO level <2.0 mg/L. Field pH values range from 7.3 to 8.6, with a mean of 8.1, indicating that groundwater in the regional aquifer is generally alkaline.

Specific Conductance and Total Dissolved Solids—Groundwater from the Taos Plateau aquifer is relatively dilute in dissolved minerals. Values for TDS range between 115 and 413 mg/L (Fig. 21), and from 133 to 588 µS/cm for specific conductance (Table 4). Dissolved solids are relatively high (>200 mg/L) along the western edge of the plateau from Antonito south to No Agua, and near the Cerro de la Olla and Red River fault zones. A Colorado well near the Rio San Antonio at Antonito (TC-227) has an anomalously high TDS value and consistently exhibits anomalous values for other chemical parameters as well. Wells in the center of the Taos Plateau and along the northern edge of the plateau near the Colorado-New Mexico border have the lowest TDS values (<150 mg/L), as do Felsenmeere spring (TS-61) and most springs in the Ute Mountain spring zone. Lava Tube spring (TS-113) and Bear Crossing spring (TS-8) each has high TDS relative to other Rio Grande gorge springs.

Chemical Characteristics of Groundwater

Major Ion Chemistry and Water Type—The contoured distribution of dissolved solids, stiff diagrams of water type, and ratios of calcium to sodium concentration are shown in Figures 21 and 22. Most groundwater in the Taos Plateau

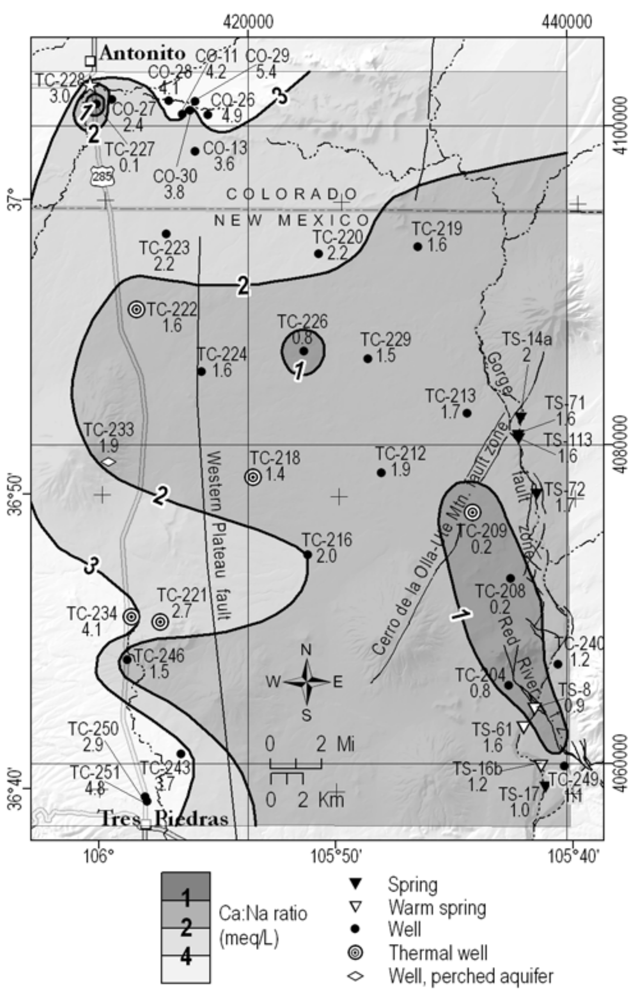

Figure 22–Contoured distribution of calcium to sodium ratio.

aquifer is calcium rich with various amounts of magnesium and sodium. Calcium concentrations range from 8.6 to 80 mg/L with a median value of 19 mg/L. Sodium concentrations range from 5.6 to 53 mg/L with a median value of 13 mg/L. A stream sample from the Rio San Antonio (TC-228) indicates that surface water is also Ca-rich, with a Ca/Na ratio of 3.0. Areas of Ca-rich groundwater (Ca/Na ratio >3) occur only near the Rio San Antonio and Arroyo Aguaje de la Petaca (Fig. 22), indicating active recharge to shallow groundwater from streams and arroyos bounding the plateau.

Sodium-rich waters (Ca/Na ratio <1) are local anomalies aligned with the Red River fault zone, the Antonito well (TC-227) and a single well in the central plateau (TC-226). Generally, wells in the center of the Taos Plateau in New Mexico and springs in the Rio Grande gorge discharge mixed calcium-sodium or calcium-sodium-magnesium type water with a Ca/Na ratio between 1 and 2. Perched groundwater on San Antonio Mountain (TC-233) is calcium-magnesium-sodium bicarbonate type water with relatively low TDS. The concentration of Mg (Fig. 23) is relatively high in the regional aquifer in New Mexico and comprises a major fraction of the total ion content near No Agua and Tres Piedras. All groundwater sampled has an ion chemistry with (Mg/Ca + Mg) <0.5 and HCO_3/SiO_2 <5.0, implying an aquifer rock rich in ferromagnesian minerals (AquaChem 2010.1.83). High aqueous Mg concentrations likely reflect the presence of magnesium-rich

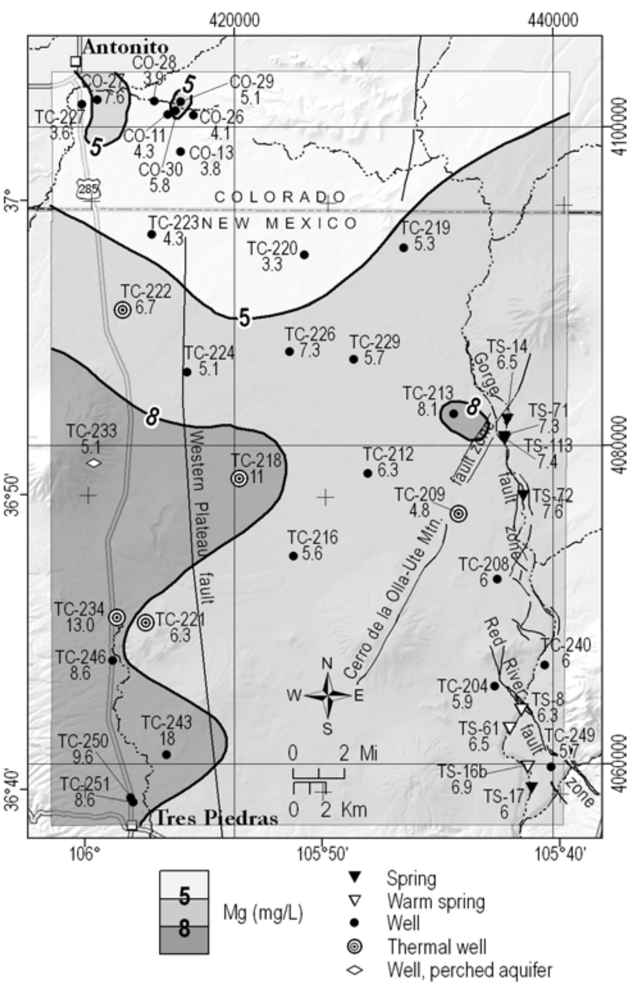

Figure 23–Contoured distribution of magnesium.

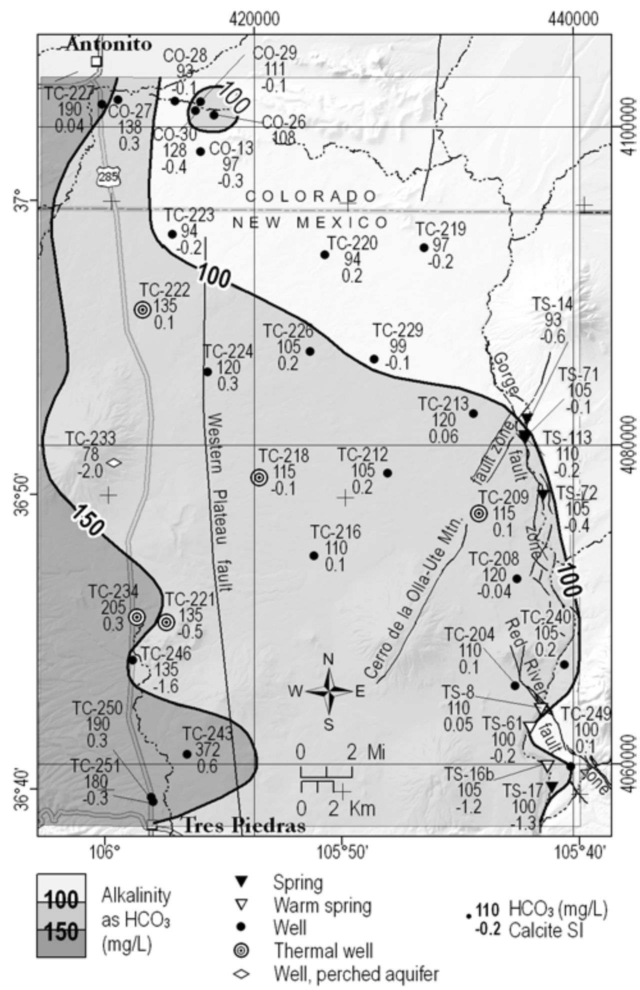

Figure 24–Contoured distribution of bicarbonate alkalinity shown with calcite saturation indices (SI) modeled with PHREEQC.

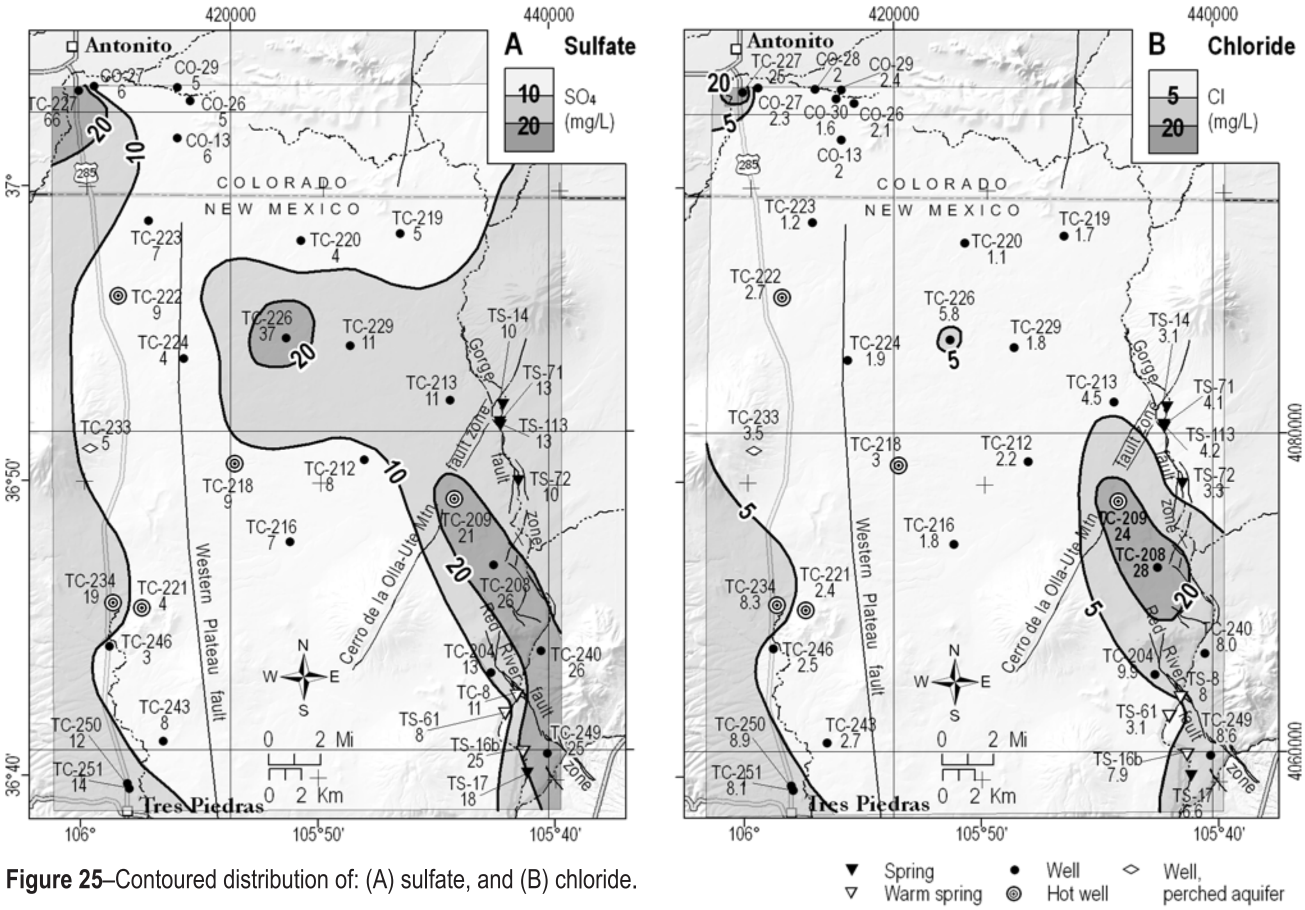

Figure 25–Contoured distribution of: (A) sulfate, and (B) chloride.

minerals in the Hinsdale Formation and Proterozoic rocks west of the Western Plateau fault.

Bicarbonate (HCO_3) is the dominant anion in the regional aquifer with concentrations ranging from 93 to 205 mg/L (Fig. 24). High values of HCO_3 alkalinity occur near No Agua Peaks and Tres Piedras. Low alkalinity is present in wells near the Rio San Antonio, in the Ute Mountain spring zone and the San Antonio Mountain perched aquifer. Modeling with PHREEQC indicates that most groundwater beneath the Taos Plateau is at or near equilibrium with respect to calcite. In general, waters with low alkalinity are also slightly undersaturated with respect to calcite. Slightly oversaturated waters are scattered throughout the aquifer, and include groundwater north and northeast of San Antonio Mountain.

Sulfate concentrations range from 4 to 66 mg/L (Fig. 25a). Low concentrations (<10 mg/L) are present in most of the regional aquifer between Antonito and Tres Piedras. Chloride, a conservative constituent in groundwater, is generally less than 5 mg/L and displays a spatial pattern similar to sulfate (Fig. 25b). The highest concentrations of Cl and SO_4 occur at the Antonito well (TC-227), in a single well in the center of the plateau (TC-226), and near the Red River fault zone (TC-209 and TC-208). Wells TC-226 and TC-227 discharge a bicarbonate-sulfate type water, and wells TC-208 and TC-209 near the Red River fault zone discharge bicarbonate-chloride water.

Concentrations of dissolved SiO_2 in groundwater generally range from 8 to 85 mg/L (Langmuir, 1997) and are not conservative due to rock-water interactions. In low-temperature systems SiO_2 is derived primarily from weathering of silicate and aluminosilicate minerals, but in this rift setting additional sources may come from mixing of geothermal waters or accelerated dissolution of silica-rich volcanic glass. Consequently, concentrations of SiO_2 in the Taos Plateau aquifer (32 to 100 mg/L) are high for groundwater, but have a well-defined geographic

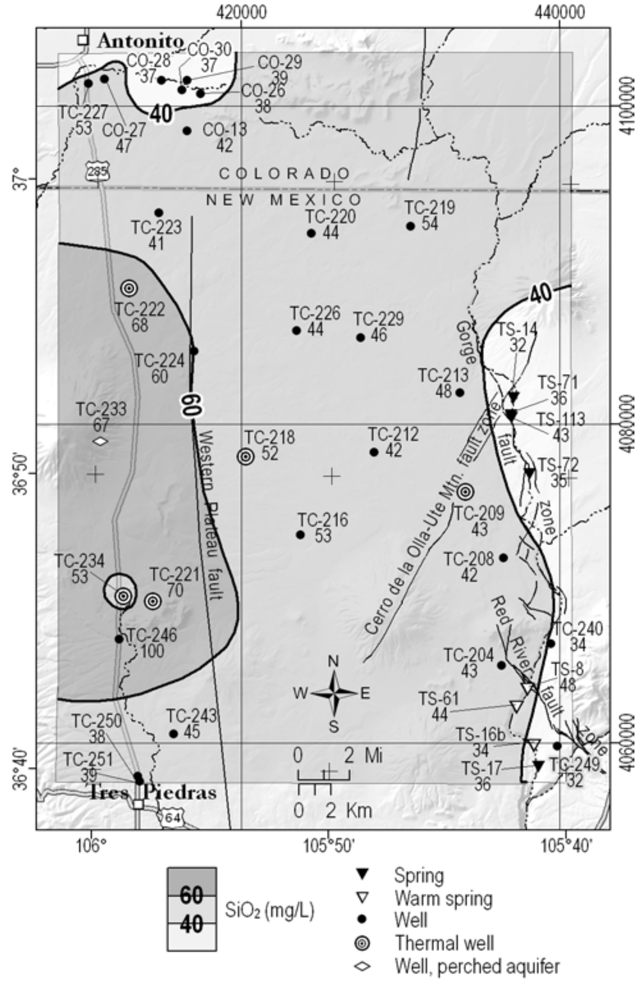

Figure 26–Contoured distribution of dissolved silica.

distribution of decreasing concentration with distance from the western boundary of the plateau (Fig. 26). High SiO_2 concentrations (>60 mg/L) are present in the western third of the plateau surrounding San Antonio Mountain. The lowest concentrations (<40 mg/L) are along the Rio San Antonio near Antonito and in the Ute Mountain spring zone in the Rio Grande gorge. Most of the Taos Plateau aquifer has SiO_2 concentrations of 40 to 50 mg/L.

A plot of the proportions of the major cations and anions for all samples is shown on a Piper diagram in Figure 27. The Piper plot provides a good summary of water type and ion chemistry for groundwater and surface water from the northern Taos Plateau and compliments the spatial figures of ion distribution (Figs. 21-25). Trends in ion chemistry observed on the Piper diagram and ion distribution figures support hydrologic interpretations of groundwater sources, recharge and flow paths for the Taos Plateau aquifer, which are summarized below.

Taos Plateau aquifer in Colorado. Groundwater in the regional aquifer in Colorado is $CaHCO_3$ water with minor added Mg and Na, no added Cl or SO_4, and is identical in ion chemistry to the Rio San Antonio. These groundwaters appear to source from infiltration of stream and surface water originating from the Rio San Antonio. The one exception is sample TC-227, which is Na-HCO_3-SO_4 water unique to its location near Antonito and not representative of local or regional water quality. Groundwater in New Mexico with a similar $CaHCO_3$ chemistry is only observed in wells adjacent to Arroyo Aguaje de la Petaca, between No Agua Peak and Tres Piedras (TC-234, -243, -250, -251), indicating a component of recharge from stream infiltration.

Taos Plateau aquifer in New Mexico. Groundwater in the Taos Plateau aquifer in New Mexico is also $CaHCO_3$ water, but contains higher amounts of Na, Mg, and dissolved solids, and locally high SO_4 and Cl, relative to groundwater from Colorado wells. Ion chemistry of New Mexico well water also has a distinct and consistent geographic distribution apparently influenced by geologic strata and structures. In general, regional groundwater along the western (up-gradient) margin of the study area is warm Ca- and Mg-rich HCO_3 water with a high dissolved ion content, suggesting these waters may originate in the Tusas Mountains to the west and enter the Taos Plateau aquifer as deep, subsurface inflow through the Hinsdale Formation. Wells in the central plateau discharge cooler groundwater with lower dissolved ion content than wells that are up-gradient on the flow path, which implies that local recharge on the plateau contributes to the regional aquifer.

Mixing of mineralized water near the Red River fault zone. Na-rich waters with relatively high Cl and SO_4 occur as isolated anomalies near

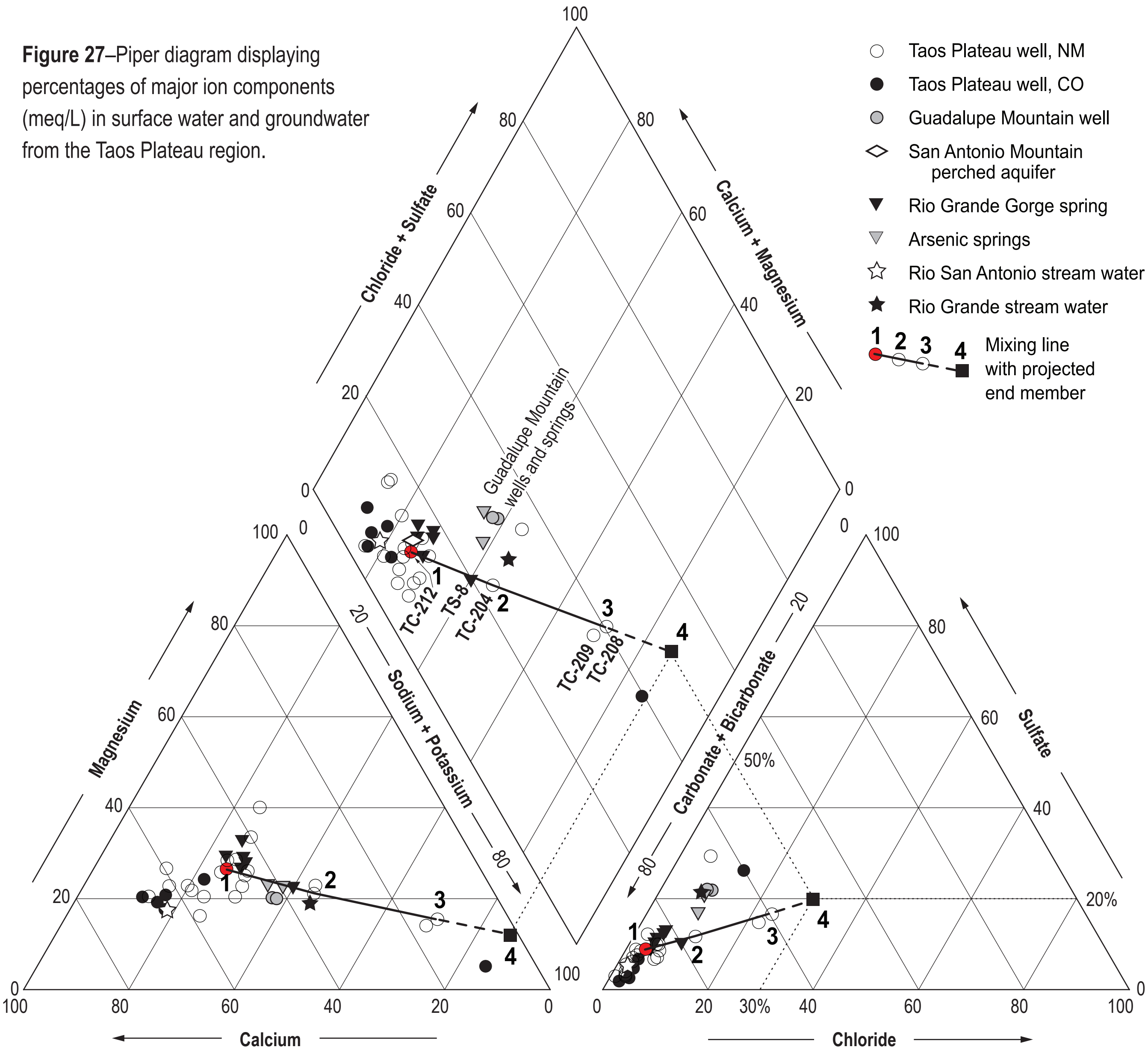

Figure 27–Piper diagram displaying percentages of major ion components (meq/L) in surface water and groundwater from the Taos Plateau region.

the Red River fault zone north of Cerro Chiflo, indicating that this major structure, particularly at its intersection with the Cerro de la Olla-Ute Mountain fault zone, facilitates upward movement of deep, warm, mineralized waters into the regional aquifer.

Mixing between two of these waters—low TDS Ca-Na-Mg-HCO_3 groundwater characteristic of the central Taos Plateau (water 1, well TC-212 for example) and high TDS Na-HCO_3-Cl groundwater from near the Red River fault zone (water 3, wells TC-208 and TC-209)—is demonstrated by a mixing line visible on the Piper plot (Fig. 27). The mixture (water 2) was sampled from a well and spring (TC-204 and TS-8) located down-gradient along the fault zone near its intersection with the Rio Grande gorge. The ratio between the mixture and the two sample end members is identical in both cation and anion triangles, suggesting simple mixing between the two waters. Water 3 is probably not a true end member representative of the deep mineralized source, but is more likely itself a mixture of deep mineralized and shallow fresh groundwater. By extending the cation mixing line to the Na axis of the triangle, and projecting that location back to the mixing lines in the combined plot and the anion plot, we can estimate the ion content of the true mineralized end member (water 4) to be Na-HCO_3-Cl-SO_4 water, with an anion content of 50% HCO_3, 30% Cl and 20% SO_4 (Fig. 27). The mixing proportions of the end members discharging at Bear Crossing Spring (TS-8) are estimated to be 80% central Taos Plateau water (water 1) and 20% Red River fault zone water (water 4).

Aquifers east of the Rio Grande. The ion chemistry of groundwater in the Taos Plateau aquifer is distinct from wells and springs near the Red River fault zone on Guadalupe Mountain east of the Rio Grande gorge (TC-240, TC-249, TS-16b, TS-17). The Ca-Na-HCO_3-SO_4 water sampled at Guadalupe Mountain is not duplicated in any sample from west of the Rio Grande gorge, although it has a similar anion content as TC-226 in the central plateau. Springs discharging in the Ute Mountain spring zone (TS-14, TS-71 and TS-113) and the Sunshine Valley reach of the Rio Grande gorge (TS-72) have unique temperature, dissolved solids and silica characteristics compared to adjacent wells on the Taos Plateau. Ion chemistry alone is insufficient to characterize spring discharge in the gorge as originating from west or east of the gorge, but isotopic characteristics provide additional evidence.

Minor Ion and Trace Element Chemistry— Bromide, like chloride, behaves conservatively in groundwater, but bromine is generally 40 to 8000 times less abundant in the environment than chlorine (Davis et al., 1998). Bromide concentrations in the Taos Plateau aquifer range from 0.020 to 0.481 mg/L, with most groundwater samples containing less than 0.05 mg/L (Fig. 28). The highest concentrations (>0.1 mg/L) occur at the Antonito well (TC-227), at TC-226 in the center of the plateau, near the Red River fault zone (TC-209 and TC-208), near No Agua Peaks (TC-234,) and at Tres Piedras (TC-250 and TC-251).

Our understanding of groundwater sources is advanced by evaluating the ratio of chloride to bromide, as relatively small changes in the total

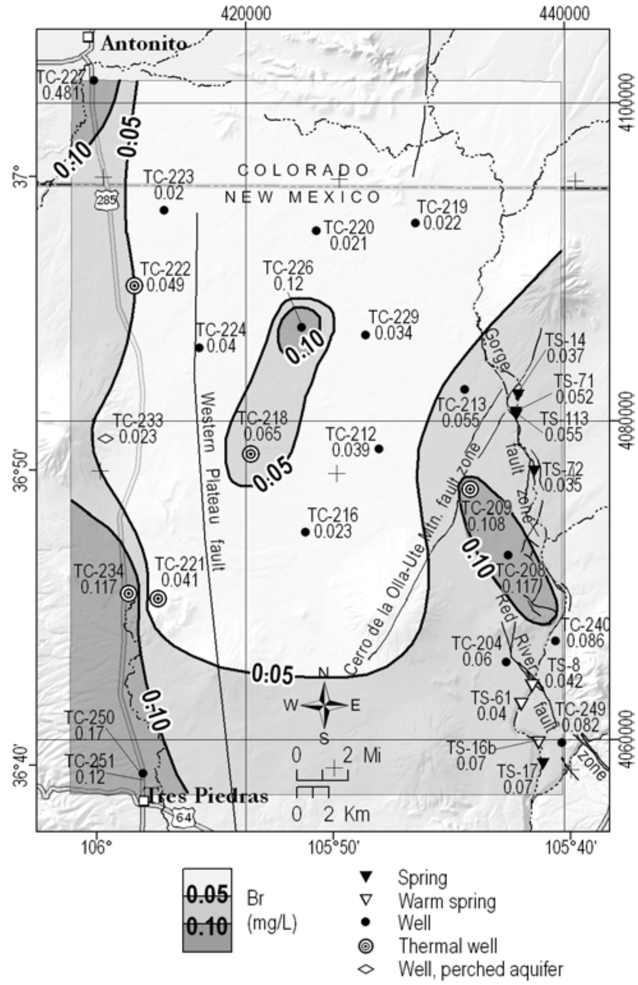

Figure 28–Contoured distribution of bromide.

mass of bromide give rise to large variations in the ratio. Chloride-bromide ratios are distinct for various natural and anthropogenic water sources (Davis et al., 1998). For example, precipitation (50-150), shallow groundwater (100-200), domestic sewage (300-600), volcanic rocks (500-545), and urban runoff and road salt (~ 1170) all possess a unique range of ratio values. Ratios of Cl to Br in the regional aquifer (Fig. 29) average about 70 and are typically less than 200. Most ratios are consistent with values for precipitation and shallow groundwater. One notable exception occurs near the Red River fault zone where ratios range from 165 (TC-204) to 239 (TC-208). Bear Crossing Spring (TS-8), which discharges from the Red River fault zone, has a Cl-Br ratio of 190. Although these values are close to the reported upper limit for shallow groundwater,

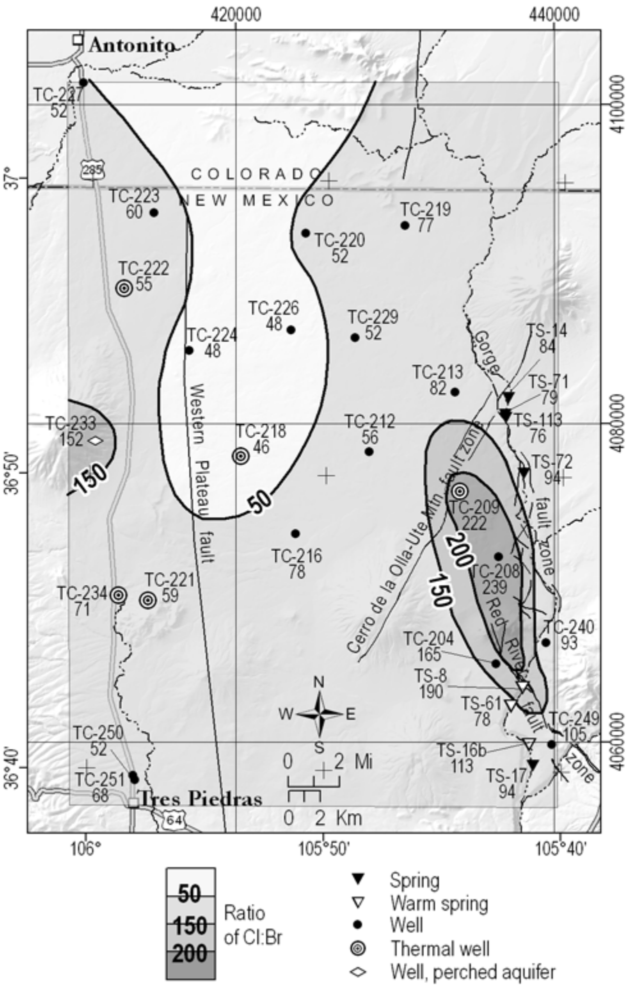

Figure 29–Contoured distribution of the ratio of chloride to bromide concentration.

they are notably elevated above those measured in the Taos Plateau aquifer. The lowest ratios, observed in the central Taos Plateau, are consistent with values for precipitation.

Fluoride concentrations in the regional aquifer range from 0.2 to 3 mg/L and are typically less than 0.5 mg/L (Fig. 30a). High values are noted at the Antonito well (TC-227) and near the Red River fault zone. High fluoride concentrations are more likely to occur in water low in calcium and high in sodium (Hem, 1985), and a comparison of fluoride concentrations with ratios of calcium to sodium (Fig. 22) indicates this is true for the Taos Plateau. High fluoride concentrations are often associated with thermal waters having high sodium and pH (Hem, 1992).

Boron concentrations in the regional aquifer range from 0.01 to 0.35 mg/L and are typically less than 0.03 mg/L (Fig. 30b). Lithium concentrations range from 0.004 to 0.113 mg/L but are typically less than 0.01 mg/L (Fig. 30c). Arsenic concentrations are generally less than 0.003 mg/L (Fig. 30d). Concentrations of F, B, Li and As are high near the Red River fault zone, and lithium is high near No Agua Peaks. The chemical constituents As, B, F and Li are usually present at much higher concentrations in hydrothermal waters than in low-temperature waters (Ellis and Mahon, 1977; Arnórsson, 2000), and particularly in thermal waters near recent volcanic systems (Tello et al., 2000). Locally high temperature, F, B, Li and As in shallow groundwater near the Red River fault zone indicates that upward flow of deep thermal water into the Taos Plateau aquifer is controlled in some way by this complex fault system.

Spatial and Statistical Correlations for Chemical Parameters—The spatial distributions of temperature, ions, and trace elements in groundwater (Figs. 20-26, 28-30) are, in many cases, similar. The western (up-gradient) margin of the Taos Plateau is characterized by relatively high temperature, TDS, Ca, Mg, HCO_3, SO_4, Cl, SiO_2, Br, F, and Li. Concentrations of these constituents decrease toward the central plateau in the direction of regional groundwater flow. Temperature, TDS, Na, SO_4, Cl, Br, F, B, and Li are also elevated at the eastern margin of the plateau near the Red River, Ute Mountain and Gorge fault systems. The lowest concentrations of most parameters are observed near Rio San Antonio and Punche Arroyo in Colorado. The Ute Mountain spring zone in the Rio Grande gorge is relatively low in temperature, TDS, and SiO_2 but displays, for most parameters, a modest but consistent trend of increasing concentrations or values downstream in the gorge.

Statistical correlations reveal links between chemical parameters in samples from the Taos Plateau aquifer. When integrated with spatial correlations they expand our understanding of mixing and geochemical processes affecting water quality along a flow path. Results of

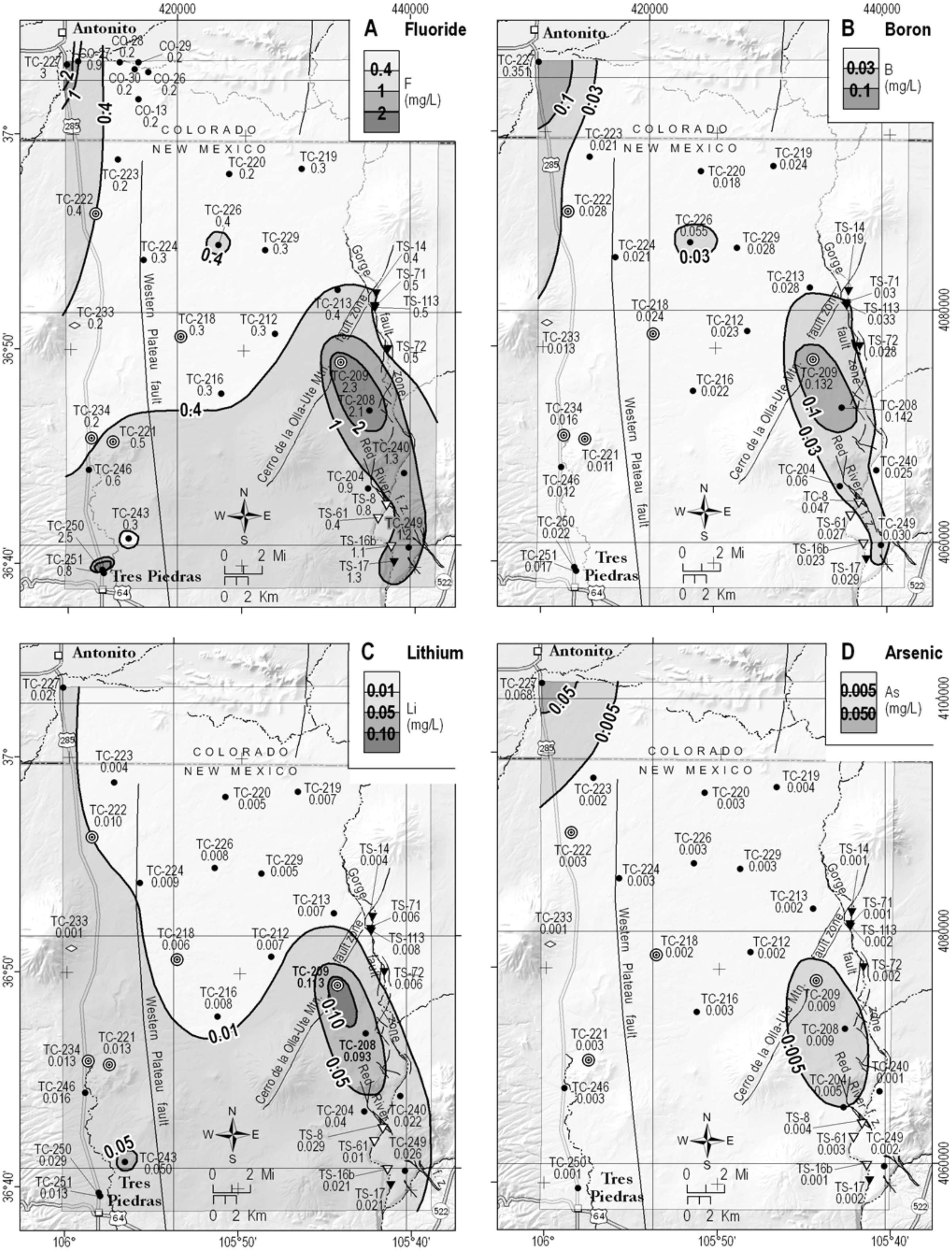

Figure 30–Contoured distribution of: (A) fluoride, (B) boron, (C) lithium and (D) arsenic.

	B	Ba	Br	Ca	Cl	δ13C	14Cpmc	δ18O	δ2H	F	HCO3	K	Li	Mg	Na	pH	SiO2	SO4	Sr	TempC	TDS	U	V	
As	0.46	-0.48		-0.42		0.49	-0.57	-0.40				0.46	0.38		0.41	0.50	0.48						0.80	As
B			0.40	-0.45	0.54				0.54	0.50			0.43		0.78	0.64		0.66						B
Ba												-0.37	-0.41		-0.43	-0.45					-0.4			Ba
Br					0.88	0.73		0.44	0.44	0.75	0.67		0.75	0.52	0.75			0.85	0.49		0.86	0.54		Br
Ca											0.43			0.49					0.81	0.54	0.36	0.56	-0.42	Ca
Cl						0.72		0.64	0.58	0.77	0.36		0.69		0.69		-0.37	0.83			0.59	0.41		Cl
δ13C									0.48	0.47	0.49		0.65		0.60			0.56			0.60			δ13C
14Cpmc								0.46			-0.64		-0.49				-0.81			-0.61	-0.7		-0.54	14Cpmc
δ18O									0.54	0.58							-0.39	0.52				0.55	-0.43	δ18O
δ2H										0.57			0.40		0.39		-0.44	0.50						δ2H
F													0.71		0.64		-0.40	0.64			0.41			F
HCO3												0.37	0.61	0.54	0.49		0.41		0.68	0.52	0.74	0.51		HCO3
K																	0.67			0.51				K
Li															0.82			0.52	0.38	0.50	0.72	0.46		Li
Mg																-0.42			0.47					Mg
Na																0.52		0.72			0.74	0.37		Na
pH																		0.45					0.42	pH
SiO2																		-0.40		0.39			0.56	SiO2
SO4																					0.56			SO4
Sr																				0.51	0.61	0.46		Sr
TempC																					0.48			TempC
TDS																						0.46		TDS
U																							-0.45	U

blank cells' – no significant correlation, P value > 0.05

Spearman correlation coefficient > 0.60

Table 7–Spearman rank correlation coefficients for pairs of chemical parameters, with a significant (P value <0.05) positive or negative correlation, in groundwater from the Taos Plateau.

Spearman Rank Order Correlation for chemical parameters in Taos Plateau groundwater (Table 7) measure the co-variance, or the degree of association, between two parameters. The stronger the correlation, the larger the correlation coefficient; a perfect correlation has a coefficient of 1.0. A plus sign signifies identical or positive correlation and a minus sign signifies reverse correlation. Where analysis indicated no significant correlation (P value >0.05) table cells are left blank. Two correlation sets are notable and are discussed below.

The correlation method indicates a significant positive covariance (rank coefficients +0.39 to +0.67) among K, SiO_2, and temperature, which is consistent with silicate weathering enhanced by elevated temperature. A reverse correlation associates elevated SiO_2 with depleted δ^2H and δ^{18}O values (rank coefficients -0.44 and -0.39) and low ^{14}C activity (rank coefficient -0.81). These associations indicate that deep, subsurface inflow into the western Taos Plateau is old, warm groundwater significantly enriched in dissolved SiO_2 through weathering of potassium feldspar from Proterozoic granitic rocks along the western margin of the field area

Strong positive covariance (rank coefficients 0.40 to 0.88) also exists between the ions Na, Cl, SO_4, HCO_3, Br, F, B, and Li, and TDS. The overlap between statistical rank association of these parameters and spatial correlation near faults, horst boundaries, or fault intersections at the eastern margin of the plateau is consistent with mixing of shallow, dilute, Ca-Na-HCO_3 groundwater from the central Taos Plateau with Na- HCO_3-Cl-SO_4 groundwater originating from a deep saline source and flowing upward along the Red River, Ute Mountain and Gorge fault systems.

Isotopic Characteristics and Groundwater Residence Time

Hydrogen-2 (δ^2H) and Oxygen-18 (δ^{18}0) Isotopes—Stable isotope values (Table 5) from wells, springs, and streams are plotted with a regression line for surface water in the southern San Luis Basin and a local meteoric water line (LMWL) for the Santa Fe area (Fig. 31). There are no isotopic data for precipitation from the Taos Plateau or southern San Luis basin, and thus a LMWL for the study area does not exist. Isotopic values for all waters (Table 5) vary over a fairly small range: -87.9 to -109.6 ‰ δ^2H and -12.0 to -15.4 ‰ δ^{18}O. Most Taos Plateau waters plot above the Santa Fe meteoric water line of Anderholm (1994) and many samples plot above the surface-water line as well.

Mountain-stream baseflow samples collected from six Rio Grande tributaries in February 2008 have δ^2H values of -96.2 to -102.5 ‰ and δ^{18}O values of -13.6 to -14.3 ‰ (Fig. 31). These samples constrain the range of stable isotope values for mountain-block recharge from the northern Sangre de Cristo Mountains east of the study area. The Rio Grande above Lava Tube spring (TS-114), sampled in September 2009 during a period of low flow, is considerably enriched (-89.7 ‰ δ^2H, -12.0 ‰ δ^{18}O) and the Rio San Antonio (TC-228), sampled during snowmelt in June 2008, is significantly depleted (-104.3 ‰ δ^2H, -14.8 ‰ δ^{18}O) relative to Sangre de Cristo mountain-front streams. A regression of the stream data forms a line with a slope of 5.5 (r^2 = 0.90), which indicates minor evaporation typical of surface water and shallow groundwater. Most spring discharge plots near or above the surface water line. Apart from the Rio San Antonio, the isotopic composition of San Luis Basin streams is enriched relative to groundwater in the Taos Plateau aquifer.

The spatial distribution of δ^2H in groundwater from the Taos Plateau (Fig. 32) illustrates a regional gradient that trends from depleted compositions (<-105 ‰) at the western margin of the plateau around San Antonio Mountain to relatively enriched compositions (>-99 ‰) near the Rio Grande gorge south of the Ute Mountain fault zone. Two springs (TS-14 and TS-113) in the Ute Mountain spring zone discharge depleted δ^2H waters relative to adjacent wells and springs (102.8 ‰ and -101.0 ‰ respectively).

To provide context for interpretation of the isotopic data, we developed a meteoric water line based on water from a shallow, hand-dug well (TC-233) completed in the San Antonio Mountain perched aquifer (sample elevation 9246 ft asl), which is representative of meteoric water from high-elevation precipitation, combined with groundwater samples from the central Taos Plateau. San Antonio Mountain perched water has the lightest ^{18}O composition of any water sampled (15.4 ‰) and plots well above the surface water line (Fig. 31). Groundwater samples from the central Plateau form a linear trend with the San Antonio Mountain sample along a regression line with the equation $\delta^2H = 7.2\ \delta^{18}O + 7.7$ (Fig. 33). We use this groundwater regression line as a proxy for a

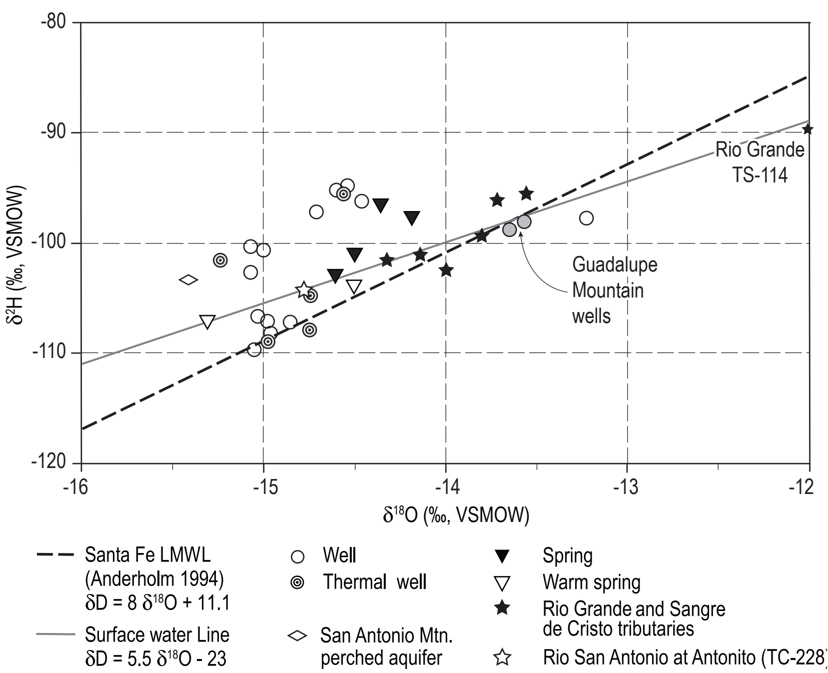

Figure 31–Isotopic data (hydrogen-2 (δ^2H) versus oxygen-18 (δ^{18}O)) for groundwater from the Taos Plateau and surface water from the southern San Luis Basin. Data (Table 5) are shown in relation to a LMWL for the Santa Fe area (Anderholm, 1994) and a Taos Plateau surface water regression line.

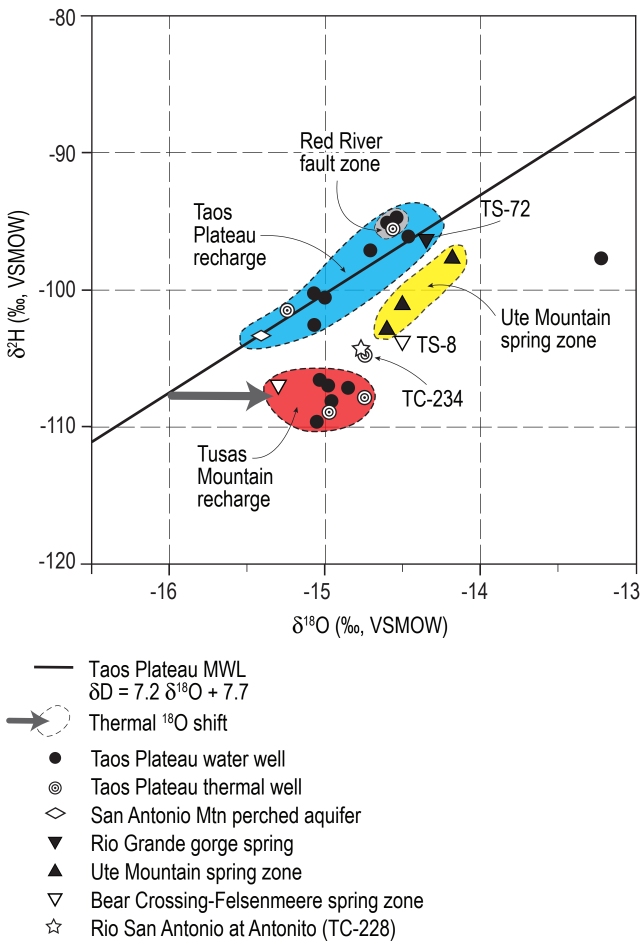

Figure 32–Contoured distribution of deuterium (δ²H, ‰) in wells and springs on the Taos Plateau. Site colors (red and blue) correspond to those for recharge sources identified on Figure 33.

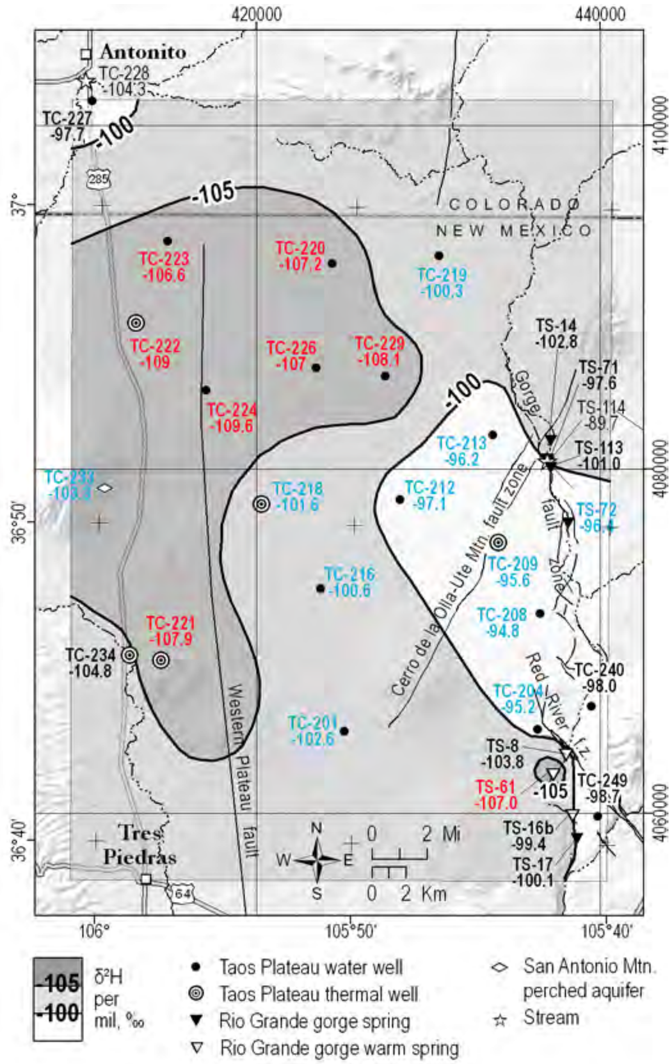

Figure 33–Stable isotope compositional groups and sources of recharge for the Taos Plateau regional aquifer. Colored zones indicate separate recharge signatures and correspond to site colors on Figure 32.

precipitation-based, local meteoric water line for the Taos Plateau (TPMWL). By evaluating isotopic data in the context of the TPMWL, we can better understand groundwater sources and flow paths in the regional aquifer.

Discussion of recharge sources, flow paths, and hydrologic and isotopic processes**—**Compositional differences in stable isotopes distinguish two sources of recharge to the Taos Plateau aquifer (Fig. 33): 1) deep groundwater underflow from the Tusas Mountains to the west, and 2) local recharge from precipitation on the Taos Plateau and volcanic domes. Waters that discharge in the Ute Mountain spring zone in the Rio Grande gorge have a unique isotopic signature and appear to be unrelated to the Taos Plateau aquifer.

Underflow from the Tusas Mountains and ^{18}O enrichment of thermal water. Groundwater at the western margin near San Antonio Mountain (Fig. 32) is depleted in ^{2}H (<-105 ‰) and plots significantly below the TPMWL (Fig. 33). These waters are more depleted in ^{2}H than any in the study area, including high-elevation meteoric water on San Antonio Mountain. The samples also display a positive shift in ^{18}O of about 0.5 to 1.0 ‰ (Fig. 33), SiO_2 concentrations above 60 mg/L (Fig. 26), and relatively warm discharge temperatures (Fig. 20). Oxygen 18 enrichment in groundwater with no corresponding enrichment in ^{2}H is typical of geothermal areas where isotopic exchange between meteoric water and silicates in the reservoir rock is accelerated by high temperature. The magnitude of the observed ^{18}O shift is similar to that documented in thermal systems where the recharging water is in equilibrium with the silicate ^{18}O content (Panichi and Gonfiantini, 1981). Waters originating as underflow from the Tusas Mountains include two thermal wells (TC-221 and TC-222) with the highest discharge temperatures measured in the study area and one warm spring (TS-61). ^{2}H depletion combined with ^{18}O enrichment in Taos Plateau samples clarifies groundwater source and flow path. Deuterium depletion distinguishes the water source as seepage from the Tusas highlands west of San Antonio Mountain. Oxygen-18 enrichment, high temperatures, and elevated dissolved silica, indicate a deep circulation pathway prior to mixing in the shallow aquifer.

Hydrologic mixing may also affect sample TC-234 from a shallow thermal well adjacent to the Arroyo Aguaje de la Petaca. This sample is identical in isotopic composition to the Rio San Antonio, but is also intermediate in composition between Tusas Mountains and Taos Plateau recharge sources (Fig. 33). This water could originate from arroyo infiltration adjacent to the volcanic field, or as some mixture of Tusas Mountain recharge, San Antonio Mountain recharge and/or arroyo infiltration.

Two well samples from the northern Taos Plateau (TC-220, TC-223) also have slight ^{18}O enrichment, plot near the surface water line (Fig. 31) and are unusually cold (Fig. 20) $CaNaHCO_3$ waters (Figs. 22, 24). They also have moderate SiO_2 concentrations of 44 and 41 mg/L. These characteristics suggest the waters are recharged in the northern Tusas Mountains, have a shallow flow path, and may be influenced by accelerated weathering of silica-rich volcanic glass. The distribution pattern for δ^2H (Fig. 32) shows that underflow from the Tusas Mountains covers a large portion of the regional aquifer beneath the western plateau as the depleted δ^2H signature persists nearly to the Taos Plateau horst. Discharge to Felsenmeere spring (TS-61) is isotopically similar to Tusas Mountain underflow.

Precipitation on the Taos Plateau. Well and spring samples from the central and eastern Taos Plateau are relatively enriched in ^{2}H (>-103 ‰) and form the TPMWL (Figs. 32 and 33). The association of these samples with San Antonio Mountain meteoric water suggests a source from local precipitation falling on the Taos Plateau and adjoining volcanic domes. These samples include five wells from the Taos Plateau (TC-201, TC-212, TC-213, TC-216, TC-219), one warm well east of San Antonio Mountain (TC-218), and a group of three wells adjacent to the Red River fault zone (TS-204, TS-208, TS-209). Some of these samples (e.g., Red River fault zone samples) have unique ion and trace chemistry and temperatures suggestive of deep circulation, as discussed in prior sections, but have no ^{18}O shift and are isotopically similar to other Taos Plateau wells. Discharge to Sunshine Trail spring (TS-72) is compositionally similar to Taos Plateau recharge. Bear Crossing spring (TS-8) appears to be a mixture of Tusas Mountain underflow and Taos Plateau recharge.

Infiltration from streams bounding the Taos volcanic field. Snow melt runoff from the Rio San Antonio (TS-228, δ^2H = -104.3 ‰), plots on the surface water line, but has a depleted isotopic composition relative to other surface waters samples (Fig. 31). The composition is nearly identical to shallow groundwater adjacent to Arroyo Aguaje de la Petaca (TC-234, δ^2H = -104.8 ‰) where the arroyo bounds the Taos Plateau volcanic field near No Agua Peaks. The isotopic signature, which characterizes modern runoff from the southern and eastern Tusas Mountains, plots between Tusas Mountain recharge and Taos Plateau precipitation (Fig. 33). This composition is unique in the regional aquifer, indicating that infiltration from modern streams draining the Tusas Mountains is not a significant source of recharge. The Antonito well in Colorado (TC-227) also plots near the surface-water line, but is unrelated to any compositional group on the Taos Plateau or in the Rio Grande gorge.

Ute Mountain recharge. Waters from the Ute Mountain spring zone (TS-14, TS-71 and TS-113) have an isotopic signature that is generally depleted in ^2H relative to adjacent Taos Plateau wells and most other springs in the upper Rio Grande gorge. The isotopic data suggest a recharge source from east of the Rio Grande gorge, from precipitation on Ute Mountain, the Sunshine Valley or the Sangre de Cristo Mountains, rather than from the Taos Plateau.

Carbon Isotope Composition and Radiocarbon Dating—Carbon-13 ($\delta^{13}C$) values for DIC range from -12.4 to -5.2 ‰, with a mean of -10.7 ‰ (Table 5). For most samples the DIC $\delta^{13}C$ is between -12 and -10 ‰. Carbon-14 activity for DIC ranges from 36.1 to 72.9 pmC, with a mean of 53.1 pmC. A plot of $\delta^{13}C$ versus ^{14}C activity (Fig. 34) shows a poor correlation (r^2 = 0.30), indicating that generally there is no dilution of ^{14}C activity from progressive dissolution of limestone or dolomite, consistent with the lack of

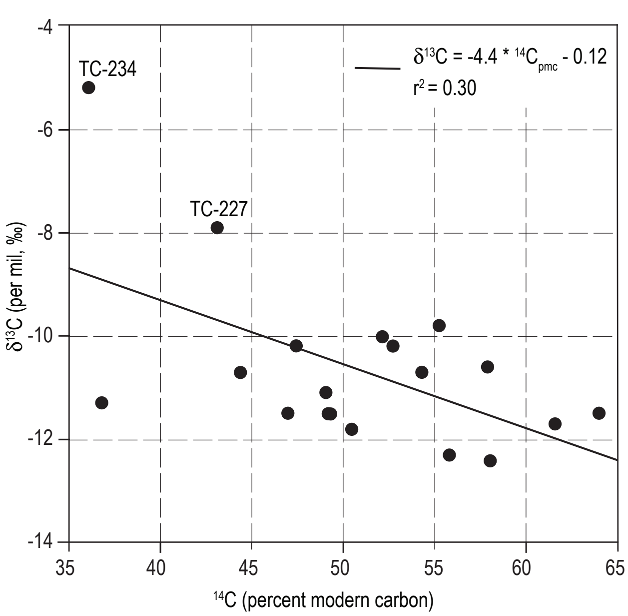

Figure 34–$\delta^{13}C$ versus ^{14}C activity of dissolved inorganic carbon (DIC).

carbonate strata in the region. However, the ^{14}C content of two samples (TC-227 and TC-234) with large (heavy) $\delta^{13}C$ values (7.9 and -5.2) and low ^{14}C activity may be diluted by another source of carbon such as hydrothermal fracture calcite or mantle CO2. The apparent radiocarbon ages for these waters are therefore likely overestimated. Although ^{14}C corrections might improve estimates of groundwater residence time in these samples, it is not undertaken in this report.

Apparent radiocarbon ages for samples from the Taos Plateau aquifer range from 8180 to 3580 years before present (Fig. 35, Table 5). The oldest groundwater occurs along the western boundary of the Taos Plateau. The youngest exists in the central closed basins. A zone of older groundwater (>5000 RCYBP) aligns with the Red River fault zone and the San Luis Hills in a northerly trend. The trend in radiocarbon age along a west-to-east flow path is remarkable for several reasons: 1) Groundwater becomes progressively younger along its flow path from San Antonio Mountain toward the central closed basins of the plateau. 2) A zone of older groundwater is coincident with the Taos Plateau horst and the Red River fault zone. 3) Discharge from the Ute Mountain and Sunshine Valley spring zones in the Rio Grande gorge is significantly younger than groundwater from adjacent Taos Plateau wells. 4) The oldest spring water, 4400 RCYBP, discharges from Felsenmeere (TS-61), the southernmost spring in the Bear Canyon spring zone.

The decrease in groundwater apparent age from west to east in the aquifer (Fig. 35) is consistent with the proposed conceptual model of groundwater sources, flow paths, and recharge developed from other hydrologic and geochemical data. Old groundwater (5500 to 8000 years old) originating in the Tusas Mountains enters the western Taos Plateau as subsurface inflow beneath the volcanic dome of San Antonio Mountain. Progressive mixing of this old groundwater with modern precipitation falling on the volcanic domes and closed basins of the central plateau produces a younger

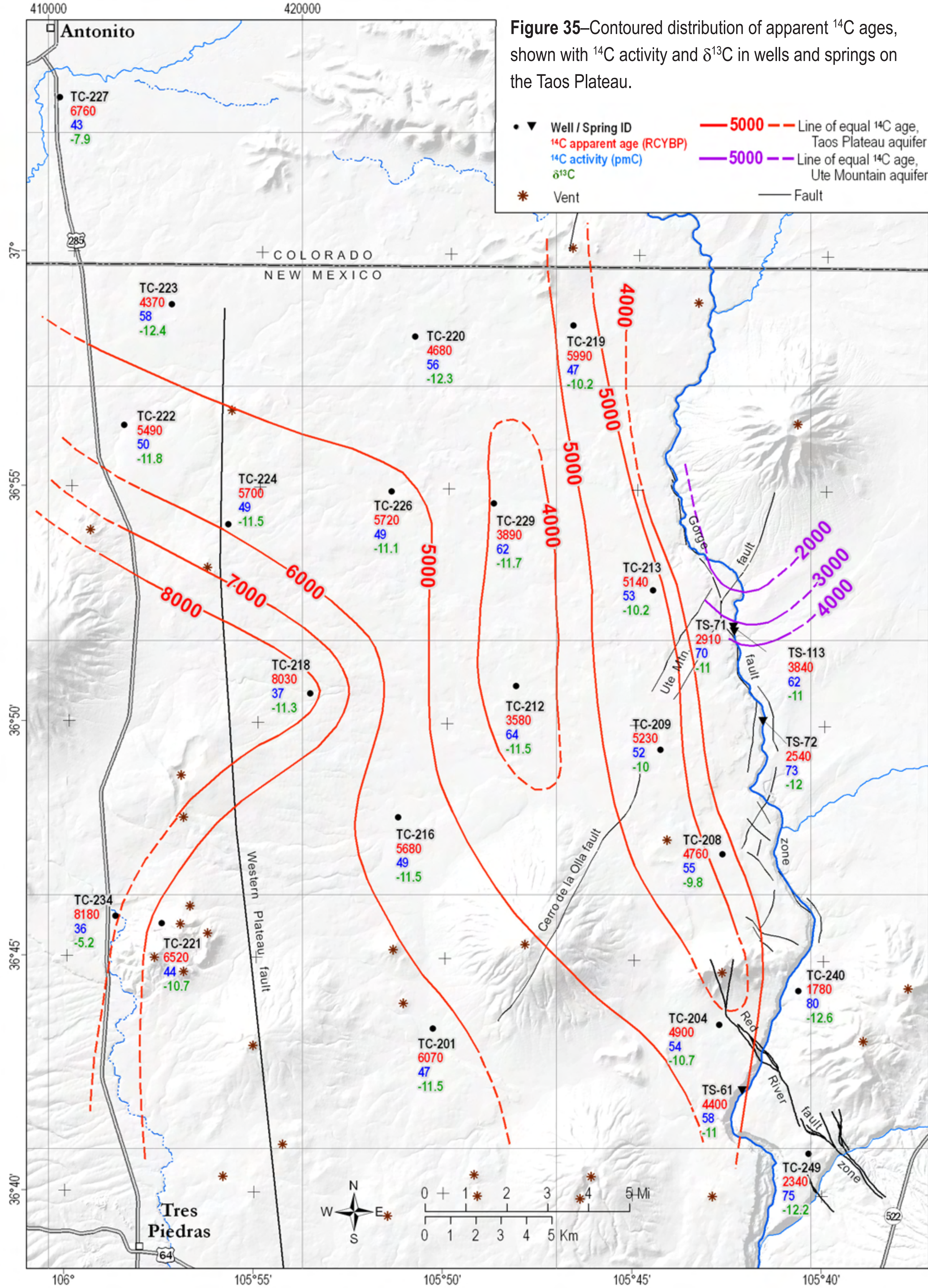

Figure 35–Contoured distribution of apparent ^{14}C ages, shown with ^{14}C activity and $\delta^{13}C$ in wells and springs on the Taos Plateau.

groundwater apparent age—3600 to 5700 years old—with higher ^{14}C activity. Additional mixing of relatively young central plateau groundwater with old groundwater ascending along rift-margin structures—the Taos Plateau horst and Red River fault zone—creates a north-trending zone of 4800 to 6000 year-old groundwater between the central plateau and the Rio Grande gorge. The age disparity (up to 3545 years) between this zone of old water and spring discharge in the Ute Mountain and Sunshine Valley spring zones indicates that sources for the springs must originate east of the gorge. The Bear Canyon-Felsenmeere spring zone discharges 4400 year-old groundwater from the Taos Plateau aquifer along the Red River fault zone.

Tritium (^3H) Composition—Tritium, a heavy radioisotope of hydrogen with a half-life of 12.32 years, is produced naturally in the upper atmosphere by cosmic radiation. Above-ground nuclear testing added large amounts of ^3H to the atmosphere from 1952 to 1980, particularly in the northern latitudes. Because ^3H enters the hydrologic cycle through precipitation, with ^3H atoms directly incorporated into the water molecule, it has been a useful groundwater dating tool. Once precipitation becomes part of the groundwater system and is isolated from the atmosphere, the original ^3H concentration drops to ½ after 12.32 years and by an additional ½ after a second period of 12.32 years, and so on. Concentrations of ^3H in groundwater that are significantly greater than modern natural production indicate recharge during peak fallout from the bomb-test period 1960-1964.

Tritium concentration in groundwater from wells and springs on the Taos Plateau ranges from 0.02 to 50.8 TU, with a mean of 2.6 TU and a median of 0.1 TU. Stream waters have 5.1 to 8.5 TU, with a mean of 7.0 TU. The mean ^3H concentration of 7.0 TU in streams provides a reasonable estimate of current atmospheric tritium levels in the northern Rio Grande rift. By applying a decay equation with a half-life of 12.32 years to an initial ^3H concentration of 7.0 TU, we can show that a residual tritium concentration of 1.0 TU corresponds to a time period of about 35 years or a recharge date around 1973. In reality, radioactive decay, mixing of old and young waters from different sources, and variation of ^3H input add complexities and make interpretation of tritium results much more difficult. Groundwater samples with a ^3H concentration >1.0 and <7.0 TU may be considered "recharge waters" or groundwater receiving some amount of modern recharge during the last 35 years. Even though high, bomb-pulse tritium concentrations have now decayed by at least 4 half-lives, groundwater with ^3H concentration much greater than 1 TU likely represents recharge from the early 1960s. For samples where the ^{14}C activity indicates an age of several thousand years and ^3H values suggest

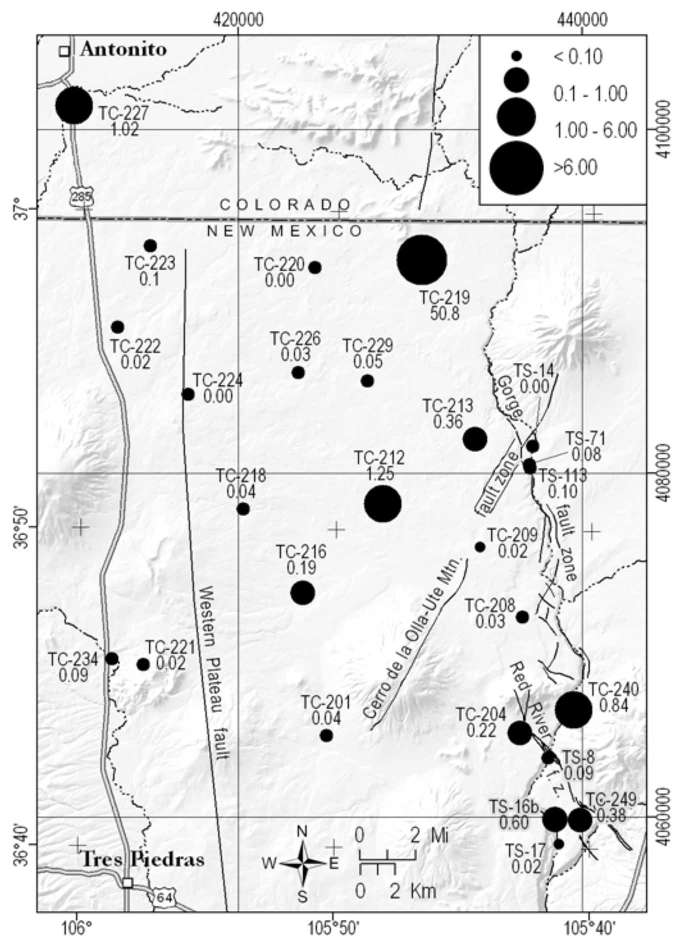

Figure 36–Distribution of tritium (^3H) content in the Taos Plateau regional aquifer. The standard analytical error for tritium is ± 0.09 TU. Samples containing <0.1 TU are considered to be tritium-free.

recharge during or after the early 1960s, mixing of water masses with distinctively different ages is indicated.

Tritium dating provides additional insight into recharge, mixing, and groundwater residence time in the Taos Plateau aquifer (Fig. 36). Most wells and springs have essentially zero tritium given the standard error of ±0.09 TU. These samples represent pre-1950s recharge or possibly a mix of old tritium-free water with a small fraction of young post-bomb recharge. Three wells samples (TC-204, TC-213, TC-216) contain significant measureable tritium between 0.1 and 1.0 TU, and likely represent a mix of old and young sources. Two well samples, TC-212 in the central plateau closed basin and TC-227 near the Rio San Antonio, have tritium contents of 1.25 and 1.02 TU. Combined with ^{14}C ages of several thousand years this indicates mixing of old tritium-free groundwater with a significant portion of modern recharge. One groundwater sample (TC-219) from a closed basin adjacent to the Rio Grande near the San Luis Hills has over 50 TU, clearly indicating a large component of recharge from the early 1960s.

Chlorofluorocarbon Composition and CFC-12 Recharge Ages—CFCs are useful tracers of groundwater flow and recharge age because they are essentially non-reactive under aerobic conditions and their input history is well known. CFC-12 (CCl_2F_2) and CFC-11 (CCl_3F) were introduced into the atmosphere in the late 1940s and CFC-113 (CCl_2FCClF_2) was first released in the 1960s. Atmospheric concentrations for CFC-113 and CFC-11 peaked in 1993 and 1994, respectively, and have since declined, complicating their use as transient tracers. The atmospheric concentration of CFC-12 peaked in 2004. Sorption of CFC-113 in aquifers with a moderate to high organic carbon content, and degradation of CFC-11 in aquifers with low dissolved oxygen can result in apparent ages that overestimate groundwater travel times (Cook et al., 1995). CFC-12 is minimally susceptible to either degradation or sorption, and CFC-12 derived recharge ages are therefore the best age estimates to use. Apparent ages obtained with CFC-12 closely match ages obtained with $^3H/He$ and hydraulic modeling for ages up to 30 years (Cook et al., 1995). Apparent CFC ages for older waters may be more uncertain than for younger waters because of lower CFC concentrations in older waters and increased sensitivity to trace contamination introduced during sampling.

CFC-12 recharge ages for the Taos Plateau (Table 6, Fig. 37) range from 29 to 59 years before the sample date. Given other chemical and isotopic evidence of mixing, these results likely reflect a mean age of mixed waters.

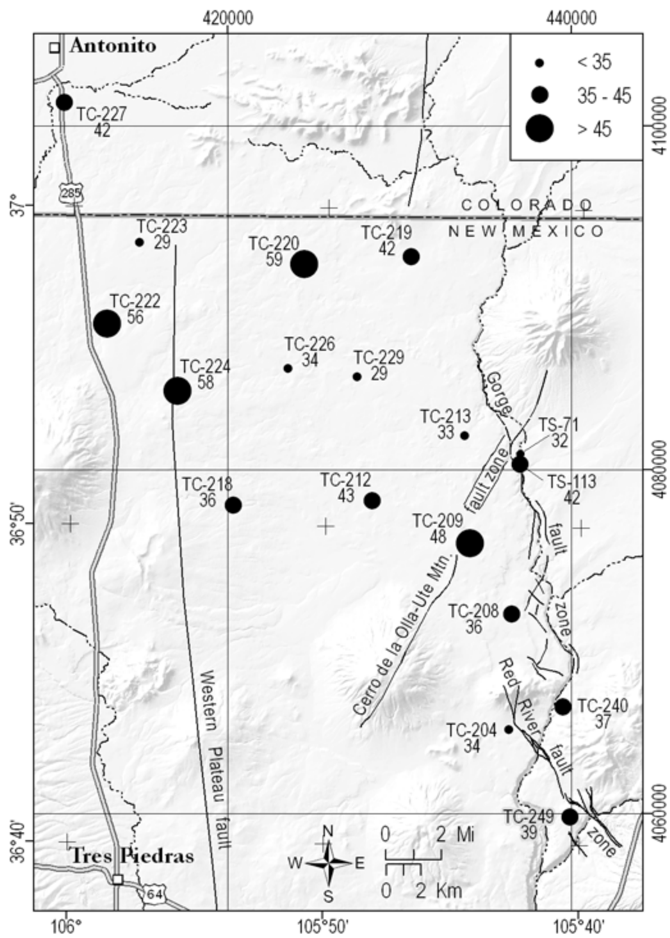

Figure 37–CFC-12 recharge ages, in years before sample date (Table 6), for the Taos Plateau regional aquifer.

VI. HYDROGEOLOGIC CONCEPTUAL MODEL OF THE NORTHERN TAOS PLATEAU

The synthesis of geologic, hydrologic, geochemical, and isotopic data from groundwater and surface water in the northern Taos Plateau enables us to create a conceptual model of the regional aquifer system that includes the following aspects of regional hydrogeology:

1) The rock units, faults, and structural features of the plateau
2) The geomorphology and surface drainage system of the Taos Plateau
3) Groundwater conditions, direction of groundwater flow and major sources and locations of recharge
4) The stratigraphic and structural controls on the groundwater system
5) The interconnection between the Taos Plateau aquifer and springs discharging in the Rio Grande gorge.

Elements of the hydrogeologic conceptual model for the Taos Plateau are illustrated in two block diagrams (Figs. 38 and 39) that present three-dimensional views of subsurface strata, rift-margin faults, horsts and grabens, water table surfaces for regional and perched aquifers, and chemical and isotopic zones within the aquifer system.

Geologic Model

Rock Units, Faults and Structural Features—Although the surface geology of the northern Taos Plateau is well mapped, the subsurface geology is not well constrained. Most of the study area is capped with Servilleta Basalt plus a variety of rhyolitic to dacitic domes and flows. Even where deep wells penetrate through the basalt cap, the thickness of the Servilleta Basalt is not necessarily constrained, as the older Hinsdale Formation basalts probably underlie the Servilleta over much of the study area, and the two basalt units can be difficult to distinguish in the field. In addition, buried volcanoes may exist in the study area, but are not discernible from the surface geology. Future geophysical studies may reveal more details of the subsurface stratigraphy of the Taos Plateau.

The San Luis Hills horst to the north and the Brushy-Timber Mountain horst to the south can be linked along the Gorge fault, which is the western boundary fault of the deep rift grabens (Taos graben and Costilla-Questa basin). We have chosen to connect the two exposed intrarift grabens with a low-relief horst informally named the Taos Plateau horst. Although the eastern boundary of the horst is a large-displacement, east-down, normal fault zone (the Gorge fault), the western boundary of the horst is thought to be a relatively small-displacement, west-down, normal fault. Along the length of the Taos Plateau horst, we show structurally high Hinsdale Formation under a thin to absent layer of Santa Fe Group and a cap of Servilleta Basalt. Future geophysical studies may better reveal the buried structural geology of the Taos Plateau.

The east-down, normal Red River fault zone is an important rift structure in the southeastern part of the study area (Fig. 39) where it appears to influence the groundwater system. Traced northward, the faults disappear near Cerro Chiflo. Our conceptual geologic model shows the Red River fault zone bending northward and merging with the east-down Gorge fault.

Based on a north-south alignment of volcanic centers along the western Taos Plateau, we hypothesize the existence of an east-down, normal fault or fault zone informally named the Western Plateau fault. In our model, the slip along this fault zone increases from north to south, resulting in major juxtaposition of stratigraphic units in the Tres Piedras area.

Geomorphology and Surface Drainage Basins—Streamflow from the Tusas Mountains is diverted around the Taos Plateau volcanic field and San Antonio Mountain via the Rio San Antonio and the ephemeral Arroyo Aguaje de la Petaca. Both the basalt-capped plateau and the lower slopes of volcanic domes lack well-integrated surface drainage systems that connect to the Rio Grande. Two-thirds of the study area (453 mi^2) consists of closed or poorly developed drainage basins, many of which contain active playa systems. Precipitation increases significantly with elevation on volcanic domes. These geomorphic and drainage features strongly suggest that the Taos Plateau volcanic field is an important recharge area for the regional aquifer.

Groundwater Conditions, Direction of Groundwater Flow, and Recharge

At the western boundary of the Taos Plateau, west of the Western Plateau fault, the regional aquifer has a relatively steep and uniform west-to-east hydraulic gradient that demonstrates subsurface groundwater inflow to the western plateau through Santa Fe Group alluvium, Hinsdale Formation, and older Tertiary rocks that underlie San Antonio Mountain and No Agua Peaks. The groundwater inflow originates as seepage from the Tusas Mountains and enters the Taos Plateau as underflow beneath the volcanic domes. It is likely that recharge through the volcanic edifices contributes to the regional aquifer.

Between the Western Plateau fault and the Rio Grande gorge, the water table flattens to a remarkably low hydraulic gradient of 2.5 to 13 ft/mi. This anomalously flat gradient is likely caused by a combination of factors, including high permeability in the fractured-basalt aquifer, flat topography, and high infiltration and recharge rates through the lava-capped plateau. Because of flat gradients and limited hydrologic data, the groundwater flow directions are poorly constrained in the eastern plateau north of Cerro de la Olla, but appear to follow a southerly or southeasterly path. Southeast of Cerro de la Olla and east of the Brushy-Timber Mountain horst, the water table grades steeply to the Rio Grande through thick Santa Fe Group alluvium. Local perched aquifers are identified in shallow wells on San Antonio Mountain and Ute Mountain.

Hydrologic, geologic and geochemical data suggest four sources of groundwater inflow and recharge for the Taos Plateau aquifer: 1) underflow from the Tusas Mountains; 2) infiltration and recharge from precipitation on the lava-capped plateau and volcanic domes; 3) upwelling of mineralized, thermal water near the Red River fault zone from a deep source; and 4) influent seepage from the Rio San Antonio, the Arroyo Aguaje de la Petaca, and the Rio Grande north of Ute Mountain.

Underflow from the Tusas Mountains—Geochemical data from this study show that groundwater underflow from the Tusas Mountains through the Hinsdale Formation and Santa Fe Group possesses many unique chemical characteristics. These waters are elevated (relative to samples from the plateau) in TDS, carbonate alkalinity, Ca, Mg, F and Li. The water apparently originated at high altitude, as indicated by ^{2}H depletion (<-105 ‰), and circulated to significant depth as indicated by anomalously warm temperatures (>19 °C). The water displays a positive isotopic shift in ^{18}O of about 0.5 to 1.0 ‰ and elevated dissolved SiO_2 (>60 mg/L) indicative of isotopic exchange between meteoric water and silicates in the reservoir rock, which is accelerated by high fluid temperatures. Carbon-14 data indicate that groundwater underflow entering the western margin of the plateau is the oldest water in the study area, with residence times ranging from about 5500 to over 8000 RCYBP. These waters

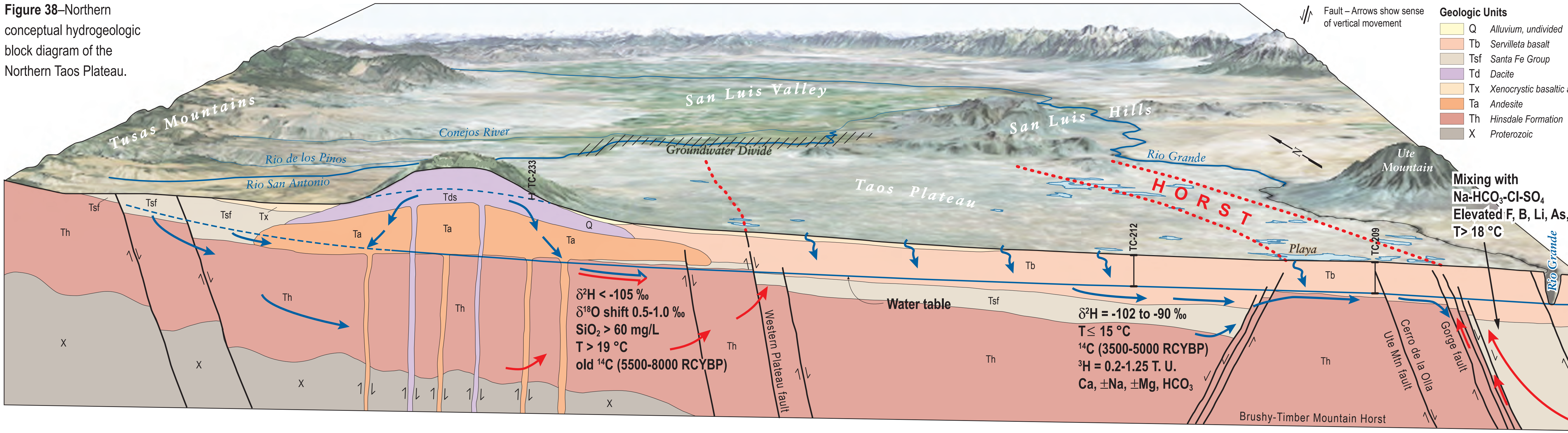

Figure 38–Northern conceptual hydrogeologic block diagram of the Northern Taos Plateau.

become progressively younger with eastward flow into the Servilleta Basalt as they mix with local recharge. The extent of ^{2}H depleted water beneath the Taos Plateau shows that underflow from the Tusas Mountains persists as a traceable component of regional groundwater nearly to the Taos Plateau horst.

Recharge from Precipitation—This study shows that substantial recharge originates from precipitation and infiltration on the lava-capped plateau and volcanic domes. A cap of fractured lava rock on the plateau and volcanic peaks dramatically increases infiltration of surface waters and results in poorly developed surface drainages. Most of the plateau consists of closed drainage basins with active playas. Precipitation rates increase significantly with elevation and temperature and evapotranspiration rates decrease, generating considerable recharge potential on the volcanic domes of the Taos Plateau. Water level data identify perched aquifers on San Antonio and Ute Mountains and recharge mounds in the regional aquifer beneath No Agua Peaks and Cerro de la Olla. Carbon-14, tritium and CFC age-dating demonstrate a downgradient decrease in groundwater residence time beneath the closed surface basins of the central plateau, and mixing of older underflow from the Tusas Mountains with tritium- and CFC-bearing recent recharge. Groundwater beneath the central and eastern regions of the Taos Plateau is relatively enriched in deuterium (typically ≥ 100 ‰) and forms a well-defined local meteoric water line (TPMWL) with San Antonio Mountain perched groundwater. These isotopic and age characteristics indicate a recharge source from local precipitation falling on the Taos Plateau and adjoining volcanic domes.

Seepage from the Rio San Antonio and the Rio Grande—Local mounds and ridges in the surface of the Taos Plateau aquifer demonstrate the effects of local topography and recharge superimposed on regional flow. Groundwater mounds exist beneath the Rio Grande in the Ute Mountain reach and the Rio San Antonio near Antonito, Colorado, indicating that channel infiltration recharges the regional aquifer. The recharge mound beneath the Rio San Antonio forms a subtle groundwater divide. West of the San Luis Hills this groundwater divide is generally coincident with a surface water divide separating the Rio San Antonio drainage from Punche Arroyo. From this divide groundwater flows southeast into New Mexico and north into the Alamosa Valley of Colorado. There is no evidence of groundwater flow directly from the Alamosa Valley north of Antonito into the Taos Plateau aquifer.

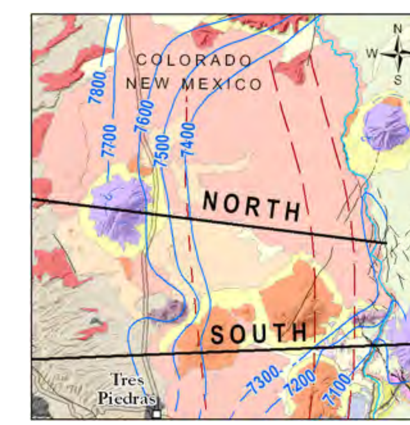

Figure 38-39–Locations of conceptional hydrogeologic cross section.

Hydrostratigraphy and Structural Controls on Groundwater Flow

Each of the geologic units exposed on the Taos Plateau and in the subsurface play some role in the regional aquifer system. Important hydrogeologic units include the Servilleta Basalt, lava domes of dacite, andesite and rhyolite, Santa Fe Group alluvial deposits that lie below the Servilleta Basalt and other lava flows and domes, the Hinsdale Formation and older volcaniclastic units, and Proterozoic granitic bedrock. The Taos Plateau aquifer is unconfined within Servilleta Basalt and the upper Santa Fe Group. Most Taos Plateau wells in New Mexico draw groundwater from the Servilleta Basalt. Just north of the Colorado border the Servilleta Basalt pinches out and wells tap Santa Fe Group sediments. West of the inferred Western Plateau

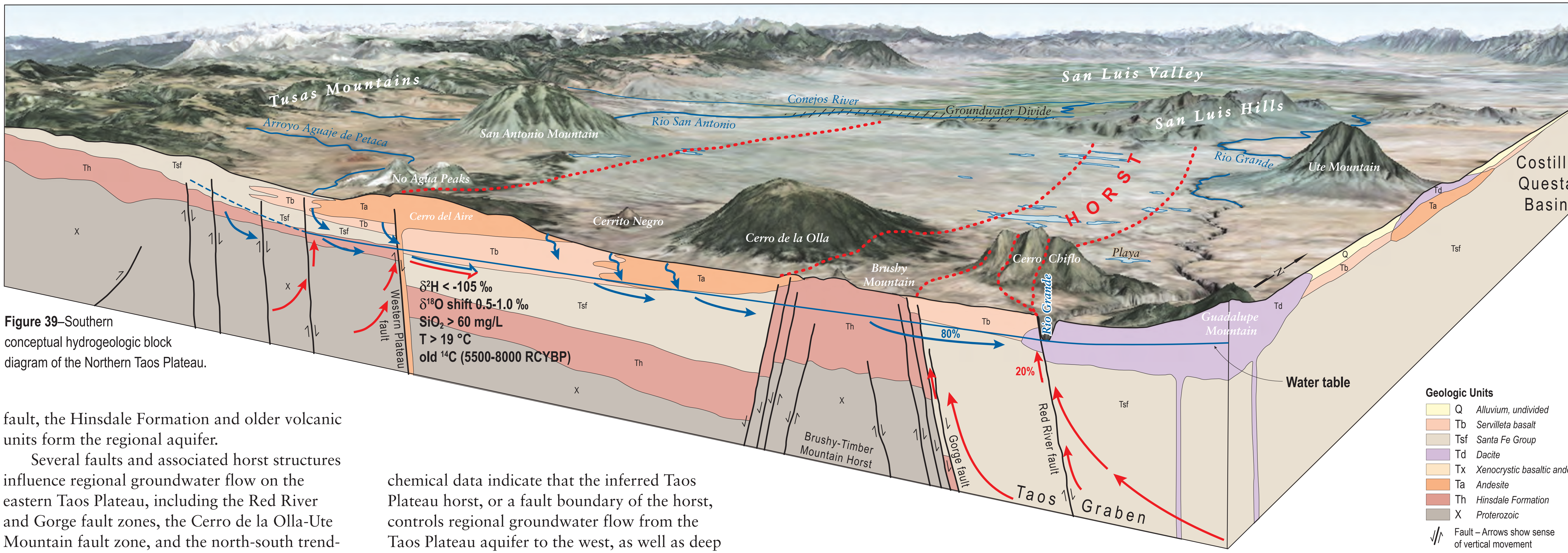

Figure 39–Southern conceptual hydrogeologic block diagram of the Northern Taos Plateau.

fault, the Hinsdale Formation and older volcanic units form the regional aquifer.

Several faults and associated horst structures influence regional groundwater flow on the eastern Taos Plateau, including the Red River and Gorge fault zones, the Cerro de la Olla-Ute Mountain fault zone, and the north-south trending San Luis Hills, Taos Plateau, and Brushy/Timber Mountain horsts. The fault-bounded horst forms a structural high in the shallow, east-dipping bedrock ramp of the western Taos Plateau and separates the ramp from the deep rift basins to the east (Taos graben and Costilla-Questa basin) along the Gorge fault. We observe that the inferred fault boundaries for the horst coincide with elevated heat flow and upwelling of warm, saline water, particularly south of the Cerro de la Olla-Ute Mountain fault zone and west of the Rio Grande gorge. The Taos Plateau horst, and the Gorge and Red River fault zones that we infer form the horst's eastern margin, influence both the flow and chemical characteristics of groundwater beneath the eastern edge of the Taos Plateau.

Taos Plateau Horst and Red River Fault Zone—Significant hydrologic, thermal and chemical data indicate that the inferred Taos Plateau horst, or a fault boundary of the horst, controls regional groundwater flow from the Taos Plateau aquifer to the west, as well as deep sources from the Taos graben to the east. West-to-east groundwater flow paths that prevail across the western half of the Taos Plateau are deflected southeast and south along the inferred eastern margin of the horst, just west of the Rio Grande gorge. Combinations of elevated groundwater temperatures and anomalously high concentrations of dissolved solids, sodium, sulfate, chloride, bromide, fluoride, boron, lithium, and arsenic are measured in wells and springs (TC-219, TC-209, TC-208, TC-204 and TS-8) aligned with the mapped Red River fault zone to the south and the inferred Taos Plateau horst to the north. Chemical and temperature anomalies in the vicinity of the Taos Plateau horst suggest a structural control for upwelling saline, thermal waters. However, lack of data from east of the Rio Grande gorge in the Taos graben make it difficult to demonstrate the water's origin.

We offer the following regional hydrogeologic model to explain observed hydrologic conditions and thermal and chemical characteristics of the eastern Taos Plateau in the context of the regional groundwater system. The inferred Taos Plateau horst, or likely the eastern fault boundary for the structure, intercepts regional groundwater flow from the shallow Taos Plateau aquifer to the west and the deep Taos graben aquifer to the east. The Red River fault zone focuses vertical upflow of deep mineralized thermal water into the Taos Plateau aquifer. Calcium-mixed cation-bicarbonate water from the Taos Plateau aquifer mixes with deep sourced $Na\text{-}HCO_3\text{-}Cl\text{-}SO_4$ thermal water and discharges to local wells and springs aligned with the structure. An ion-based mixing model estimates that discharge to the warm Bear Crossing spring in the Rio Grande gorge represents a mixture of about 20% fault-zone water and 80% Taos Plateau groundwater. Mineralized thermal waters may originate from deep groundwater circulation through the Taos graben, which is forced upward by the Taos Plateau horst and/or Red River fault zone, or from upflow of deep thermal fluids along the horst-bounding basement faults. Either or both deep sources may contribute to elevated groundwater temperatures and chemical anomalies in the southeastern corner of the Taos Plateau. A forced convection model has been proposed for a similar hydrogeologic rift setting – the Cañada Ancha graben and Caja del Rio horst – in the southern Española Basin (Johnson et al., 2012), and we prefer a similar model for this study area.

Ute Mountain Fault Zone—The Ute Mountain and Gorge faults appear to exert structural control over groundwater discharge to the Ute Mountain spring zone. First discharge (spring

TS-14) occurs where the Ute Mountain fault intersects the gorge and last discharge (spring TS-113) is located at the intersection of the Gorge fault. Waters from these springs are generally depleted in ^{2}H relative to Taos Plateau recharge, but are significantly enriched relative to Tusas Mountains water. The waters also have chemically distinct concentrations of fluoride, boron and silica and significantly younger apparent ^{14}C ages, relative to the Taos Plateau. The combination of hydrologic, chemical, and isotopic data suggests a source from Ute Mountain to the northeast or from the Costilla-Questa basin to the east.

***Western Plateau Fault*—**The Western Plateau fault, an inferred east-down, normal fault or fault zone, is approximately coincident with a north-south alignment of volcanic centers along the western Taos Plateau. In our model, the slip along this fault zone increases from north to south, resulting in major juxtaposition of stratigraphic units in the Tres Piedras area. The Western Plateau fault is also coincident with a west-to-east reduction in hydraulic gradient – from 70 ft/mi to about 4 ft/mi – in the regional aquifer east of San Antonio Mountain that marks a change in aquifer permeability between the Hinsdale Formation and the Servilleta Basalt, which we suspect are juxtaposed across the fault.

Interaction between the Taos Plateau Aquifer and Rio Grande Gorge Springs

Gains in Rio Grande stream flow result from discharge of groundwater from aquifers west (Taos Plateau) and east (Sunshine Valley) of the gorge via large springs and spring zones. Two principal spring zones – the Ute Mountain spring zone (river mile 19.5 to 21) and the Bear Crossing-Felsenmeere spring zone (river mile 33 to 34) – coincide with two structural features of the Taos Plateau, the Ute Mountain and Red River fault zones.

The start of the Ute Mountain spring zone correlates with the start of Winograd's (1959) accretion zone as well as the intersection of the Ute Mountain fault with the Rio Grande gorge. Discharge vents along both banks are commonly located 5 to 15 feet above river level, thus demonstrating a hydraulic head elevated well above the channel bottom. The number and discharge of springs increases downstream, culminating in a large subaqueous spring, with an artesian head that rises several feet above river level, that discharges approximately 13 cfs (6000 gpm) from a cavern in the river channel (Bauer and Johnson, 2010). This spring, named Lava Tube spring, demarcates the end of the Ute Mountain spring zone and spatially coincides with the Gorge fault. Geochemical data indicate that spring water chemistry is not representative of the Taos Plateau aquifer and radiocarbon dating indicates groundwater ages younger than any sampled from the Taos Plateau. Our model suggests that recharge from Ute Mountain, possibly via the Ute Mountain fault, provides at least a major component of flow to the Ute Mountain spring zone.

The Taos Plateau aquifer first discharges to the Rio Grande 33 miles downstream from the Colorado border in a 1.5-mile-long river reach at the Red River fault zone. The Bear Crossing springs emerge from numerous, high-volume vents situated 50 to 100 or more feet above river level where the Red River fault zone intersects the west wall of the Rio Grande gorge. The high-volume (~ 9700 gpm; 21.6 cfs) Felsenmeere springs discharge as columns of water that emerge from the basalt talus about 100 ft above the river. The spring zones are structurally controlled by the Red River fault zone and deep incision of the Rio Grande gorge into the Taos Plateau aquifer.

PROJECT PERSONNEL AND ACKNOWLEDGMENTS

Project Personnel

Peggy S. Johnson, Senior Hydrogeologist, New Mexico Bureau of Geology & Mineral Resources, peggy@gis.nmt.edu
Tasks: Data collection, compilation, and interpretation; technical report.

Paul Bauer, Ph.D., Principal Geologist, New Mexico Bureau of Geology & Mineral Resources, bauer@nmt.edu
Tasks: Project management; data collection, compilation, and interpretation; technical report.

Support Personnel

Stacy Timmons, M.S., Senior geologic research associate, New Mexico Bureau of Geology & Mineral Resources, stacyt@gis.nmt.edu
Tasks: Analytical geochemistry coordination.

Brigitte Felix, GIS Specialist, New Mexico Bureau of Geology & Mineral, bfk@gis.nmt.edu
Tasks: GIS; cartography; drafting; report design, layout and production.

Trevor Kludt, Ph.D., Hydrogeologic Lab Associate, New Mexico Bureau of Geology & Mineral Resources, tkludt@gis.nmt.edu
Task: Data collection.

Mark Mansell, GIS Specialist, New Mexico Bureau of Geology & Mineral Resources.
Tasks: GIS; cartography.

Acknowledgments

We thank Rolf Schmidt-Petersen of the New Mexico Interstate Stream Commission for arranging the principal funding for this study. Trudy and Ed Healy provided a grant from the Healy Foundation for an overlapping study of the adjacent Rio Grande gorge springs. The funding and project planning were facilitated by the efforts of Ron Gardiner of Questa. We are especially indebted to Herb Chavez, James Harmon, Stuart Smith, and Greg Gustina (BLM, Taos Field Office) for invaluable assistance in finding, measuring, and sampling the BLM wells on the Taos Plateau. Mark Sundin (BLM, Taos Field Office) assisted with several aspects of the project. Ron Gervason and Tony Benson of the Taos Soil & Water Conservation District provided UTM locations of inventoried water wells in the study area. Ren Thompson (USGS, Denver) was kind enough to review the geologic cross sections and share his expertise on the geology of the northern Taos Plateau. Tien Grauch and Benjamin Drenth (USGS, Denver) shared their insights from a developing geophysical model of the basin. Andrew Campbell provided general comments and a critical review of geochemical methods and interpretations. Hamilton Brown and Jeff Ogburn collected winter tributary stream-flow samples for geochemical analyses. Finally, we are much obliged to the land owners and permittees who graciously allowed us access to their wells for water level measurements and sampling.

REFERENCES

Anderholm, S. K., 1994, *Ground-water recharge near Santa Fe, north-central New Mexico:* U.S. Geological Survey Water-Resources Investigations Report 944078, 68 p.

Appelt, R. M., 1998, *40Ar/39Ar geochrolology and volcanic evolution of the Taos Plateau volcanic field, northern New Mexico and southern Colorado:* M.S. thesis, New Mexico Tech, 58 p. plus appendices.

Arnórsson, S., 2000, *Reactive and conservative components, in Arnórsson, S., ed., Isotopic and Chemical Techniques in Geothermal Exploration, Development and Use:* Vienna, International Atomic Energy Agency, p. 40–48.

Bankey, V., Grauch, V. J. S., Drenth, B., and Geophex, Inc., 2006, *Digital data from the Santa Fe East and Questa-San Luis helicopter magnetic surveys in Santa Fe and Taos Counties, NM, and Costilla County, Colorado:* U.S. Geological Survey Open-file Report 2006–1170, 4 pp with maps; available as digital product only at http://pubs.usgs.gov/of/2006/1170/.

Bauer, P. W. and Johnson, P. S., 2010, *A rare, large artesian subaqueous spring in the upper Rio Grande:* New Mexico Geology, v. 32, no. 1, p. 26–27.

Bauer, P. W., Johnson, P. S. and Timmons, S., 2007, *Springs of the Rio Grande Gorge, Taos County, New Mexico:* Inventory, Data Report, and Preliminary Geochemistry: New Mexico Bureau of Geology and Mineral Resources, Open-File Report 506, 20 p., plus appendices and oversize plate.

Benson, A. L., 2004, *Groundwater geology of Taos County:* New Mexico Geological Society Guidebook 55, p. 420–432.

Bliss, J. H. and Osgood, E. P., 1928, *Seepage study on Rio Grande between State line bridge, Colorado, and Embudo, New Mexico, and between Alamosa, Colorado, and Embudo, New Mexico:* New Mexico State Engineer, 9th Biennial Report, 1928–1930, July 1928, p. 27–40.

Brister, B. S., and Gries, R. R., 1994, *Tertiary stratigraphy and tectonic development of the Alamosa Basin (northern San Luis Basin), Rio Grande rift, south-central Colorado; in Keller, G. R., and Cather, S. M. (eds.), Basins of the Rio Grande rift—structure, stratigraphy, and tectonic setting:* Geological Society of America, Special Paper 291, p. 39–58.

Brister, B. S., Bauer, P. W., Read, A. S., and Lueth, V. W., 2004, *Geology of the Taos Region:* New Mexico Geological Society, Guidebook 55, 448 p.

Bryan, K., 1928, *Preliminary report on the geology of the Rio Grande Canyon as affecting the increase in flow of the Rio Grande south of the New Mexico-Colorado boundary:* Ninth Annual Report, State Engineer of New Mexico, 1928–1930; p. 108–120.

Bryan, K., 1938, *Geology and ground-water conditions of the Rio Grande depression in Colorado and New Mexico, in Regional Planning, Part 6, The Rio Grande Joint Investigation in the Upper Rio Grande:* U.S. National Resources Commission, p. 197–225.

Burck, P., Barroll, P., Core, A., and Rappuhn, D., 2004, *Taos regional groundwater flow model:* New Mexico Geological Society Guidebook 55, p. 433–439.

Chapin, C. E. and Cather, S. M., 1994, *Tectonic setting of the axial basins of the northern and central Rio Grande rift, in G. R. Keller and S. M. Cather (eds.), Basins of the Rio Grande rift: structure, stratigraphy and tectonic setting:* Geological Society of America Special Paper 291, p. 5–25.

Cook, P. G., Solomon, D. K., Plummer, L. N., Busenberg, E. and Schiff, S. L., 1995, *Chlorofluorocarbons as tracers of groundwater transport processes in a shallow, silty sand aquifer:* Water Resources Research, vol. 31, no. 3, p 425–434.

Coons, L. M., and Kelly, T. E., 1984, *Regional hydrogeology and the effect of structural control on the flow of groundwater in the Rio Grande Trough, northern New Mexico:* New Mexico Geological Society, 35th Field Conference, p. 241–244.

Daniel B. Stephens and Associates, 2007, *Taos Regional Water Plan, Volume 1:* Water Plan, January 2007, http://www.ose.state.nm.us/isc_regional_plans7.html.

Davis, S. N., Whittemore, D. O., and Fabryka-Martin, J., 1998, *Uses of chloride/bromide ratios in studies of potable water:* Ground Water, vol. 36, no. 2, p. 338–350.

Dungan, M. A., Muehlberger, W. R., Leininger, L., Peterson, C., McMillan, N. J., Gunn, G., Lindstrom, M., and Haskin, L., 1984, *Volcanic and sedimentary stratigraphy of the Rio Grande gorge and the Late Cenozoic geologic evolution of the southern San Luis Valley:* New Mexico Geological Society Guidebook 35, p. 157–170.

Dungan, M. A., Thompson, R. A., and Stormer, J. S., 1989, *Rio Grande rift volcanism: Northeastern Jemez zone, New Mexico:* New Mexico Bureau of Mines and Mineral Resources, Memoir 46, p. 435–486.

Edwards, C. L., Reiter, M. Shearer, C., and Young, W., 1978, *Terrestrial heat flow and crustal radioactivity in northeastern New Mexico and southeastern Colorado:* Geological Society of America Bulletin, v. 89, p. 1341–1350.

Ellis, A. J. and Mahon, W. A. J., 1977, *Chemistry and Geothermal Systems:* New York, Academic Press, 392 p.

Garrabrant, L. A., 1993, *Water resources of Taos County, New Mexico:* U.S. Geological Survey Water-Resources Investigations Report 93–4107, 86 p.

Goff, F., Laughlin, A., Aldrich, J., Ander, M., Arney, B., Decker, E., Gardner, J., Heiken, G., Kron, A., LaDelfe, C., Pettitt, R., and Shannon, S., 1981, *Hot dry rock geothermal prospects:* Geothermal Resources Council Transactions, v. 5, p. 173–176.

Grauch, V. J. S., and Keller, G. R., 2004, *Gravity and aeromagnetic expression of tectonic and volcanic elements of the southern San Luis Basin, New Mexico and Colorado:* New Mexico Geological Society Guidebook, 55th Field Conference, Geology of the Taos Region, p. 230–243.

Green, G. N. and Jones, G. E., 1997, *The digital geologic map of New Mexico in ARC/INFO format:* U.S. Geological Survey, Open-file Report, v. 97–0052, pp. 1–9.

Harder, V., Morgan, P., and Swanberg, C. A., 1980, *Geothermal resources in the Rio Grande rift: origins and potential:* Geothermal Resources Council Transactions, v. 4, p.61–64.

Hearne, G. A., and Dewey, J. D., 1988, *Hydrologic analysis of the Rio Grande Basin north of Embudo, New Mexico, Colorado and New Mexico:* U.S. Geological Survey Water-Resources Investigations Report 86–4113, 244 p.

Hem, J. D., 1992, *Study and interpretation of the chemical characteristics of natural water:* U.S. Geological Survey Water-Supply Paper 2254 (4th ed.), 263 p.

Johnson, P. S., 1998, *Surface-Water Assessment, Taos County, New Mexico:* New Mexico Bureau of Geology & Mineral Resources, Open-File Report OF-440, 36 p. plus tables and appendices.

Johnson, P. S., Koning, D. J., and Partey, F. K., 2012, *Shallow groundwater geochemistry in the Española Basin, Rio Grande rift, New Mexico – evidence for structural control of a deep thermal source, in M. Hudson and V. J. S. Grauch (eds.), New Perspectives on the Rio Grande Rift:* From Tectonics to Groundwater, Geological Society of America Special Paper.

Kelson, K. I. and Bauer, P. W., 2003, *Geologic map of the Los Cordovas 7.5-minute quadrangle, Taos County, New Mexico:* New Mexico Bureau of Geology & Mineral Resources, Open-file geologic map OF-GM 63, scale 1:24,000.

Kelson, K. I. and Bauer, P. W., 2006, *Geologic map of the Arroyo Hondo 7.5-minute quadrangle, Taos County, New Mexico:* New Mexico Bureau of Geology & Mineral Resources, Open-file geologic map OF-GM 116, scale 1:24,000.

Kelson, K. I., Bauer, P. W., and Thompson, R. A., 2008, *Preliminary geologic map of the Guadalupe Mountain 7.5-minute quadrangle, Taos County, New Mexico*: New Mexico Bureau of Geology & Mineral Resources, Open-File Geologic Map OF-GM 168, scale 1:24,000.

Kinzli, K.D., Shafike, N., Bauer, P., Lundahl, A., Schmidt-Petersen, R., Harris, S., Lewis, G., Johnson, P., and Timmons, M., 2011, *Quantifying river accretion in the upper Rio Grande gorge, New Mexico, by using an Accoustic Doppler Current Profiler*: River Research and Applications, published in Wiley Online Library (wileyonlinelibrary.com) DOI: 10.1002/rra.1581.

Langmuir, D., 1997, *Aqueous environmental geochemistry:* Prentice-Hall, Inc., New Jersey, 600 pp.

Lipman, P. W. and Mehnert, H. H., 1975, *Late Cenozoic basaltic volcanism and development of the Rio Grande depression in the southern Rocky Mountains:* Geological Society of America Memoir 144, p. 119–154.

Lipman, P. W. and Mehnert, H. H., 1979, *The Taos Plateau volcanic field, northern Rio Grande rift, New Mexico: in Riecker, R. C., ed., Rio Grande rift – Tectonics and magmatism:* American Geophysical Union, Washington D.C., p. 289–311.

Machette, M. N., Coates, M-M., and Johnson, M. L., 2007, *2007 Rocky Mountain Section Friends of the Pleistocene Field Trip—Quaternary geology of the San Luis Basin of Colorado and New Mexico, September 7–9, 2007:* U.S. Geological Survey Open-File Report 2007–1193, 197 p.; available at pubs.usgs.gov/of/2007/1193.

Mailloux, B. J., Person, M., Kelley, S., Dunbar, N., Cather, S., Strayer, L., and Hudleston, P., 1999, *Tectonic controls on the hydrogeology of the Rio Grande Rift, New Mexico:* Water Resources Research, v. 35, no. 9, p. 2641–2659.

Manning, A. H., 2009, *Ground-water temperature, noble gas, and carbon isotope data from the Española Basin, New Mexico:* U.S. Geological Survey Scientific Investigations Report 2008–5200, 69 p.

Mazor, E., 2004, *Chemical and Isotopic Groundwater Hydrology:* Marcel Dekker, Inc., Basel, Switzerland, 455 pp.

Morgan, P., Harder, V., Swanberg, C. A., and Daggett, P. H., 1981, *A groundwater convection model for Rio Grande rift geothermal resources:* Geothermal Resources Council Transactions, v. 5, p. 193–196.

Panichi, C. and Gonfiantini, R., 1981, *Geothermal Waters, in J. R. Gat and R. Gonfiantini (eds.), Stable Isotope Hydrology – Deuterium and Oxygen-18 in the Water Cycle:* IAEA Technical Reports Series No. 210, International Atomic Energy Agency, Vienna, p. 241–271.

Peterson, C. M., 1981, *Late Cenozoic stratigraphy and structure of the Taos Plateau, northern New Mexico:* M.S. thesis, University of Texas at Austin, 57 p.

Plummer, L. N., Bexfield, L. M., Anderholm, S. K., Sanford, W. E., and Busenberg, E., 2004a, *Geochemical characterization of ground-water flow in the Santa Fe Group aquifer system, Middle Rio Grande Basin, New Mexico:* U.S. Geological Survey Water-Resources Investigations Report 03–4131, 395 p.

Plummer, L. N., Bexfield, L. M., Anderholm, S. K., Sanford, W. E., and Busenberg, E., 2004b, *Hydrochemical tracers in the Middle Rio Grande Basin, U.S.A., 1. Conceptualization of groundwater flow:* Hydrogeology Journal, v. 12, p. 359–388.

Reiter, M., Edwards, C. L., Hartman, H. and Weidman, C., 1975, *Terrestrial heat flow along the Rio Grande rift, New Mexico and Southern Colorado:* Geological Society of America Bulletin, v. 86, p. 811–818.

Seager, W.R., 1975, *Cenozoic tectonic evolution of the Las Cruces area, New Mexico:* New Mexico Geological Society Guidebook 26, p. 241–250.

Shomaker, J. W. and Johnson, P., 2005, *Hydrology and water supply in the Taos region:* New Mexico Decision-Makers Field Guide No. 4, Mining in New Mexico – the Environment, Water, Economics, and Sustainable Development, p. 16–20.

Siebenthal, C. E., 1910, *Geology and water resources of the San Luis Valley, Colorado:* U.S. Geological Survey Water Supply Paper 240, p. 15–18.

Steele, K. F. and Wagner, G. H., 1981, *Warm springs of the western Ouachita Mountains, Arkansas:* Geothermal Resources Council Transactions, v. 5, p. 137–140.

Summers W. K. and Hargis, L. L., 1984, *Hydrogeologic cross section through Sunshine Valley, Taos County, New Mexico:* New Mexico Geological Society, 35th Field Conference, p. 245–248.

Swanberg, C. A., 1981, *Subsurface temperatures of geothermal resources – Catalogue of thermal waters, in L. Icerman, A. Starkey, and N. Trentman (eds.), State-coupled low temperature geothermal resource assessment program, fiscal year 1979:* New Mexico Energy Research and Development Program, New Mexico State University, p. 118 – 1–30.

Swanberg, C. A., 1984a, *Temperature gradient studies near two groundwater constrictions in northern New Mexico, in L. Icerman (ed.), Regional geothermal exploration in north central New Mexico*: New Mexico Energy Research and Development Institute, p. 114–148.

Swanberg, C.A., 1984b, *Geothermal resources of the Rio Grande rift, in L. Icerman (ed.), Regional geothermal exploration in north central New Mexico:* New Mexico Energy Research and Development Institute, p. 165–183.

Swanberg, C. A. and Morgan, P., 1978, *The linear relation between temperatures based on the silica content of groundwater and regional heat flow: a new heat flow map of the United States:* Pure and Applied Geophysics, vol. 117, p. 227–241.

Tello, E. H., Verma, P. M., and Tovar, R. A., 2000, *Chemical and isotopic study to define the origin of acidity in the Los Humeros (Mexico) geothermal reservoir:* Geothermal Resources Council Transactions, vol. 24, p. 441–449.

Thompson, R. A. and Machette, M. N., 1989, *Geologic Map of the San Luis Hills Area, Conejos and Costilla Counties, Colorado:* U.S. Geological Survey, Miscellaneous Investigations Series Map I–1906, scale 1:50,000.

Thompson, R. A., Dungan, M. A., and Lipman, P. W., 1986, *Multiple differentiation processes in early-rift calc-alkaline volcanics, northern Rio Grande rift, New Mexico:* Journal of Geophysical Research, v. 91, p. 6046–6058.

Thompson, R. A., Johnson, C. M., and Mehnert, H. H., 1991, *Oligocene basaltic volcanism of the north Rio Grande rift: San Luis Hills, Colorado:* Journal of Geophysical Research, v. 96, p. 13,577–13,592.

Trainer, F. W. and Lyford, F. P., 1979, *Geothermal hydrology in the Rio Grande rift, North-Central New Mexico:* New Mexico Geological Society Guidebook, v. 30, p. 299–306.

Upson, J. E., 1939, *Physiographic Subdivisions of the San Luis Valley, Southern Colorado:* The Journal of Geology, Vol. 47, No. 7, p. 721–736.

Wilson, L., Anderson, S. T., Jenkins, D. and Lovato, P., 1978, *Water availability & water quality, Taos County, New Mexico: Phase A Report: Basic data on geography, climate, geology, surface water, groundwater, water rights, water use, water supply and water quality:* Technical Report to the Taos County Board of Commissioners by Lee Wilson & Associates, Inc., 66 p. plus tables and appendices.

Winograd, I. J., 1959, *Ground-water conditions and geology of Sunshine Valley and western Taos County, New Mexico:* New Mexico State Engineer Office, Technical Report 12, 70 p.

Witcher, J. C., 1981, *Thermal springs of Arizona:* FIELDNOTES From the State of Arizona, Bureau of Geology and Mineral Technology, v. 11, no. 2, p 1–4.

Witcher, J. C., Reiter, M., Bland, D., and Barroll, M.W., 1992, *Geothermal resources in New Mexico:* New Mexico Geology, v. 14, no. 1, p. 14–16.

APPENDICES

APPENDIX C–GEOLOGIC MAP UNIT DESCRIPTIONS

(Adapted principally from Kelson et al. (2009), Read et al. (2009), and Lipman and Mehnert (1979)

Qal Stream channel and valley-floor alluvium, and active floodplains (Holocene)—Poorly to moderately sorted sand, pebbles, and boulders with clasts of granitic, metamorphic, volcanic, and sandstone rock types. Clasts along Red River, Rio Grande, and tributaries draining the Sangre de Cristo Mountains are dominated by granitic rock, quartzite, and basalt. Clasts along tributaries draining the western side of the Rio Grande are dominated by volcanic rock types. Weak or no soil development.

Qe Eolian deposits (Pleistocene to Holocene)—Well-sorted, fine-to-medium sand with some silt and rare gravel lags. Poorly exposed except in small road cuts. Predominantly on eastern side of the Rio Grande. Weak-to-moderate soil development.

Qcl Colluvial mantle on slopes and landslide deposits (middle Pleistocene to Holocene)—Colluvium consists of poorly sorted sand, pebbles, and boulders which mantles slopes. Consists of thin mantle overlying volcanic bedrock. Landslide deposits consist of poorly sorted sand to boulders. Includes large rotational slide blocks within the Rio Grande gorge which contain rotated and detached beds of Servilleta Formation basalt. May also include areas underlain by Holocene colluvium in Rio Grande and Red River gorges.

Qf Alluvial fan deposits, undivided (middle Pleistocene to Holocene)—Poorly sorted silt, sand, pebbles, and cobbles. Clasts are primarily quartzite, schist, granite, and volcanic rock types. Associated soils typically have some degree of calcium carbonate development.

Qt Stream terrace deposits, undivided (middle Pleistocene to Holocene)—Poorly sorted silt, sand, pebbles, cobbles, and boulders. Clasts are primarily quartzite, schist, granite, and volcanic rock types. Associated soils typically have some degree of calcium carbonate development.

QTg Old alluvium (late Tertiary to middle Pleistocene)—Poorly sorted sand, pebbles, and cobbles. Clasts of basalt, quartzite, and other metamorphic and volcanic rock types. Locally high percentage of angular to subangular quartzite pebbles and cobbles. Present along piedmont between Sangre de Cristo Mountains range front and Red River and Rio Grande gorges. Correlative with the Lama Formation of Lambert (1966), and probably correlative with the Blueberry Hill deposit in the Arroyo Hondo and Taos quadrangles. Contains an ash layer in the uppermost strata dated by 40Ar/39Ar at 1.6 Ma (elevation ca. 7660 ft, M. Machette, USGS, personal comm., 2008). Contains undated ash layer in road cut near Red River Fish Hatchery (elevation ca. 7160 ft) that is chemically similar to ca. 3 Ma Jemez volcanic units (N. Dunbar, NMBGMR, personal comm., 2008).

Tb Servilleta Formation, basalt (Pliocene)— Flows of dark-gray tholeiitic basalt characterized by small olivine phenocrysts, diktytaxitic texture, and local vesicle pipes and segregation veins. Formed thin, fluid, widespread pahoehoe basalt flows that erupted principally from five large shield volcanoes in the central part of the Taos Plateau (Lipman and Mehnert, 1979) but also from small shields and vents in the northwestern study area (Thompson and Machette, 1989). The flows commonly form columnar-jointed cliffs where exposed with a maximum thickness of approximately 200m in the Rio Grande gorge in the southeastern map area. Individual flows, up to 12 m thick, are grouped into packages of from one to ten flows (Peterson 1985; Dungan et al., 1984). These packages are separated by sedimentary intervals that are as much as 70 m thick in in the Rio Grande gorge. Tabular plagioclase and sparse olivine are the only phenocrysts. 40Ar/39Ar ages from basalts exposed in the Rio Grande gorge south of the map area range in age from 4.81 +/- 0.03 Ma for the lowest basalt near the Gorge Bridge, to 3.12 +/- 0.13 Ma for the highest basalt flow at the Gorge Bridge (Appelt, 1998). Servilleta lava flows represent the youngest eruptive activity in the map area where uppermost Servilleta lava flows are as young as 3.32 +/- 0.15 Ma south of Cerro Chiflo.

Tg Servilleta Formation, interbasalt gravel (Pliocene)—In cross sections only. Sedimentary intervals between basalt flow members, as much as 70 m thick in the Rio Grande gorge near the Red River. Typically rounded to subrounded pebble- to cobble-size clasts in a sand to silt matrix.

Tsf Santa Fe Group, undivided (Miocene to Pliocene)—Consists primarily of rift-related, clastic sedimentary deposits of the Tesuque Formation(?) that underlie the Servilleta Formation. Mixed conglomerate, sandstone, and mudrock were derived from the Sangre de Cristo Mountains, Tusas Mountains, and the Rio Grande. Includes Quaternary surficial deposits in the southwestern map area. The eolian Ojo Caliente Sandstone Member (middle to late Miocene) may exist in the subsurface. Older volcaniclastic units—equivalent to the Los Pinos Formation, Chama-El Rito Member of the Tesuque Formation, and Picuris Formation—may exist in the subsurface. Thickness unknown, but probably highly variable over study area.

Tdu Dacite of Ute Mountain (Pliocene)—Eroded, monolithologic, phenocryst-poor dacite domes, flows, and spires that form the large, steep-sided volcano of Ute Mountain. Dacites flows are typically thick, locally flow layered near flow margins, and locally cut by radial dikes. The two-pyroxene dacites form dark gray to black, non-vesicular lava flows containing augite+orthophyroxene+p lagioclase in a typically glassy groundmass. Approximate age of 2.7 Ma (Read et al., 2004).

Tds Dacite of San Antonio Mountain (Pliocene)—Eroded, monolithologic, phenocryst-poor dacite domes, flows, and spires that form the large, steep-sided volcano of San Antonio Mountain. Dacites flows are typically thick, locally flow layered near flow margins, and locally cut by radial dikes. The two-pyroxene dacites form dark gray to black, non-vesicular lava flows containing augite+orthophyroxene+plagioclase in a typically glassy groundmass. Approximate age of 3.05 Ma (Read et al., 2004).

Tx Xenocrystic basaltic andesite (Pliocene)—A series large of lava flows that erupted along the flanks of San Antonio Mountain. These andesites are compositionally similar to the olivine andesites but carry abundant xenocrysts of sodic plagioclase and resorbed quartz. In the San Antonio Mountain area, these lava flows overlie Servilleta basalts.

Approximate ages of 2.34 Ma for Pinebetoso Peaks and 3.53 Ma for La Segita Peaks (Read et al., 2004).

Taa **Andesite of Cerro del Aire (Pliocene)—** Large, monolithologic shield edifice of calc-alkaline, olivine-bearing andesite. The andesites occur as weakly to moderately vesicular aa flows and associated near-vent cinder, spatter, and agglutinate. Andesites contain olivine±plagioclase ±augite±orthopyroxene in an intergranular groundmass. Olivine phenocrysts are euhedral to skeletal, weakly zoned, and in equilibrium with whole-rock compositions. Approximate age of 3.6 Ma (Read et al., 2004).

Tr **Rhyolite of No Agua Peaks (Pliocene)—** Silicic alkalic rhyolite erupted from a cluster of four steep-sided lava domes at No Agua Peaks. The margins of the domes consist of tan, frothy, hydrated perlitic glass with obsidian inclusions (often called “apache tears”). The interiors of the lava domes are light-gray, flow laminated, and mostly devitrified. Rhyolites are nearly aphyric, containing less than 1% plagioclase+sanidine+quartz (Lipman and Mehnert, 1979). Approximate age of 4.1 Ma (Read et al., 2004).

Tdm **Dacite of Unamed Cerrito East of Montoso (Pliocene)—**Dark gray, sparsely phyric, low-silica, calc-alkaline dacite lava flows erupted from two vent areas east of Cerro Montoso. Dacites contain rare, skeletal, pyroxene phenocrysts and resorbed, subhedral olivine and quartz xenocrysts in a microcrystalline to glassy groundmass. Locally includes small volume, aerially restricted andesite flows (McMillan and Dungan, 1988). Scoria and spatter agglutinate common near poorly defined vent areas. Isotopic age determination on lava flow groundmass concentrate yielded an age of 4.11 +/- 0.13 Ma (Kelson et al., 2009).

Tvr **Volcanic rocks of Red River volcano (Pliocene)—**Includes a sequence of volcanic rocks and near vent pyroclastic deposits of moderate relief on the south side of Guadalupe Mountain and in canyon exposures in the middle and upper reaches of the Red River. Lava flows of the Red River volcanic sequence include a series of lower, predominantly basaltic andesite and andesite lava flows overlain by dacite lava flows capping the gorge sequence on both sides of the Red River. Near vent spatter, agglutinate and volcanic bombs are locally common. Locally, deposits of the Red River volcano overlie and in rare cases are intercalated with dacite lava flows of Guadalupe Mountain and consistently overlie basalt and rare andesite of the Servilleta Fm near the base of the Red River gorge. Isotopic ages for andesite and dacite lava flows within the Red River gorge are 4.87 +/- 0.16 Ma and 4.83 +/- 0.09 Ma respectively (Kelson et al., 2009).

Tao **Andesite of Cerro de la Olla (Pliocene)—** Dark gray to black, porphyritic olivine andesite lava flows erupted from vents on Cerro de la Olla, the largest monogenetic shield volcano of the Taos Plateau volcanic field (Lipman and Mehnert, 1979). Contains 2-3% phenocrysts of olivine in a microcrystalline groundmass of plagioclase, olivine, augite, and Fe-Ti oxides. The lower slopes of Cerro Montoso in the western side of the map area are often mantled in colluvium and rarely preserve well-developed flow morphology. Instead outcrops typically reflect blocky flow tops and remnants of numerous discontinuous and aerially restricted flow lobes. Appelt (1998) reported an 40Ar/39Ar age of 4.97 +/- 0.06 Ma for a groundmass separate from the south flank of Cerro de la Olla.

Tag **Dacite of Guadalupe Mountain (Pliocene)—** Predominantly trachydacite lava flows and associated near-vent pyroclastic deposits of the Guadalupe Mountain volcano complex. Contains sparse, small phenocrysts of plagioclase, hypersthene and augite in a pilotaxitic glassy groundmass. Distal lava flows exposed in the Rio Grande gorge and the Red River gorge are highly elongate and individual flows are laterally restricted, typically forming overlapping finger-like lobes characterized by radial cooling fractures and concentric brecciated carapaces where exposed in cross section. Flows exposed in Rio Grande gorge vary in thickness from a few meters to several tens of meters. Guadalupe Mountain dacite lava flows overlie both Cerro Chiflo dome deposits and lower Servilleta Formation basalt lava flows in the Rio Grande gorge and locally underlie and are intercalated with lava flows of the Red River volcano. Appelt (1998) reported 40Ar/39Ar ages of 5.11 +/- 0.08 Ma, 5.34 +/- 0.06 Ma, and 5.21 +/- 0.07 Ma.

Tvc Trachyandesite of Cerro Chiflo (Pliocene)— Eroded remnants of large lava dome of porphyritic trachyandesite at Cerro Chiflo, forms prominent cliff outcrops along Rio Grande gorge. Light brown to gray, weakly to strongly flow laminated, contains phenocrysts of plagioclase, hornblende, and sparse biotite in a devitrified groundmass. Xenoliths of Precambrian schist, gneiss, and granite are common up to 10 cm in diameter. Flow breccias preserved around margins of dome and ramp structures common throughout the exposed interior. Appelt (1998) reported 40Ar/39Ar ages of 5.31 +/- 0.31 Ma and 5.32 +/- 0.08 Ma.

Tam Andesite of Cerro Montoso (Pliocene)— Dark gray to black, porphyritic olivine andesite lava flows erupted from vents on Cerro Montoso, one of the largest, petrologically uniform, shield volcanoes of the Taos Plateau volcanic field (Lipman and Mehnert, 1979). Contains 2–3 percent phenocrysts of olivine in a microcrystalline groundmass of plagioclase, olivine, augite, and Fe-Ti oxides. The lower slopes of Cerro Montoso are typically mantled in colluvium and rarely preserve well-developed flow morphology. Instead outcrops typically reflect blocky flow tops and remnants of numerous discontinuous and aerially restricted flow lobes. Appelt (1998) reported an 40Ar/39Ar age of 5.88±0.18 Ma from the west side of Cerro Montoso.

Ta Older andesite lavas (Miocene or Pliocene)—Poorly exposed, eroded, olivine andesitic edifices that are mostly buried by the modern dacitic cones of Ute Mountain and San Antonio Mountain. Olivine andesite lava flows in the Rio Grande gorge west of Ute Mountain contain rare, well-developed primary pahoehoe flow textures (Ruleman et al., 2007). Ages unknown, but predates eruption of Servilleta basalt at Ute Mountain.

Ti Intrusive rocks of the San Luis Hills (Oligocene)—Fine- to medium-grained, equigranular to slightly porphyritic, gray to tan stocks of quartz monzonite in the southern San Luis Hills.

Tat Amalia Tuff (Oligocene)—Light gray to light brown moderately welded porphyritic, peralkaline, rhyolite ash-flow tuff. Consists primarily of quartz and sanidine phenocrysts in a devitrified matrix. Fe-Ti oxides, sphene, and alkali amphibole phenocrysts are minor. Forms low erosional hills of distal outflow in Brushy Mountain area. Miggins et al. (2002) reported a 40Ar/39Ar sanidine age of approximately 25.1 Ma. Erupted from the Questa caldera to the east (Lipman and Reed, 1989).

Tvb Volcanic deposits of Brushy Mountain (Oligocene)—Volcanic rocks and deposits consisting primarily of andesite to dacite lava flows and flow breccias and rhyolite block-and-ash flows and ash-flow tuff with volumetrically minor air-fall deposits

(Thompson et al., 1986; Thompson and Schilling, 1988). Light tan, poorly welded, lithic-rich, rhyolite ash-flow tuff forms base of section near low saddle of Brushy Mountain. Lower rhyolite contains phenocrysts of plagioclase and altered biotite, sparse light brown altered pumice and angular to subangular vitrophyric inclusions containing plagioclase phenocrysts and reddish-brown dacite inclusions. Locally overlain by thin outflow deposits of Amalia Tuff. Post-Amalia Tuff deposits include light grey to white rhyolite dome deposits including locally, block-and-ash flows, ash-flow tuffs, and air-fall deposits. All deposits are mineralogically similar containing sanidine, quartz and minor biotite phenocrysts in a devitrified glass matrix. K-Ar dating of sanidine yielded an age of 22.3 +/- 0.08 (Lipman and Mehnert, 1979) and a 40Ar/39Ar sanidine age of 25.01 +/- 0.05 Ma (Kelson et al., 2009).

Tvt **Volcanic deposits of Timber Mountain (Oligocene to Miocene)**—Volcanic rocks and deposits consisting primarily of andesite to dacite lava flows and flow breccias and lesser rhyolite flows and ash-flow tuff (Thompson and others, 1986; Thompson and Schilling, 1988). Light-brown, lithic-poor, densely welded rhyolite ash-flow tuff forms base of section and contains moderately to highly flattened pumices, phenocrysts of plagioclase, sanidine, quartz, and biotite with subordinate amounts of Fe-Ti oxides, clinopyroxene and orthopyroxene in a glassy to partially devitrified matrix. K-Ar dating of biotite and sanidine separates yielded ages of 26.5 +/- 1.3 and 24.4 +/- 0.9 Ma, respectively (Lipman and Mehnert, 1979). Appelt (1998) reported an 40Ar/39Ar age of 17.47 +/- 0.05 Ma for groundmass separates from a lava flow.

Th **Hinsdale Formation (Oligocene)**—Basaltic lava, breccia, and near-vent pyroclastic deposits of the San Luis Hills and northwestern map area. According to Thompson and Machette (1989) includes fine-grained silicic alkali-olivine basalt, basaltic andesite, tholeiitic basalt, and minor andesite and xenocrystic basaltic andesite. Ages range from about 26.4 to 25.7 Ma in southern San Luis Hills area (Thompson and Machette, 1989). Thickness ranges from 0 to 300 m.

Tu **Older Tertiary rocks (Oligocene)**—In cross sections only. Tertiary volcaniclastic and volcanic rocks that predate the Hinsdale Formation. Consists of the Los Pinos Formation and its equivalents.

X **Proterozoic rocks, undivided (Paleo- and Mesoproterozoic)**—Includes the Tres Piedras granite and other crystalline Proterozoic rocks.

APPENDIX D–REGIONAL CLIMATE DATA

Figure D1–Regression of mean annual precipitation versus elevation for regional climate data stations in Taos County.

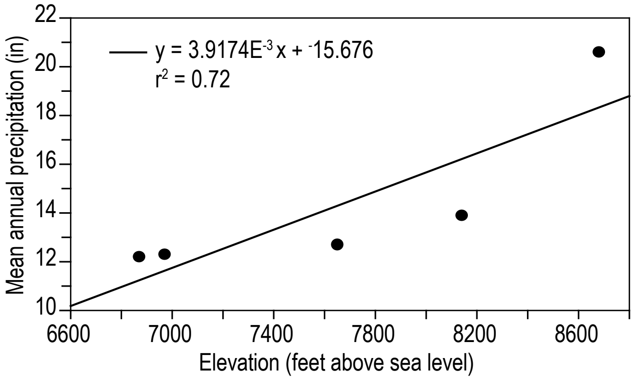

Figure D2–Regression of mean annual air temperature versus elevation for regional climate data stations in the San Luis Basin, northern New Mexico and southern Colorado.

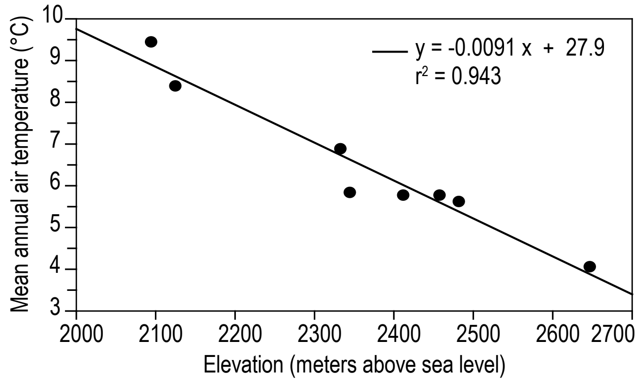

Table D1–Climate data from regional weather stations in the San Luis Valley, northern New Mexico and southern Colorado.

Station	Period of record	Longitude (dd)	Latitude (dd)	Elevation (ft)	Elevation (m)	Precipitation (inches)	Mean annual temperature (°F)	Mean annual temperature (°C)
Alamosa	1948-2006	105.87	37.45	7540	2299	7.1	41.4	5.2
Cerro	1932-2006	105.6	36.75	7650	2332	12.7	44.4	6.9
Conejos3 NNW	1948-1960	106.03	37.13	7910	2412	8.05	42.5	5.8
El Rito	1933-2006	106.183	36.333	6870	2095	12.2	49	9.4
Manassa	1948-2006	105.95	37.167	7690	2345	7.6	42.6	5.8
Red River	1915-2006	105.4	36.7	8680	2646	20.6	39.3	4.1
San Luis 1E	1980-2006	105.43	37.183	8060	2457	9.6	42.4	5.8
Taos	1914-2006	105.6	36.38	6970	2125	12.3	47.1	8.4
Tres Piedras	1914-2006	105.983	36.633	8140	2482	13.9	42.1	5.6

Western Regional Climate Center: New Mexico and Colorado Climate Summaries, http://www.wrcc.dri.edu

Table D2–Precipitation estimates for volcanic highlands in the northern Taos Plateau study area.

	Elevation (ft asl)	Precipitation (inches)*
Cerro Chiflo	8882	19.1
Cerro del Aire	9023	19.7
Cerro de la Olla	9475	21.4
Cerro Montoso	8655	18.2
Cerro Negro	8205	16.5
No Agua Peaks	9003	19.6
San Antonio Mountain	10,908	27
San Luis Hills @ state line	8200	16.4
Ute Mountain	10,093	23.9

* Mean annual precipitation estimated for volcanic highlands from precipitation-elevation regression (Fig. D1)

New Mexico Bureau of Geology and Mineral Resources

A Division of New Mexico Institute of Mining and Technology

Socorro, NM 87801
(575) 835-5490
Fax (575) 835–6333
www.geoinfo.nmt.edu